3.00
+8

Batholithic Rocks of Southern California—A Model for the Petrochemical Nature of their Source Materials

U.S. GEOLOGICAL SURVEY PROFESSIONAL PAPER 1284

Batholithic Rocks of Southern California—A Model for the Petrochemical Nature of their Source Materials

By A. K. BAIRD *and* A. T. MIESCH

U.S. GEOLOGICAL SURVEY PROFESSIONAL PAPER 1284

A mathematical model is used to remove the effects of magmatic differentiation from the chemical data on 480 samples

UNITED STATES GOVERNMENT PRINTING OFFICE, WASHINGTON : 1984

UNITED STATES DEPARTMENT OF THE INTERIOR

WILLIAM P. CLARK, *Secretary*

GEOLOGICAL SURVEY

Dallas L. Peck, *Director*

Library of Congress Cataloging in Publication Data
Baird, Alexander K.
Batholithic rocks of southern California.
(Geological Survey Professional Paper ; 1284)
Bibliography: 42 p.
1. Batholiths—California, Southern. I. Miesch, A. T. (Alfred T.) II. Geological Survey (U.S.) III. Title. IV. Series.
QE461.B24 1983 552'.3 82-21048

For sale by the Branch of Distribution
U.S. Geological Survey
604 South Pickett Street
Alexandria, VA 22304

CONTENTS

ILLUSTRATIONS

TABLES

BATHOLITHIC ROCKS OF SOUTHERN CALIFORNIA—A MODEL FOR THE PETROCHEMICAL NATURE OF THEIR SOURCE MATERIALS

By A. K. BAIRD[1] and A. T. MIESCH

ABSTRACT

Major-element analyses of 497 composite samples of batholithic rocks (quartz diorites, granodiorites, and quartz monzonites) from the northern Peninsular Ranges and Transverse Ranges Provinces, southern California, form the basis for a mixing model that accounts for most of the compositional variation in the rocks. The compositional structure in the batholithic rocks as a group was found to be similar to that in the Sierra Nevada batholith, and indicates that four end members are sufficient to account for 85–97 percent of the variability in each of the eight major oxides. According to the model, the batholithic rocks formed from the mixing of basaltic and quartzo-feldspathic end-member magmas, and the removal of variable proportions of plagioclase and mafic minerals, principally hornblende. Gabbroic rocks, common only in the western part of the region, could have formed from nearly uncontaminated magmas of the basaltic end member. Variations in the mixtures of basaltic and quartzo-feldspathic magmas are presumed to reflect variations in their source materials at depth. According to the model, the compositions of the source materials do not vary smoothly over the region, but display a discontinuity along a line approximately coincident with the present San Jacinto fault zone. The discontinuity is roughly coincident with previously noted petrologic and isotopic discontinuities in the northern Peninsular Ranges and is interpreted as the western limit of significant contribution of continental materials to the batholithic rocks. The model gives no evidence of a discontinuity in the vicinity of the San Andreas fault zone.

INTRODUCTION

The batholithic rocks of late Mesozoic age in southern California are exposed over 18,000 km^2 (square kilometers) in parts of two geologic provinces, the Peninsular Ranges Province and the Transverse Ranges Province (fig. 1), and range in composition from gabbro to quartz monzonite. Composite samples from 548 localities were analyzed for eight major elements (Baird and others, 1979) and these data form the basis for compositional modeling with an extended method of *Q*-mode factor analysis (Miesch, 1976b). The method was used to determine the number and nature of end members required to adequately explain the observed chemical variations. Areal variations in the corresponding mixing proportions and in the derived compositions of the end-member magmas, or magma-source materials, display a distinct discontinuity in the eastern part of the Peninsular Ranges Province.

[1]Present address: Pomona College, Claremont, CA 91711

REGIONAL GEOLOGIC SETTING

The northern Peninsular Ranges lie at the northern end of a narrow (120 km) belt of batholithic rocks of Mesozoic age that can be traced southward for hundreds of kilometers into Baja California, Mexico. The eastern limit of this belt, over all its length, is in the flooded depression of the Gulf of California and its northward extension, the Salton Trough. The Gulf is interpreted to have formed in latest Tertiary time by oceanic spreading on the East Pacific Rise; the Salton Trough is believed to have formed by a series of rhombochasms developed along the San Andreas fault zone (fig. 2). The northern terminus of the Peninsular Ranges Province, and the southern boundary of the Transverse Ranges Province, is at the east-striking Malibu Coast-Cucamonga fault zone and its possible eastward continuation, the Banning fault (fig. 2). The San Andreas fault zone continues northwestward from the northern margin of the Peninsular Ranges diagonally across the Transverse Ranges Province. Other fault zones, especially the San Jacinto and Elsinore (both subparallel to the San Andreas) and the east-striking Pinto Mountain fault, provide boundaries for further subdivisions of the provinces. We recognize six structurally-bounded units or blocks (fig. 2): San Gabriel, San Bernardino, and Little San Bernardino (Transverse Ranges), and San Jacinto, Perris, and Santa Ana (Peninsular Ranges).

To claim that this region is the most geologically enigmatic part of California is an understatement. Certain petrologic-structural aspects have been agreed to by most workers, but other aspects have received diverse interpretations. General, if not universal, agreement exists on the following aspects:

1. Plutonic igneous rocks are mostly late Mesozoic in age and are intrusive into metamorphic rocks apparently no older than Triassic in the Peninsular Ranges but as old as late Precambrian in the Transverse Ranges.

2. Plutonic igneous rocks vary compositionally from southwest to northeast, from mafic to felsic. Gabbroic rocks are found only in the Peninsular Ranges and most are southwest of the San Jacinto fault.

3. Plutonic igneous rocks are dominantly the product

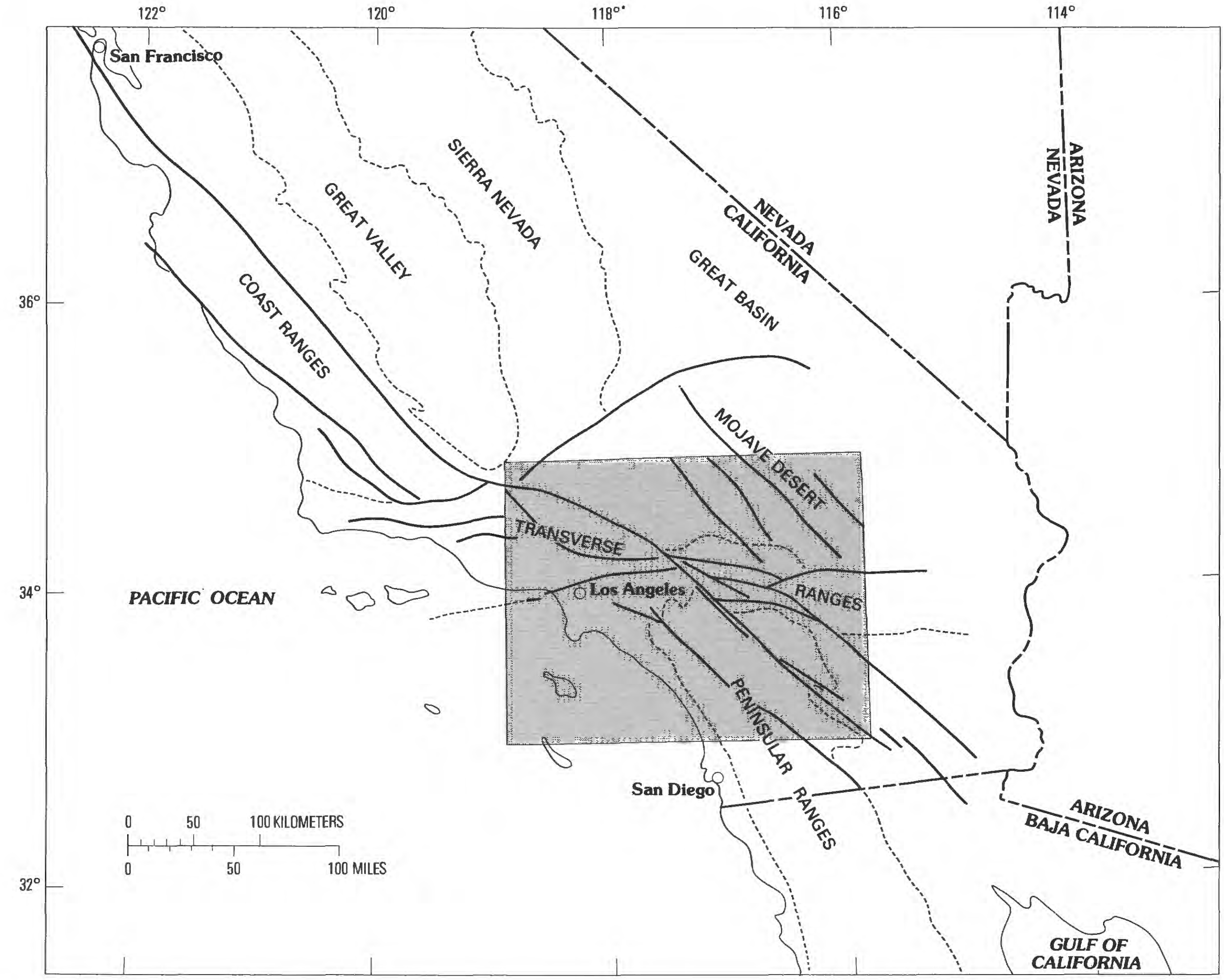

FIGURE 1.—Geologic provinces of southern and central California and northern Baja California, Mexico (dotted lines). Heavy lines delineate major fault patterns, dashed where inferred. Shaded rectangle outlines area of figures 2 and 3.

of magmatic activity; that is, they form numerous individual plutons that have internal structures characteristic of flow.

4. At least some, if not most, of the faults that bound structural blocks postdate the emplacements of the plutonic rocks, and movements on the faults have continued to Holocene times.

The nature and magnitude of separation on the San Andreas fault in southern California remain subjects of major disagreement. (The total separations on the Elsinore and San Jacinto faults have been relatively small—15 km or less—by most interpretations.) The San Andreas fault has been judged (1) a major strike-slip fault in California with hundreds of kilometers of movement dating back to (perhaps) early Mesozoic time (Hill and Dibblee, 1953), (2) a major continental transform and plate boundary also with hundreds of kilometers of movement (Atwater, 1970), (3) a boundary of minor importance in the Transverse Ranges (Hadley and Kanamori, 1977; Yeats, 1981), (4) an important strike-slip fault in southern California that has 250 km of separation (Crowell, 1979), (5) a relatively minor strike-slip fault in southern California that has 35–70 km of right separation at the Transverse Ranges (Baird, Morton, Woodford, and Baird, 1974), (6) a minor structure that does not significantly offset bedrock patterns in southern California (Woodford, 1960), and, finally, (7) a minor participant in large-scale rotational tectonics of southern California that does not cut the Transverse Ranges (Luyendyk and others, 1979). Thus, depending upon the interpretation, the San Andreas fault in this part of California may be young, may be old, or may

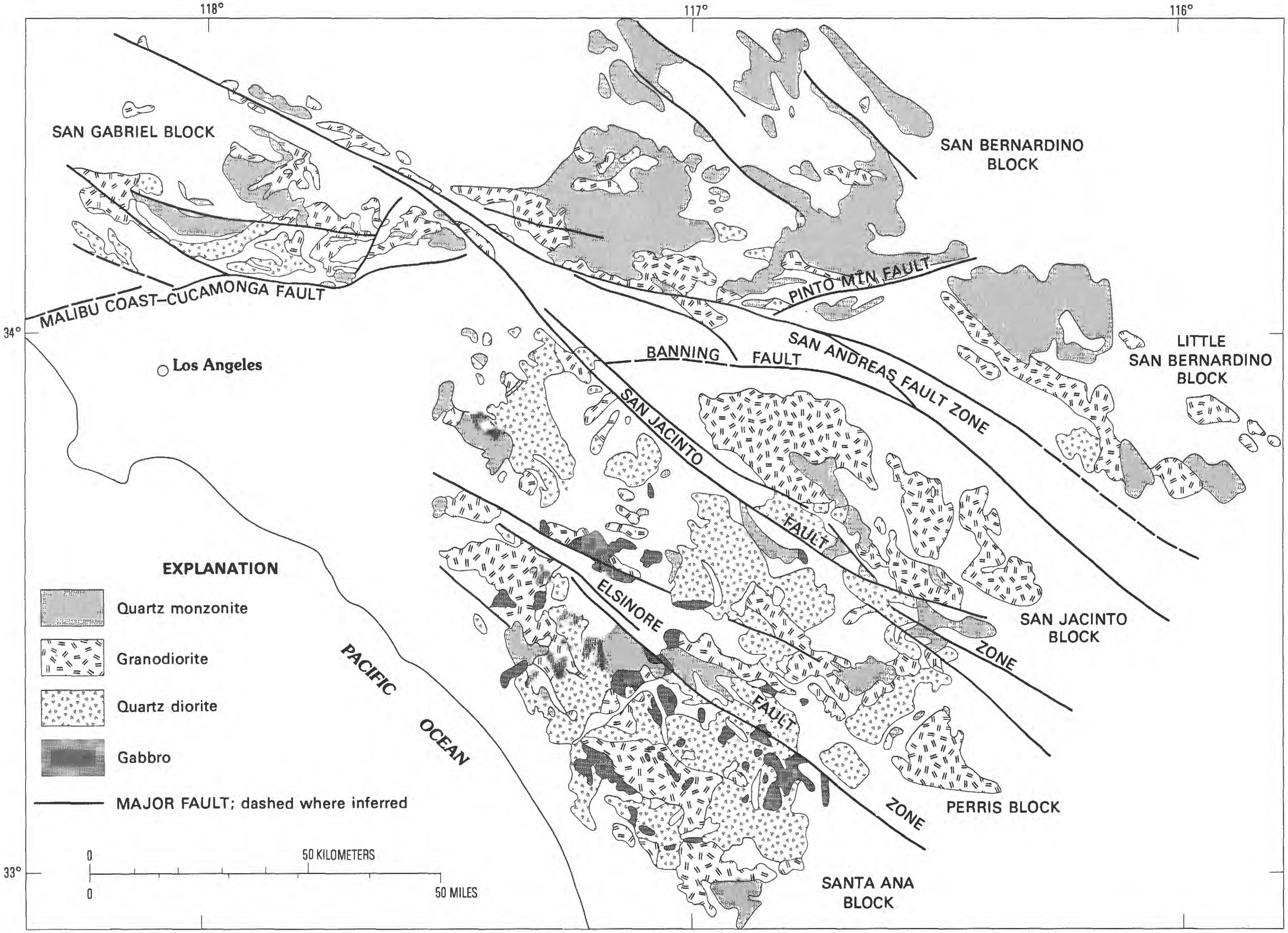

FIGURE 2.—Generalized map for the Mesozoic plutonic rocks of the northern Peninsular and Transverse Ranges Provinces, Calif. Fault-bounded structural blocks are indicated. Rock nomenclature follows that of Bateman and others (1963). Map modified from Baird, Baird, and Welday (1979).

have only a few kilometers or more than 1000 km of separation. If the separation since Mesozoic time has been large then, obviously, it is fortuitous that the plutonic rocks east of the San Andreas (San Bernardino and Little San Bernardino blocks) are presently adjacent to similar rocks west of the fault, it is accidental that apparently continuous areal patterns of petrologic variation occur across the region, and a happenstance that distinct, internally consistent patterns of chemical variations in all these rocks suggest a common origin and evolution that are different from those of other Cordilleran batholithic masses (Baird and others, 1979).

PREVIOUS GEOCHEMICAL STUDIES

The first extensive and the definitive work on the batholithic rocks of the area was by E. S. Larsen, Jr. (1948) who described a number of plutonic units in the northern Peninsular Ranges and published dozens of chemical and modal analyses. Through his work, these rocks became known as the "southern California batholith," although Larsen clearly recognized that the same batholithic mass extends great distances into Mexico. The area he studied and mapped is essentially that of the Perris and Santa Ana blocks of the present paper (fig. 2). The name "southern California batholith" has been restricted to the Peninsular Ranges Province and has not been extended to include the Transverse Ranges, perhaps mainly because of Larsen's work.

Within and southeast of the area described by Larsen, a number of more detailed studies bearing on the geochemistry of plutonic rocks have been made (for example, Morton and others, 1969; Miesch and Morton, 1977; Morton and Baird, 1976; Nishimori, 1976; Todd and Shaw, 1979; Taylor and Silver, 1978; Walawender, 1979). Reconnaissance work in Mexico by Gastil and others (1975) has established the general geology of the batholithic rocks there. Isotope, trace-element and radiometric-dating studies have been pursued by Silver and colleagues (for example, Silver and others, 1975; Taylor and Silver, 1978; Gromet and Silver, 1979), by Krummenacher and others (1975), and by DePaolo (1980). Much of this work, especially as it pertains to the southern Peninsular Ranges within California, has been carefully summarized by Abbott and Todd (1979).

To the north, in the Transverse Ranges, considerably less work bearing on the geochemistry of batholithic rocks has been done. However, individual plutons have been studied (for example, Baird and others, 1967; Richmond, 1965), problems of the older Mesozoic syenitic rocks have been described (Miller, 1977), and radiometric dates for both wallrock and some intrusives have been reported (Silver, 1971).

The basis for the present report is the group of 548 composite samples collected by Baird and his colleagues (fig. 3). The purpose of the sampling was to provide unbiased representative samples of the batholithic rocks that could be used to determime areal distributions of the major and minor elements. Details of the methods, analyses, and discussions of elemental distributions are given elsewhere (Baird, 1975; Baird, Morton, Woodford, and Baird, 1974; and Baird, Baird, and Welday, 1974, 1979). In summary, the principal findings from these prior studies are:

1. All elements, except aluminum and titanium, have statistically significant regional trends that increase or decrease to the northeast.
2. Silicon, potassium, and to a lesser extent sodium, increase markedly toward the northeast in a fashion directly predictable from areal distributions of rock types (gabbro to quartz monzonite) and from position with respect to the continental margin.
3. Within individual quartz-rich rock types (quartz monzonite, granodiorite and quartz diorite), however, silicon varies antipathetically with potassium.
4. Potassium, the element that exhibits the strongest trend, seems to vary independently of the other elements within the quartz-rich rock types, but dependently in gabbroic rocks.
5. Chemical variations are continuous, without the stepwise sequences thought to characterize the Sierra Nevada trends (Bateman and Dodge, 1970).
6. Monzo-syenitic rocks in the Transverse Ranges are genetically unrelated to the quartz plutonites.
7. Gabbroic rocks have patterns of geochemical behavior different from the quartz plutonites and probably had different sources.

For the present investigation, we have eliminated from consideration 23 samples from localities underlain by monzo-syenites, and an additional 26 samples from localities at which the rocks are gabbroic, for the reasons cited and because attempts to develop a model with these analyses included in the data gave evidence of the petrogenetic differences. A final two samples were removed from the San Gabriel block because the rocks are probably Miocene in age and genetically are unrelated to the batholith (D. M. Morton, oral commun. 1980). Thus, a total of 497 composite samples from the studies summarized have been considered in this investigation.

PETROLOGIC NOMENCLATURE

This report uses the terminology of Bateman and others (1963, fig. 2), rather than that of the IUGS (International Union of Geological Sciences) Commission (Streckeisen, 1973) for several reasons: (1) for consistency with prior discussions of the same chemical data; (2) for consistency with studies in the Sierra Nevada; and (3) for flexibility because the Bateman classification provides five divisions of quartz plutonites whereas the IUGS scheme uses only four (effectively three because no rocks in southern California fall in the alkali granite category).

ACKNOWLEDGMENTS

We are indebted to T. H. McCulloh and V. R. Todd of the U.S. Geological Survey and to W. B. Wadsworth of Whittier College for helpful criticism of the manuscript.

DEVELOPMENT OF THE MODEL

Chemical variation in nearly all rock bodies has resulted from processes of mixing and unmixing (for example, differentiation), and appropriate petrogenetic models are comprised of end-member compositions and estimated mixing proportions for representative rock samples. The observed compositions of the rock samples can be approximated by combining (forming linear combinations of) the end-member compositions according to the derived mixing proportions. The first task in the development of such a model is to determine the number of end members required; the next is to derive the end-member compositions. The first task can be accomplished rather objectively by mathematical analysis, but the second requires geologic reasoning and speculation as well as mathematics. Once the number of end members and their compositions have been determined, each individual sample composition can be examined to see if it can be approximated by reasonable combinations of the end members. If most or all the samples can be explained, the model is said to be mathematically adequate. Whether the model is valid or not depends on whether the end-member compositions are those of the materials that were actually involved in the mixing or unmixing processes that caused the compositional variations in the rocks. The methods used here serve to reject some selected end-member compositions as mathematically impossible, but the final selections are not unique.

The modeling methods used here have been described elsewhere (Miesch, 1976a, b, c) and have been applied previously to a variety of petrogenetic problems (for example, Miesch and Morton, 1977; Miesch and Reed, 1979; Miesch, 1979; Stuckless and others, 1981; Stuckless and Miesch, 1981). The mathematical development is not repeated here and the reader is referred to the cited papers for details.

However, an easily visualized application of the modeling concepts involves the plagioclase feldspar system. If one were given a number of feldspar crystals as unknowns (when in reality they were all samples of oligoclase, andesine, labradorite and bytownite), one could determine analytically that they were composed principally of four oxides: SiO_2, Al_2O_3, Na_2O and CaO. But, the compositions of the plagioclases can be described at least approximately in terms of only two end members, albite and anorthite. Similarly, although the batholithic rocks of southern California are composed mostly of eight major-oxide constituents, we will show that the compositions of these rocks can be approximated in terms of only four end members. The end members chosen for the plagioclase series, albite and anorthite, are conventional, but they are not the only end members that could be used. In a study of island arcs, for example, An_{30} and An_{55}, rather than Ab and An, might be appropriate. In fact, the only requirement for the plagioclase end members is that they be some combination of albite and anorthite. Otherwise, they would not be mathematically compatible with the plagioclase series. That is, the compositions of the plagioclase crystals could not be approximated as linear combinations of the end members. Just as there is a choice for the plagioclase end members, there is a choice of end members that can be used to describe the compositional variation within the batholithic rocks of southern California; the choices must be made on the basis of both mathematical evidence and geologic observation or speculation regarding the materials actually involved in the mixing processes.

NUMBER OF END MEMBERS

The data matrix (Appendix 1) consists of 497 rows that represent composite samples and eight columns that represent the oxide variables: SiO_2, Al_2O_3, FeO (total iron), MgO, CaO, Na_2O, K_2O, and TiO_2. The 497 rows of the original data matrix were adjusted so that the eight variables in Appendix 1 sum to 100 percent for each sample. This constant row-sum is required in order to recalculate the results of conventional *Q*-mode factor analysis into the end-member compositions and mixing proportions that comprise the model. The original data are given in Baird and others (1979) where they are keyed with rock-type designations and the U–V geographic coordinates identified on figure 3 of this report. The average compositions of all samples and of the samples from each of the six structural blocks identified in figure 2 are given in table 1. In order to give each oxide equal weight in the modeling procedure, each column of the matrix was scaled to have the same mean and variance, according to a technique described previously (Miesch, 1980). Also, in order to treat the data for each sample as a vector of unit length, the scaled data for each sample were divided through by the square root of the sum of squares (that is, normalized). The scaled and normalized data were then regarded as the coordinates of 497 unit vectors with a common origin in eight-dimensional space.

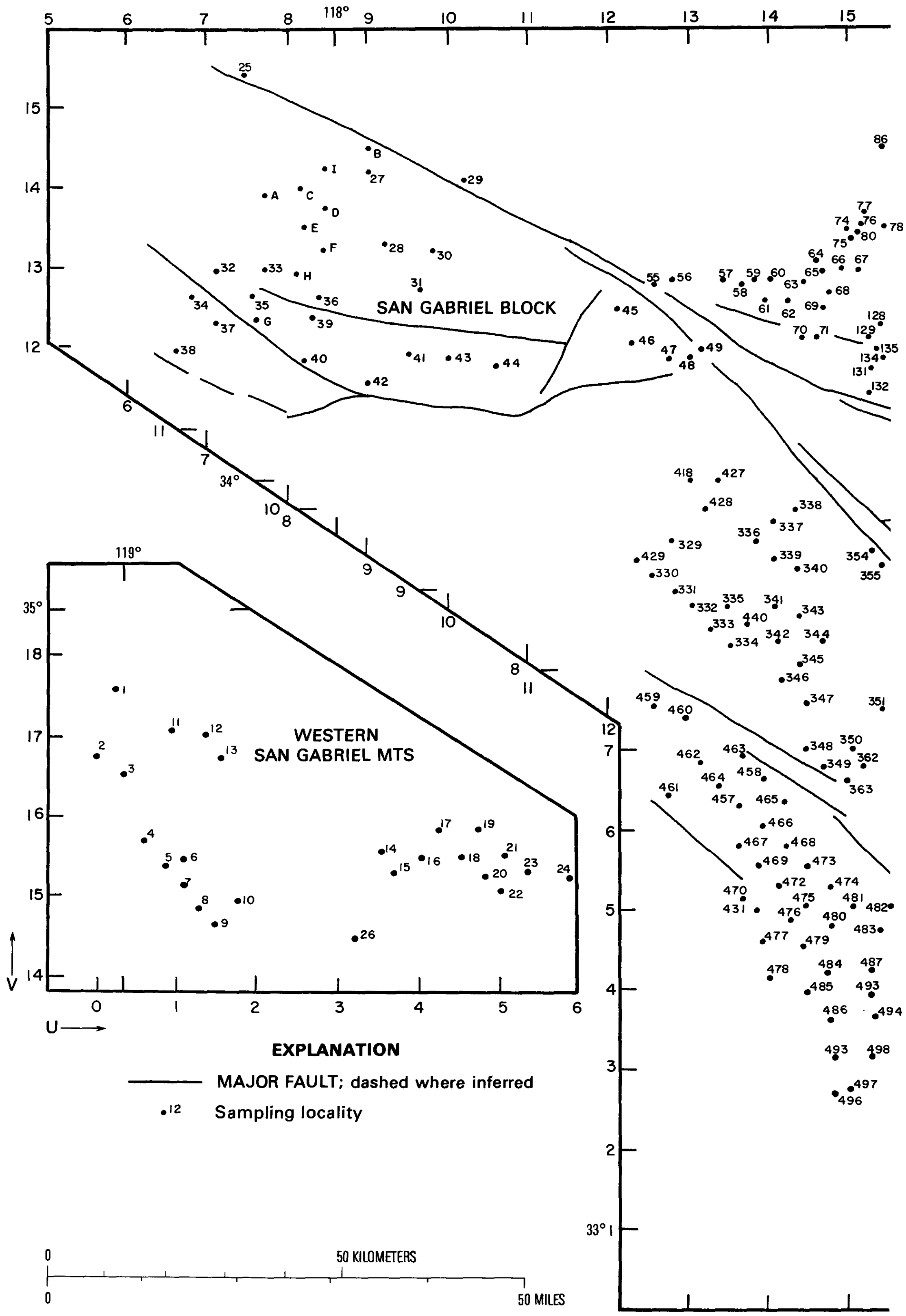

FIGURE 3.—Sampling localities in Mesozoic plutonic rocks of the nothern Peninsular and Transverse Ranges, Calif. Locality numbers are used in Baird and others (1979) for

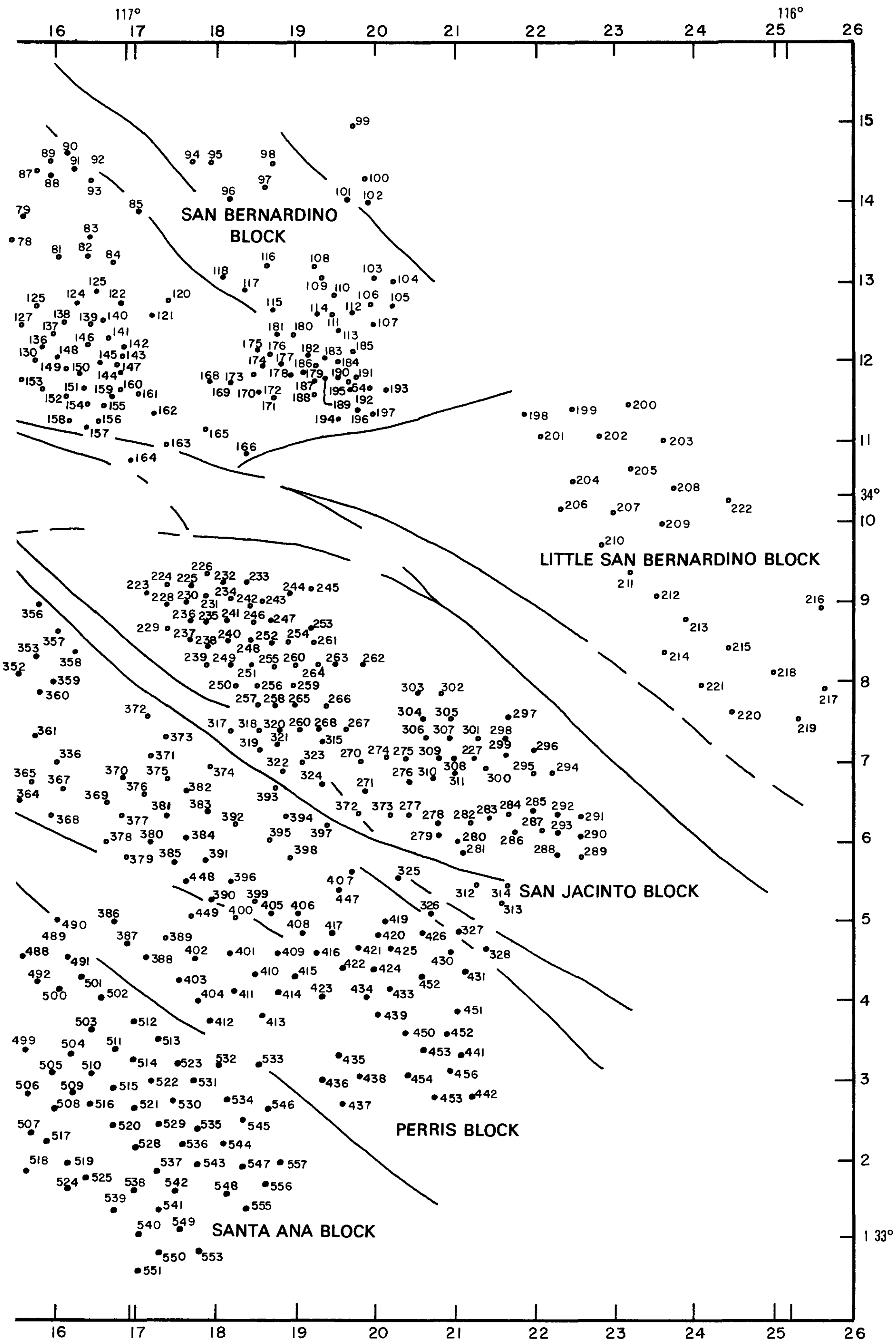

keyed to Appendixes 1 and 2 (prefix B has been deleted from locality numbers on map to save space). The U-V coordinate system was convenience in referring to sampling localities.

TABLE 1.—*Average compositions (in percent) of the batholithic rocks within structural blocks of southern California*

[All analyses were expressed as oxides and recomputed to 100 percent before computation of averages]

Structural block	Number of samples	Oxide							
		SiO_2	Al_2O_3	FeO	MgO	CaO	Na_2O	Ka_2O	TiO_2
San Gabriel block	47	67.10	16.41	3.81	1.58	3.47	3.90	3.15	0.57
San Bernardino block	125	70.22	15.45	2.22	0.88	2.86	3.76	4.06	0.55
Little San Bernardino block	25	69.90	15.65	2.56	1.16	2.59	3.87	3.88	0.40
San Jacinto block	101	67.54	16.41	3.56	1.45	3.89	3.65	2.76	0.73
Perris block	119	67.12	15.99	4.02	1.85	4.43	3.78	2.23	0.59
Santa Ana block	80	68.38	15.17	4.07	1.70	3.99	3.91	2.27	0.52
All batholithic rocks	497	68.32	15.83	3.39	1.44	3.67	3.79	2.97	0.58

Methods of principal-components analysis were then used to project the vectors into two dimensions, then three, and so forth up to seven dimensions (one less than the number of oxides). After each projection, the compositions represented by the projected vectors were determined and were compared with the compositions represented by the vectors in the original eight-dimensional space. The correlation coefficients between the original and recomputed data were determined and squared to give coefficients of determination for each oxide. These latter values are measures of the variances in the original data that can be explained by mixing models with two to seven end members, and are summarized in the factor-variance diagram in figure 4. This figure clearly shows that the original data can be closely approximated as a four-dimensional vector system, or as a four-factor, four-component, or four-end-member compositional series. Figure 4 shows that a model with only three end members would explain only about 71 percent of the variance in Al_2O_3 and that a five-end-member model offers no substantial improvement over a four-end-member model. The values of the coefficients of determination for four factors range from 0.85 to 0.97 (fig. 4), indicating that a four-end-member model can account for 85–97 percent of the variance in each oxide constituent. Thus, 3–15 percent of the variance in each constituent is ascribed to analytical imprecision and to other factors, such as minor petrologic processes that will not be represented in the model. Also, at least some part of this unaccounted for variance may be attributed to the fact that the four end-member compositions to be derived, in actuality, rather than being fixed, varied somewhat in both space and time. The absolute variances accounted for and not accounted for by four factors are listed in table 2.

COMPOSITIONAL STRUCTURE

The concept of compositional structure in igneous bodies and rock series was described in a previous report (Miesch and Reed, 1979) and refers to the nature of the relations among the oxide constituents as represented by a factor-variance diagram. These relations determine the number of end members that will be required in a petrogenetic mixing model. The compositional structure in the southern California batholithic rocks is closely similar to that of the Sierra Nevada batholith (Miesch and Reed, 1979, fig. 7). The fact that the variances in the eight oxides can be closely accounted for by the mixing and unmixing of four end members is not accidental. It has arisen from the fact that the southern California batholithic rocks originated mostly as a result of a simple combination of processes that involved only four dominant compositions, or perhaps four compositional extremes. That is, the batholithic rocks might have formed mainly by the separation of three independent mafic phases from a magma, by the separation of two phases from mixtures of two magmas, or by some other process that involved four, and only four, dominant end members. A likely possibility is that the batholithic rocks formed primarily by the separation of differentiates (mineral assemblages) that varied in composition between two end members from a magma that also varied within a two-end-member system. We shall assume that the magma varied in composition between an end member (which we label M–1) derived from near the present continental margin and another end member (labeled *M*–2) derived from farther to the northeast. Composition *M*–1 may represent a magma that has undergone relatively little or no contamination by continental materials, and *M*–2 may represent a magma that includes more continental material. We shall also assume that the differentiates varied between extremes which we shall label *D*–1 and *D*–2. The compositions of the differentiates, presumably, varied with the composition of the magma, temperature, and other local conditions.

Now the task is to estimate the compositions *M*–1, *M*–2, *D*–1, and *D*–2 in the most reasonable way and then to describe the compositions of all 497 samples in terms of these four components. The only mathematical requirement for each of the four compositions is that they be representable as vectors in the four-dimensional

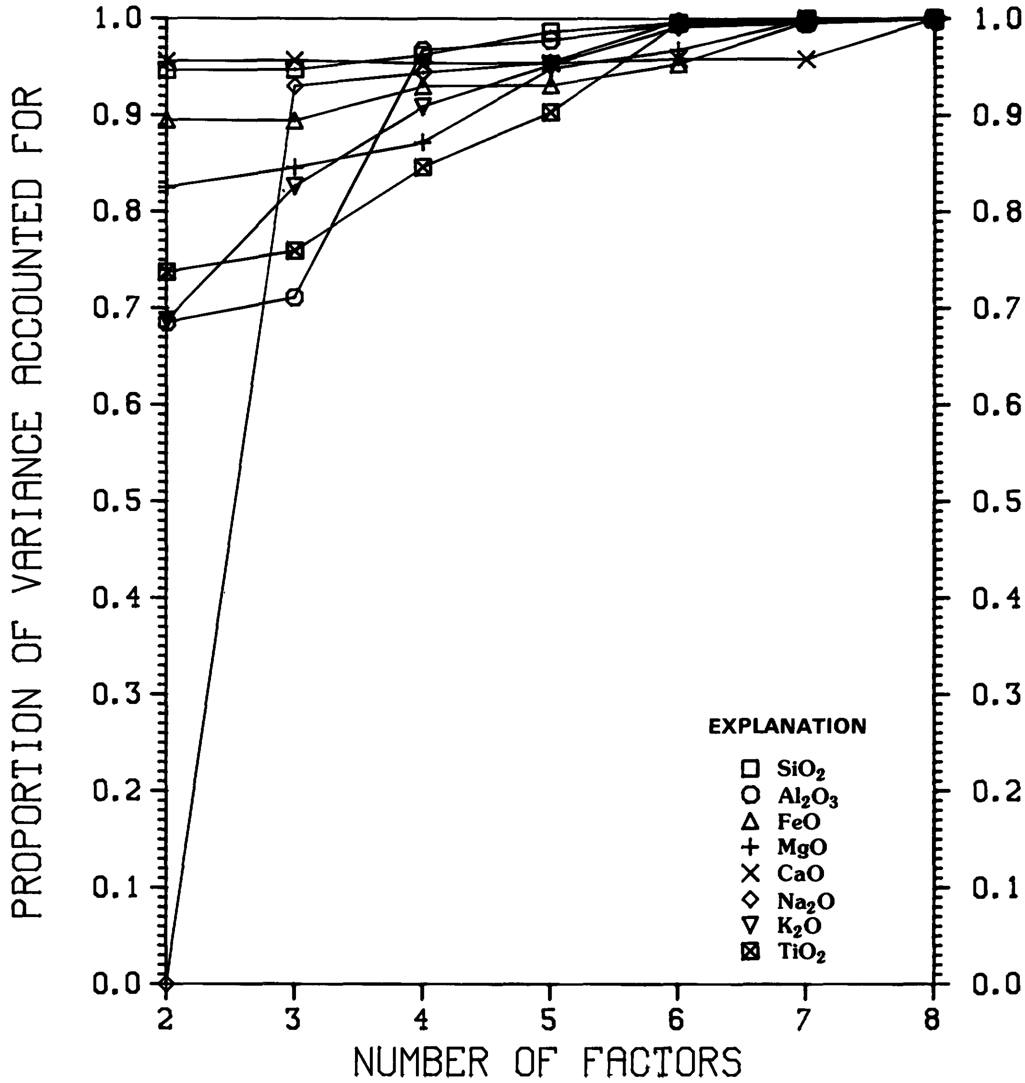

FIGURE 4.—Factor-variance diagram for the batholithic rocks of southern California.

TABLE 2.—*Chemical variances in the batholithic rocks of southern California that can and cannot be accounted for by a four-end-member mixing (factor) model*

Oxide	Variance		
	Accounted for	Not accounted for	Total
SiO_2	22.3617	0.8719	23.2336
Al_2O_3	1.9365	.0656	2.0018
FeO	2.7419	.2062	2.9481
MgO	.9547	.1404	1.0951
CaO	2.7561	.1334	2.8895
Na_2O	.1515	.0089	.1604
K_2O	1.1326	.1138	1.2464
TiO_2	.0493	.0089	.0582

space that contains the projected sample vectors. Any four compositions that can be represented in this manner can be mixed in varying proportions to approximate the original data to the degree indicated in figure 4 for a four-factor model and will lead to variances accounted for and not accounted for as listed in table 2.

The need to select *M*–1, *M*–2, *D*–1, and *D*–2 so that they can be represented as vectors in the four-dimensional space of the sample vectors is analogous to the need to describe the plagioclase compositions in terms of combinations of albite and anorthite.

DERIVATION OF THE DIFFERENTIATE END-MEMBERS *D*–1 AND *D*–2

The principal minerals in the quartz diorite, granodiorite, and quartz monzonite are quartz, potassium feldspar, plagioclase, hornblende, biotite, and iron oxides, chiefly magnetite and ilmenite. Presumably, the differentiates that were precipitated from the magmas consisted mainly of the least-soluble phases, plagioclase, hornblende, biotite, and the iron oxides. Consequently, the compositions of end members *D*–1 and *D*–2 were sought by testing mixtures of the compositions of these minerals. Plagioclase was represented by the ideal compositions of albite and anorthite, and ideal compositions were also used to represent magnetite and ilmenite. Biotite was represented by the average of eight analyses (table 3) from Larsen and Draisin (1950, p. 69). Hornblende was first represented by the average of eleven analyses given by Larsen and Draisin (1950, p. 71), then by the average analysis of the six hornblendes from nongabbroic rocks, and finally by the individual analyses. The best results were achieved using the single hornblende analysis given in table 3. A computer program similar to the EQSCAN program described previously (Miesch, 1976c) was used to form 53,130 systematic mixtures of the six selected compositions. The value 53,130 is the number of points at 5-percent increments within the six-dimensional space representing the six compositions. Each mixture was represented as a unit vector in the original eight-dimensional space of the 497 sample vectors, and then projected into the four-dimensional space containing the projected sample vectors. After each projection, the vector communality (square of vector length) was computed and taken as a direct measure of the nearness of the original unit vector to the four-dimensional subspace. The average communality of the 497 sample vectors in four-dimensional space is 0.9951. Of the vectors representing the 53,130 mathematical mixtures, only a few were represented by vectors with communalities this high. The two that led to the highest communalities were mixtures of (1) 33.9 percent anorthite, 63.3 percent hornblende, 0.9 percent magnetite, and 1.9 percent ilmenite (assemblage 1); and (2) 60.6 percent albite, 35.5 percent anorthite, 2.0 percent magnetite, and 1.9 percent ilmenite (assemblage 2). No biotite is included in either mixture. Thus, of all possible combinations of plagioclase, hornblende, biotite and the iron oxides, these two assemblages, and any combinations of them, come closest to satisfying the mathematical requirements for the differentiates, *D*–1 and *D*–2. The requirements of the model are perfectly satisfied, however, by the two vectors representing these compositions after projection into the four-dimensional space. The compositions represented by the projected vectors are given in table 4 (*D*–1 and *D*–2) along with the compositions rep-

TABLE 3.—*Biotite and hornblende compositions (in percent) used in determination of end-member compositions, D–1 and D–2*

Oxide	Biotite[1]	Hornblende[2]
SiO_2	37.96	47.57
Al_2O_3	17.70	8.64
FeO	21.20	17.46
MgO	9.52	11.22
CaO	0.39	11.82
Na_2O	0.22	1.18
K_2O	9.49	0.72
TiO_2	3.51	1.37

[1]Average of eight analyses from Larsen and Draisin (1950, p. 69).
[2]Analysis 7 from Larsen and Draisin (1950, p. 71).

TABLE 4.—*Compositions (in percent) of two mineral assemblages and end members D–1 and D–2*

Oxide	Mineral assemblage[1]		End member	
	Assemblage 1	Assemblage 2	*D*–1	*D*–2
SiO_2	44.75	57.00	44.68	56.31
Al_2O_3	17.89	24.81	18.49	25.12
FeO	12.87	2.87	13.01	3.55
MgO	7.10	0.00	8.01	0.44
CaO	14.31	7.16	12.81	5.91
Na_2O	0.75	7.16	0.72	7.39
K_2O	0.46	0.00	0.42	0.14
TiO_2	1.88	1.00	1.83	1.13

[1]Assemblage 1 contains the following percentage concentrations of minerals: anorthite, 33.89; hornblende (see table 3), 63.27; magnetite, 0.91; and ilmenite, 1.92. Assemblage 2 contains the following percentage concentrations of minerals: albite, 60.59; anorthite, 35.53; magnetite, 1.97; and ilmenite, 1.90.

resented by the vectors before projection (assemblage 1 and assemblage 2). The bulk compositions of all materials precipitated from the magmas in the formation of the observed samples, therefore, are assumed to have ranged between composition *D*–1 and composition *D*–2. Materials rich in *D*–1 and sparse in *D*–2 contained a more calcic plagioclase and were more mafic. Those rich in *D*–2, on the other hand, contained a more sodic plagioclase and were more felsic.

DERIVATION OF THE MAGMA END-MEMBERS *M*–1 AND *M*–2

The remaining problem is to estimate the compositions of the extremes, *M*–1 and *M*–2, in the range of magmas from which the batholithic rocks were derived. Like compositions *D*–1 and *D*–2, compositions *M*–1 and *M*–2 must also be representable as vectors in the four-dimensional space of the 497 sample vectors. But, an additional requirement in the selection of compositions *M*–1 and *M*–2 pertains to the mixing proportions that will be required for the 497 samples. Acceptable mixing proportions will necessarily be positive for magma compositions *M*–1 and *M*–2 and must be generally negative for differentiate compositions *D*–1 and *D*–2, inasmuch as the differentiates should be separated from the magmas, not added to them, in the formation of most of the batholithic rocks. If compositions *M*–1 and *M*–2 are selected arbitrarily, for example, many samples may require negative proportions of *M*–1 and (or) *M*–2. Also, some samples may require opposite signs in the mixing proportions for *D*–1 and *D*–2, suggesting that the differentiates separated from the magmas had bulk compositions outside the range for *D*–1 and *D*–2 (table 4); possibly the required bulk composition of the differentiate may be partly negative. In addition, the mixing proportions must not be large in absolute value. The sum of the mixing proportions for *M*–1, *M*–2, *D*–1 and *D*–2 will always equal unity, so if the sum of those for *M*–1 and *M*–2 equals 20, for example, the sum of those for *D*–1 and *D*–2 must equal *minus* 19. Mixing proportions such as these would indicate that the specific sample resulted from a differentiation process that went 95 percent of the way towards completion—possible for some individual samples, but not likely for any large mass of batholithic rocks.

The two structural units within the region that are the most widely separated in a direction perpendicular to the continental margin are the Santa Ana and San Bernardino blocks (fig. 2). The chemical data for samples from these two blocks were extracted from the main data matrix (Appendix 1) and were examined by independent factor analyses of the same type used to examine the entire data set. Factor-variance diagrams for the two subsets of the data are given in figures 5 and 6. Both diagrams indicate that the chemical data from the corresponding structural blocks can be well represented in three-dimensional vector systems. Stereograms showing the configurations of the vector systems are given in figures 7 and 8; the compositions represented by selected vectors on the stereograms are given in tables 5 and 6. Tables 5 and 6 may be used to observe the nature of compositional changes in various directions across the stereograms. Note that both configurations of sample vectors (figures 7 and 8) are approximately triangular and that those points near the lower left corners represent compositions relatively low in SiO_2 and high in FeO and MgO, whereas those points to the right represent more siliceous compositions. The compositions of the parent magmas for each of these groups of samples seem to be at or near the point "N" on the corresponding stereogram; the compositions represented by these points are given in tables 5 and 6. These compositions were represented as vectors in the four-dimensional space of the 497 sample vectors. They were then taken tentatively as the *M*–1 and *M*–2 vectors being sought and as representing two of the end members for the model. Vectors *D*–1 and *D*–2, previously deduced as representative of the range of precipitates separated from the magmas to form the batholithic rocks, were taken to represent the other two end members. We found, however, that the compositions of many samples could be approximated in the mixing computations only by using negative proportions of composition *M*–1. Consequently, alternative compositions for *M*–1 and *M*–2 were sought by trying vectors in the same plane as those representing *M*–1 and *M*–2, but separated by a wider angle. This procedure led to the identification of the compositions *M*–1 and *M*–2 listed in table 7. The four end-member compositions given in table 7 can be mixed in various proportions (Appendix 2) to approximate the compositions (to the degrees indicated for four factors in fig. 4 and table 2) of all 497 samples (Appendix 1). With the exception of one sample, all the proportions for end members *M*–1 and *M*–2 are positive and in the range from:

	Minimum		*Maximum*
M–1	0.0	to	2.5641
M–2	0.0	to	1.8051

With the exception of 16 samples, the mixing proportions for *D*–1 and *D*–2 are of the same sign and in the range from:

	Minimum		*Maximum*
D–1	–1.4776	to	0.1996
D–2	–1.0498	to	0.1304

Only a few of the samples required positive mixing proportions for *D*–1 and *D*–2, indicating that compositions *D*–1 and *D*–2 must be subtracted from compositions *M*–1 and *M*–2 in order to approximate the compo-

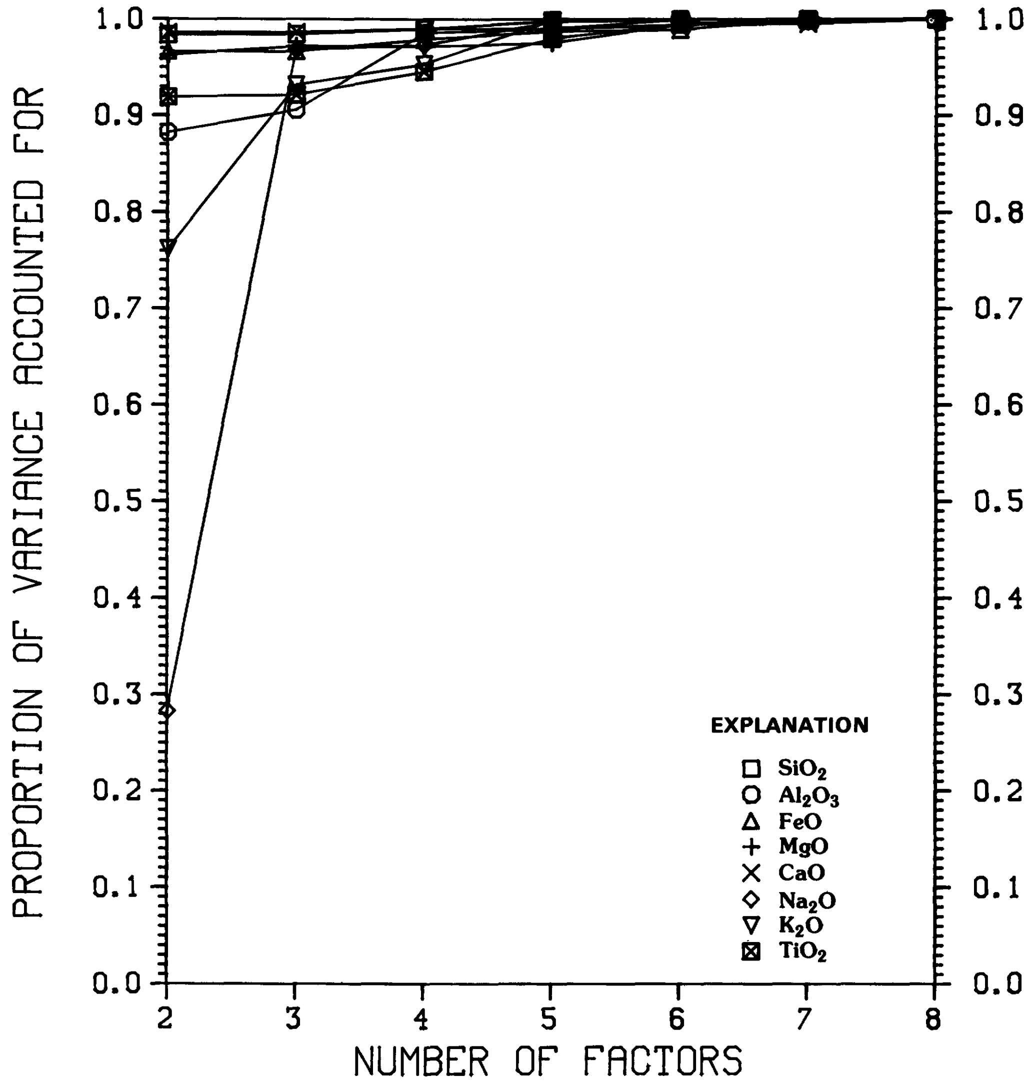

FIGURE 5.—Factor-variance diagram for the batholithic rocks of the Santa Ana block of southern California.

sitions of most samples. The compositions of the 16 samples that require mixing proportions of opposite sign for *D*–1 and *D*–2 can be produced from compositions *M*–1 and *M*–2 only by adding or subtracting compositions that include negative values for one or more oxides. Therefore, these 16 samples and one (B429)[2] that requires a negative amount of *M*–1 are not accounted for by the model proposed here. Of the 17 anomalous samples, 11 are from the San Jacinto block (B226, B229, B283, B286, B301, B302, B303, B304, B306, B308, and B321), 4 from the Perris block (B338, B392, B420, and B429), and 1 each from the San Bernardino (B99) and Santa Ana blocks (B513). The anomalous samples are discussed in a later section of this report.

[2] See figure 3 for sampling localities and Appendix 1 for the analyses.

CHARACTERISTICS OF THE MODEL

PETROLOGY OF THE MAGMA END-MEMBERS *M*–1 AND *M*–2

The normative mineralogy of *M*–1 (table 7) is that of a saturated basaltic or gabbroic rock. The 26 gabbro compositions (heretofore not considered in the modeling) were each tested for compatibility with the more silicic rocks of the Santa Ana block by computation of vector communalities. The two gabbros most compatible (highest communalities) are B545 and B511 (table 8). The compositions of these two samples need only be slightly modified to be perfectly representable as vectors (*G*–1 and *G*–2) in the three-dimensional vector space formed by the Santa Ana block sample compositions (fig. 7). The compositions represented by vectors

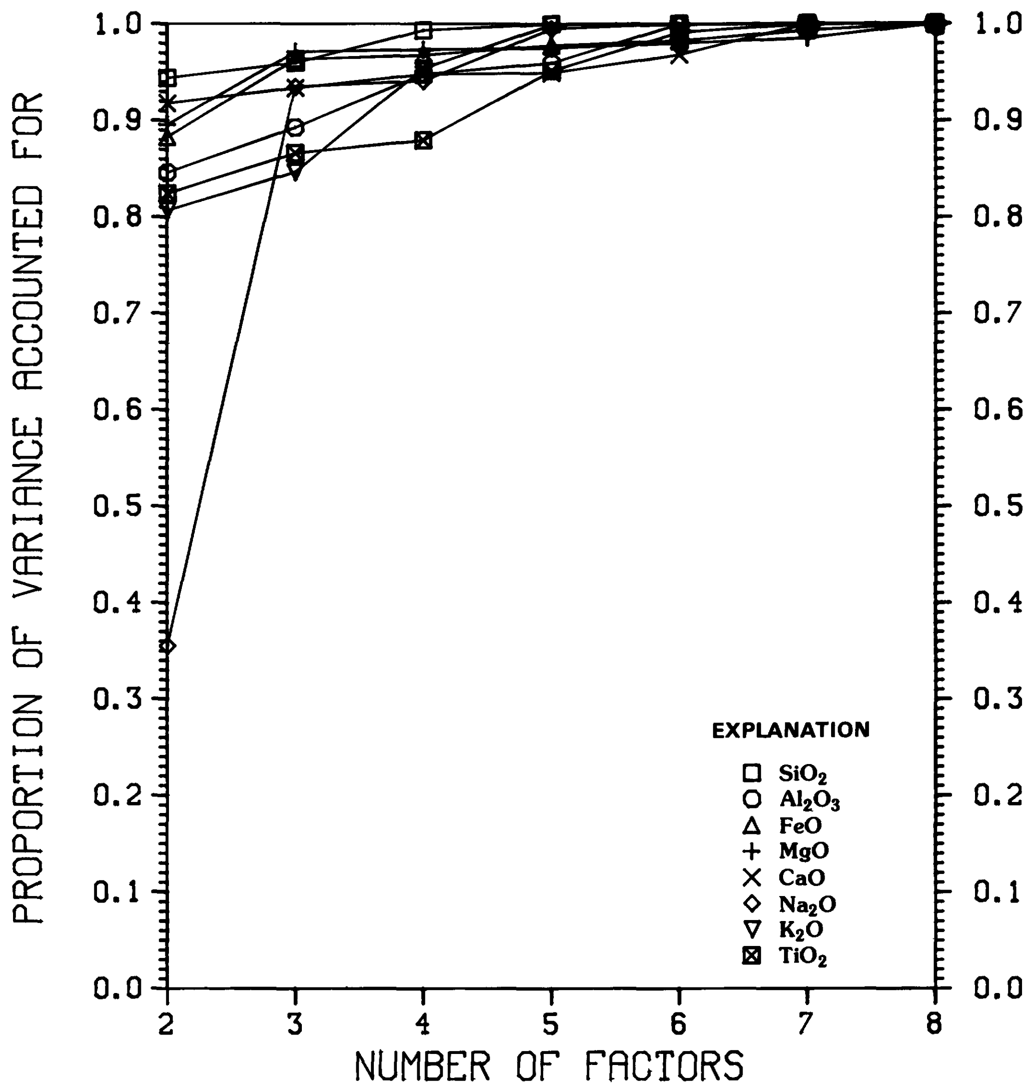

FIGURE 6.—Factor-variance diagram for the batholithic rocks of the San Bernardino block of southern California.

G–1 and G–2 are given in table 8. The compositions are notably close to that of end member M–1 (table 7). Nockolds and Allen (1953) used variation diagrams to deduce the compositions of parental magmas for calc-alkaline rocks. Their average values, compared with M–1 (table 7), are only slightly higher in MgO and K_2O, and slightly lower in FeO and CaO.

Because both compositions M–1 and M–2 (table 7) were derived by mathematical procedures, we were interested in determining how closely they correspond to actual rock compositions. Although composition M–1 is close to the compositions of some gabbros from the region, as pointed out in the preceding paragraph, none of the batholithic rocks have compositions close to composition M–2. Consequently, a search was made of the RASS computer-based file (Van Trump and Miesch, 1977) which contains about 130,000 rock analyses by laboratories of the U.S. Geological Survey since 1967. The analyses are of samples collected throughout the United States. The igneous rock analyses in the RASS file closest to compositions M–1 and M–2 are given in table 9. The measure of closeness used was *cosine theta* of Imbrie and Purdy (1962). The closest match to M–1 is a gabbro of Jurassic age from the Alaska-Aleutian Range batholith (Reed and Lanphere, 1973). The closest matches to M–2 are an andesite from southwest Nevada and tuffaceous rocks from southwest Colorado and northern Washington, all of Tertiary age. The average norm for these matches to M–2 includes 16 percent quartz, 23 percent orthoclase, and 53 percent sodic andesine, consistent with a leucocratic granodiorite. Composition M–2 is incompatible with any magma or source material of an oceanic nature.

One possible origin for end-member M–2 is by mixing

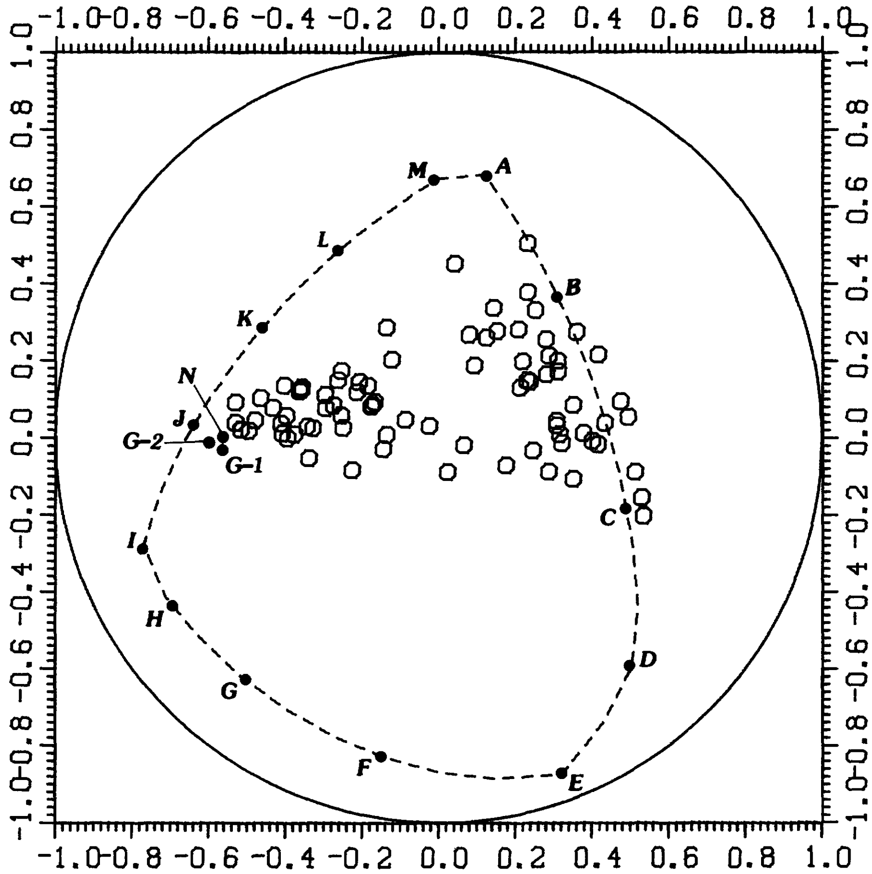

FIGURE 7.—Sterogram showing the three-dimensional vector system for the batholithic rocks of the Santa Ana block of southern California. Open circles represent 80 sample vectors. Dashed line outlines area wherein all vectors represent compositions that are entirely nonnegative. All vector projections have been from an upper hemisphere vertically onto the plane of the stereogram. See table 5 for compositions represented by vectors *A* through *N*.

TABLE 5.—*Compositions represented by some points on figure 7*

Oxide	*A*	*B*	*C*	*D*	*E*	*F*	*G*	*H*	*I*	*J*	*K*	*L*	*M*	*N*
SiO_2	71.46	74.67	77.79	80.45	81.20	65.97	51.52	37.21	32.12	48.31	56.70	62.04	68.47	54.30
Al_2O_3	15.75	14.03	12.35	10.82	9.16	13.29	17.23	21.15	22.91	20.07	18.59	17.65	16.52	18.60
FeO	3.29	2.27	1.29	0.44	.011	4.62	8.90	13.13	14.67	9.99	7.57	6.03	4.17	8.23
MgO	0.00	0.00	0.00	0.09	1.04	4.10	6.98	9.83	10.56	6.14	3.85	2.39	0.63	4.81
CaO	2.63	1.69	0.77	0.00	0.05	5.38	10.43	15.44	17.14	11.15	8.04	6.07	3.69	9.02
Na_2O	6.08	4.78	3.52	2.29	0.05	0.00	0.00	0.00	0.59	3.01	4.25	5.05	6.01	3.27
K_2O	0.40	2.29	4.14	5.88	8.39	6.01	3.72	1.43	0.00	0.00	0.00	0.00	0.00	0.67
TiO_2	0.39	0.26	0.14	0.03	0.00	0.62	1.21	1.79	2.00	1.34	0.99	0.78	0.51	1.09

of the gabbroic magma represented by *M*–1 with a partial melt from the continental crust. For example, composition *M*–2 of table 7 could have been produced by mixing 11.76 percent magma of composition *M*–1 with 88.24 percent melt with a composition as follows:

SiO_2	Al_2O_3	FeO	MgO	CaO	Na_2O	K_2O	TiO_2
68.02	18.70	1.29	0.00	2.76	4.78	3.79	0.67

The equivalent normative composition is:

Q	C	Or	Ab	An	Fs	Il
19.2	1.7	22.4	40.4	13.7	1.7	1.3

MIXING PROPORTIONS

A statistical summary of the mixing proportions for the four end members, as required for the 480 samples accounted for by the model, is given in table 10. Some parameters derived from these values are summarized in table 11. The first of these parameters is the sum

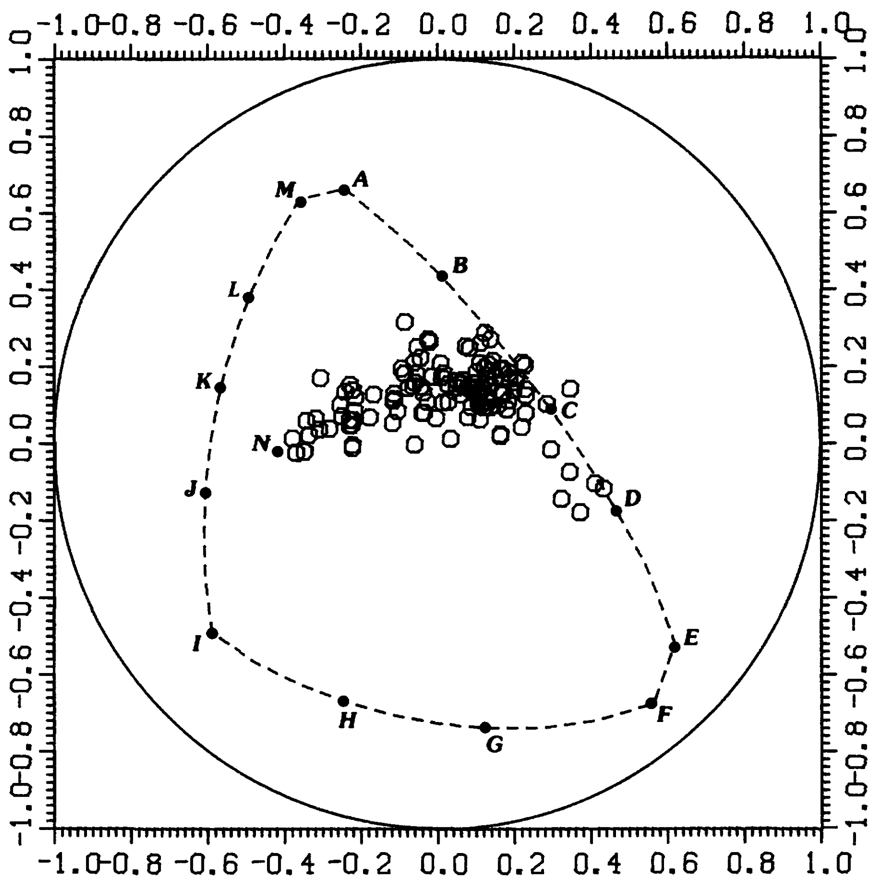

FIGURE 8.—Stereogram showing the three-dimensional vector system for the batholithic rocks of the San Bernardino block of southern California. Open circles represent 125 sample vectors. Dashed line outlines area wherein all vectors represent compositions that are entirely nonnegative. All vector projections have been from an upper hemisphere vertically onto the plane of the stereogram. See table 6 for compositions represented by vectors *A* through *N*.

TABLE 6.—*Compositions represented by some points on figure 8*

Oxide	*A*	*B*	*C*	*D*	*E*	*F*	*G*	*H*	*I*	*J*	*K*	*L*	*M*	*N*
SiO_2	68.12	72.37	75.29	77.16	80.54	80.06	66.25	49.93	9.94	33.21	46.51	55.78	62.86	56.67
Al_2O_3	20.09	16.50	14.04	12.44	9.53	8.04	10.68	13.82	21.77	21.85	21.93	21.96	22.02	18.33
FeO	0.02	0.28	0.46	0.59	0.84	2.18	7.83	14.49	30.64	17.85	10.52	5.43	1.51	7.55
MgO	0.00	0.00	0.00	0.00	0.00	0.60	3.38	6.65	14.60	8.53	5.05	2.64	0.78	3.52
CaO	3.51	2.31	1.49	0.96	0.01	0.11	3.85	8.27	19.10	12.88	9.32	6.84	4.95	6.54
Na_2O	6.63	4.75	3.46	2.62	1.08	0.00	0.00	0.00	0.23	3.30	5.08	6.30	7.26	3.96
K_2O	1.20	3.41	4.94	5.92	7.72	8.64	6.97	5.01	0.00	0.00	0.00	0.00	0.00	2.25
TiO_2	0.42	0.36	0.33	0.30	0.26	0.37	1.03	1.82	3.72	2.36	1.58	1.04	0.62	1.18

of the mixing proportions for end members *M*–1 and *M*–2, which gives the amount of magma from which each unit amount of sample was derived. The mean value of this parameter for all 480 samples is 1.8744, indicating that, according to the model, the average sample was formed by removal of 0.8744 parts of the differentiates (*D*–1 and *D*–2) from 1.8744 parts of magma (*M*–1 plus *M*–2); this corresponds to differentiation of about 47 percent. Inspection of the mean values for batholithic rocks from the individual structural blocks (table 11) shows that those for the San Jacinto block call for the least amount of differentiation and that, in general, the amount of differentiation required tends to increase from the northeast to the southwest. This regional variability is also apparent from the map of individual sample values for this parameter in figure 9. (Note: The class intervals in figures 9–12 are defined by the 20th, 40th, 60th, and 80th percentiles of the mapped variable.)

The second parameter derived from the mixing pro-

TABLE 7.—*Chemical and normative compositions of the end members for the mixing model*

	End member			
	M–1	*M*–2	*D*–2	*D*–2
Chemical composition (in percent)				
SiO_2	54.41	66.42	44.68	56.31
Al_2O_3	18.37	18.66	18.49	25.12
FeO	8.86	2.18	13.01	3.55
MgO	4.76	0.56	8.01	0.44
CaO	8.89	3.48	12.81	5.91
Na_2O	3.18	4.59	0.73	7.39
K_2O	0.30	3.38	0.42	0.14
TiO_2	1.24	0.74	1.83	1.13
Normative composition (in percent)				
Q	4.2	17.3	0.0	0.0
C	0.0	1.1	0.0	2.1
Or	1.7	20.0	2.5	0.8
Ab	26.9	38.8	6.2	59.8
An	35.0	17.2	45.9	29.3
Ne	0.0	0.0	0.0	1.5
Wo	3.8	0.0	7.4	0.0
En	11.9	1.4	8.3	0.0
Fs	14.2	2.8	8.7	0.0
Fo	0.0	0.0	8.2	0.8
Fa	0.0	0.0	9.4	3.6
Il	2.4	1.4	3.5	2.1

TABLE 8.—*Compositions (in percent) of two samples of gabbros and the compositions represented by vectors G–1 and G–2 on figure 7*

	Sample		Vector	
Oxide	B545	B511	*G*–1	*G*–2
SiO_2	53.96	53.02	53.89	52.65
Al_2O_3	18.01	19.25	18.64	19.02
FeO	8.86	8.71	8.35	8.72
MgO	5.04	4.73	4.96	5.16
CaO	9.14	9.66	9.18	9.60
Na_2O	3.17	3.19	3.15	3.23
K_2O	0.71	0.44	0.74	0.46
TiO_2	1.13	1.00	1.11	1.16

portions is the percentage of end member *M*–2 in the total magma (*M*–1 plus *M*–2) required for each sample. The mean values (table 11) and the map of individual values (fig. 10) show that this parameter increases from the southwest to the northeast, suggesting that the more silicic and potassic extreme, *M*–2, was only a minor component in the magmas that formed the rocks of the Santa Ana and Perris blocks, but a major component in the magmas farther to the northeast. A major discontinuity in the map pattern on figure 10 occurs near the San Jacinto fault, in the eastern part of the Perris block. This discontinuity is discussed further in the next section of this report.

The third parameter is the percentage of end member *D*–2 in the total of the differentiates (*D*–1 plus *D*–2) that separated from the magmas to yield the liquids that later crystallized to form each sample. The mean values (table 11) and the map of individual values (fig. 11) show that this parameter is somewhat higher for the easternmost blocks of batholithic rocks, indicating that, according to the model, the precipitates in the eastern part of the region included a more sodic plagioclase and less hornblende than those farther west in the Santa Ana and Perris blocks. The discontinuity in the pattern of figure 10 is also present in figure 11, but is somewhat less distinct.

REGIONAL VARIATION IN THE COMPOSITIONS OF THE MAGMAS AND DIFFERENTIATES

The compositions of the magmas and, presumably, the source materials required for each of the 480 samples, according to the model, can be determined by

TABLE 9.—*Analyses from the U. S. Geological Survey RASS data file that compare closely with end-member compositions M–1 and* M–2

[Analyses of end members *M*–1 and *M*–2 are from table 7. See NOTE for description of samples (from RASS data file) for analyses 1–7. All analyses were recomputed to sum to 100 percent]

	M–1	1	*M*–2	2	3	4	5	6	7
SiO_2	54.41	54.01	66.42	66.05	65.90	65.56	65.49	66.58	66.39
Al_2O_3	18.37	19.06	18.66	18.78	18.22	18.19	18.43	18.67	18.75
FeO	8.86	8.39	2.18	3.17	3.27	3.21	3.18	2.33	2.53
MgO	4.76	4.92	.56	.38	.61	.74	.76	.42	.76
CaO	8.89	8.61	3.48	3.44	2.97	3.35	3.50	3.39	3.79
Na_2O	3.18	3.48	4.59	3.86	4.30	4.27	4.12	3.59	5.22
K_2O	.30	.52	3.38	3.76	4.20	4.17	4.02	4.62	2.15
TiO_2	1.24	1.00	.74	.56	.53	.50	.49	.40	.41

NOTE.—Description of samples for analyses 1–7:
Analysis 1. Gabbro of Jurassic age from southern Alaska, collected by B. L. Reed, 1970.
Analysis 2. Andesite of Eocene age from southwest Nevada, collected by D. F. Crowder, 1969.
Analysis 3. Quartz-latite welded tuff of Oligocene age from the San Juan Mts., Colo., collected by R. G. Luedke, 1969.
Analysis 4. Welded tuff of Oligocene age from the Sand Juan Mts., Colo., collected by R. G. Luedke, 1970.
Analysis 5. Crystal-rich welded tuff of Oligocene age from the Sand Juan Mts., Colo., collected by R. G. Luedke, 1970.
Analysis 6. Quartz-latite welded tuff of Oligocene age from the San Juan Mts., Colo., collected by P. W. Lipman, 1974.
Analysis 7. Volcanic tuff of Eocene age from northern Washington, collected by R. C. Pearson, 1973.

TABLE 10.—*Statistical summary of mixing proportions required for the batholithic rocks within structural blocks of southern California*

Structural block	Number of samples	End member							
		M–1	*M*–2	*D*–1	*D*–2	*M*–1	*M*–2	*D*–1	*D*–2
		Mean				Standard deviation			
San Gabriel block	47	0.8805	0.8571	–0.3889	–0.3488	0.2284	0.2924	0.1809	0.1875
San Bernardino block	124	0.6422	1.1517	–0.3376	–0.4563	0.1828	0.2756	0.1321	0.1760
Little San Bernardino block	25	0.8778	1.0627	–0.4678	–0.4727	0.2997	0.2691	0.1846	0.1528
San Jacinto block	90	0.7294	0.8825	–0.2816	–0.3303	0.2681	0.2459	0.1958	0.1872
Perris block	115	1.2651	0.6742	–0.5421	–0.3973	0.3547	0.2669	0.2711	0.2105
Santa Ana block	79	1.6256	0.6400	–0.7744	–0.4912	0.3828	0.3055	0.3581	0.2422
All batholithic rocks	480	1.0053	0.8691	–0.4598	–0.4146	0.4645	0.3394	0.2883	0.2062

TABLE 11.—*Mean values of parameters computed from the mixing proportions summarized in table 10*

Structural block	Relative amount of crust from which batholithic rocks were derived	Percentage of *M*–2 in crustal material (*M*–1 plus *M*–2) from which the batholithic rocks were derived	Percentage of *D*–2 in materials (*D*–1 plus *D*–2) separated from the crust to form the batholithic rocks
San Gabriel block	1.7377	48.68	47.26
San Bernardino block	1.7938	63.74	57.12
Little San Bernardino block	1.9405	55.04	51.04
San Jacinto block	1.6119	55.08	56.19
Perris block	1.9394	34.71	41.75
Santa Ana block	2.2656	27.12	38.04
All batholithic rocks	1.8744	47.21	48.84

mathematical mixing of end members *M*–1 and *M*–2 (table 7) according to the mixing proportions derived for each sample (Appendix 2), followed by adjustment of each mixture so that the sum of the oxide values is 100 percent. The average compositions of the magmas required for each structural block, and for the batholithic rocks as a whole, are given in table 12. Note that the magma composition required for the batholithic rocks of the Little San Benardino and San Jacinto blocks, on opposite sides of the San Andreas fault zone,

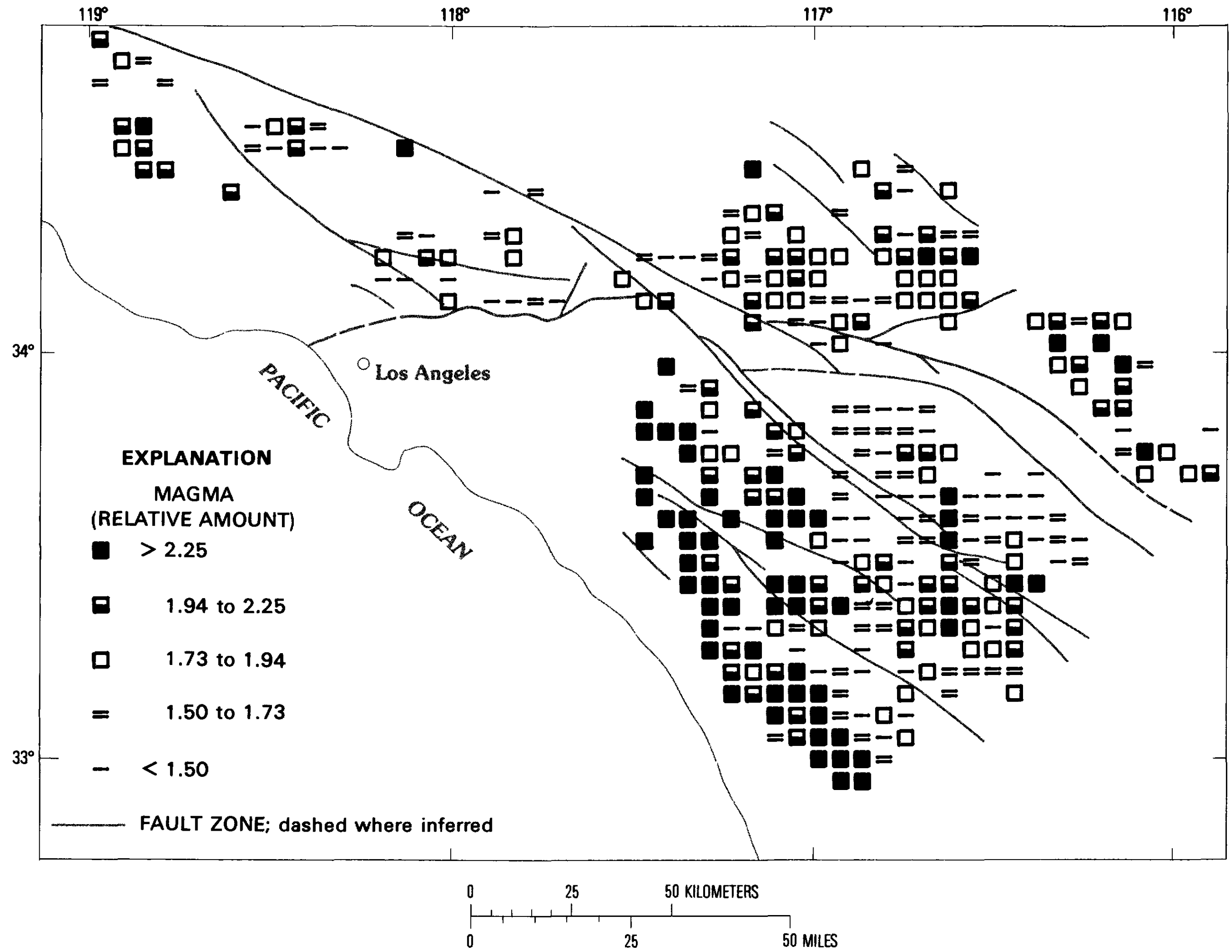

FIGURE 9.—Relative amounts of magma required for the formation of the batholithic rocks.

are almost identical even though the average compositions of the samples from these two blocks are somewhat different (table 1). Average compositions of the differentiates that were separated from the magmas to form the batholithic rocks are given in table 13; these averages were obtained from compositions *D*–1 and *D*–2 in table 7 and the mixing proportions for these end members in Appendix 2.

Maps of chemical variation in the batholithic rocks of southern California, as determined from the original data (Appendix 1) on the 480 samples accounted for by the model, are given in figure 12. This figure also shows the areal compositional variations in the magmas and in the differentiates according to the model. As described previously, the original chemical data show continuous patterns of areal change from the southwest toward the continental interior. In marked contrast, most maps of model-derived parameters (figs. 9–11) and compositions of magmas and differentiates (fig. 12) show pronounced discontinuities near the boundary between the Perris and San Jacinto blocks, within the Peninsular Ranges Province. The exact locations of these discontinuities differ slightly from map to map. Nevertheless, we regard the discontinuity as a single feature, although of uncertain exact location. No other feature is as prominent in these map patterns as is this discontinuity. Certainly, the San Andreas fault, both east of the Peninsular Ranges and through the Transverse Ranges, does not correlate with any map pattern as significant as the discontinuity near the San Jacinto fault trace. In fact, if these maps, derived from the model, were used to establish petrologic provinces, two such provinces would emerge: one composed of the San Gabriel, San Jacinto, San Bernardino, and Little San Bernardino blocks and another composed of the Perris and Santa Ana blocks.

ANOMALOUS SAMPLES

The distribution of sampling localities whose chemical compositions are not accounted for by the model proposed here is far from random; 11 of 17 are in the San

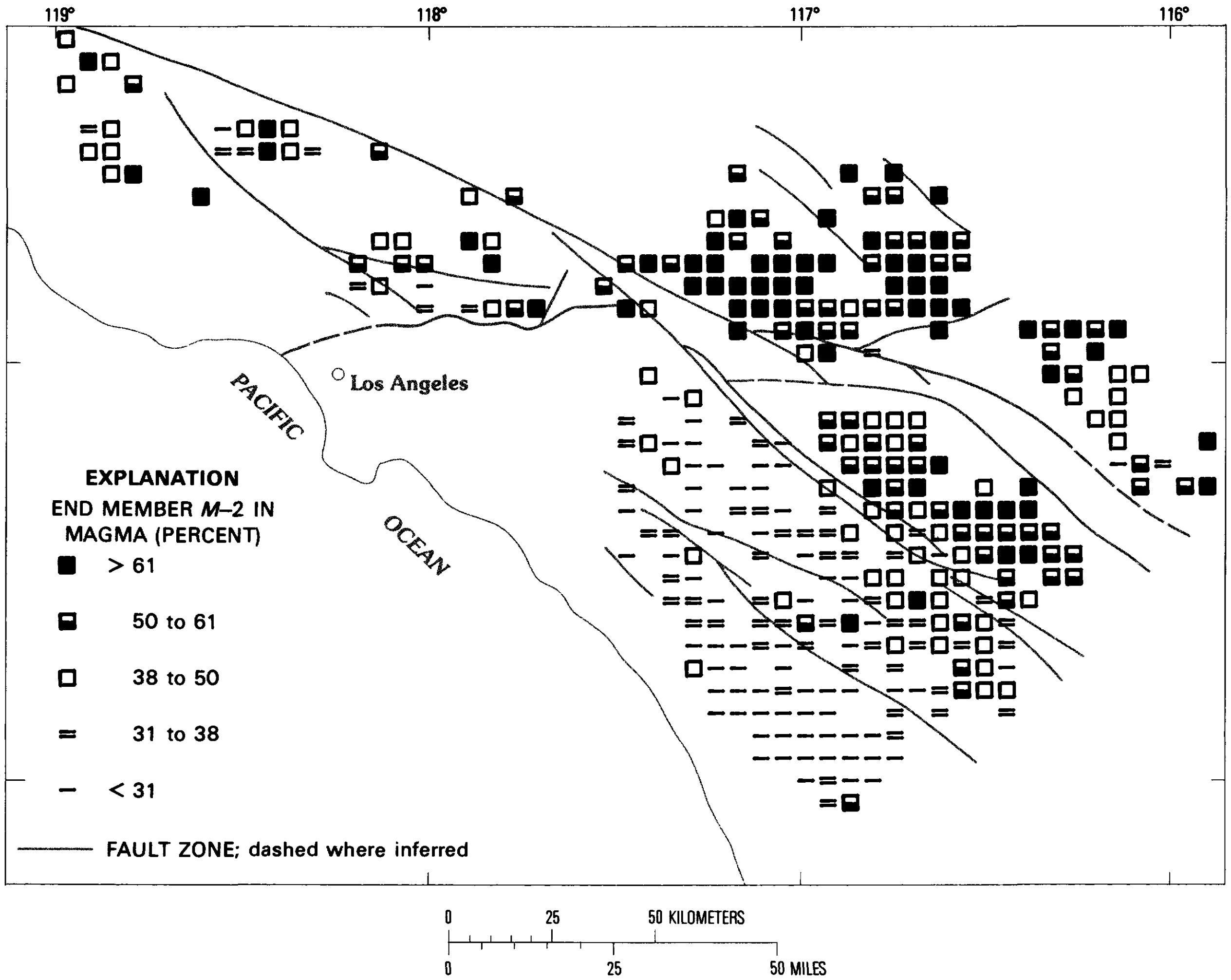

FIGURE 10.—Percentages of end-member *M*-2 in the magmas.

Jacinto block. Further, 8 of the 11 localities are tightly clustered (fig. 3) in the easternmost part of the block. On the basis of strontium and oxygen isotopes, Taylor and Silver (1978, p. 425) interpreted the batholithic rocks of the San Jacinto block to be anomalous and "derived from a distinctive source rock at depth." Further, high values of $\delta^{18}O$, exceeding +10 in the easternmost San Jacinto block, show an anomalous circular low that coincides with the cluster of eight sampling localities that are anomalous with respect to our model (fig. 3). With two exceptions in the Perris block, all other anomalous localities are at or near the exposed margins of the batholithic rocks, or in the zones of faulting that mark the boundaries between blocks.

RELATIONS TO OTHER GEOLOGIC FEATURES

The discontinuity in the areal distributions of the model parameters and compositions derived from the model correlate well with a number of field relations, age relations, and petrologic and structural features of the batholithic and pre-batholithic rocks. However, except that the most pronounced breaks in the map patterns occur near the San Jacinto fault, there is a poor correlation with the pattern of major faults and especially no correlation with the San Andreas fault zone. This lack of correlation is surprising in view of the huge displacements widely accepted (for example, Crowell, 1979) for the San Andreas fault in southern California.

Regional asymmetries that appear to correlate with the discontinuity in the model parameters have been described by many investigators working over a larger area than that considered here. In each of the asymmetries, regional gradients are interrupted by sharp changes in the eastern Peninsular Ranges, near the trace of the San Jacinto fault:

1. *Pre-batholithic rock types.*—Metavolcanic rocks in the west are succeeded eastward by metasedimentary rocks (Gastil and others, 1978) over much of the length of the Peninsular Ranges. A belt of carbonate (shelf?) rocks has been recognized in the Transverse Ranges (Woodford, 1960). The overall west-to-east sequence

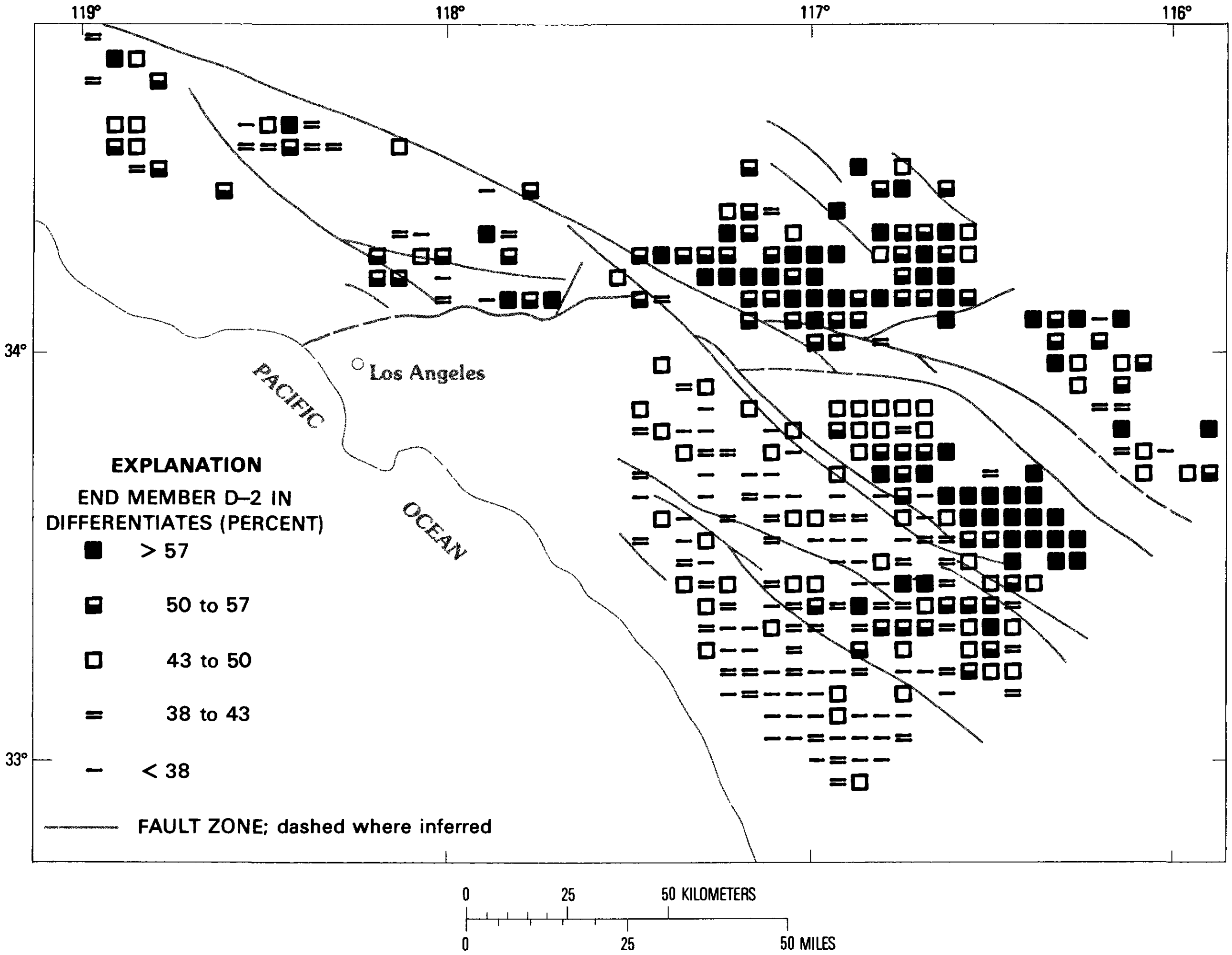

FIGURE 11.—Percentages of end-member *D*-2 in the differentiates.

seems to be blueschist-metavolcanic-metasedimentary (clastic)-metasedimentary(carbonate). Batholithic rocks are emplaced in all types, except in blueschist. The most mafic parts of the batholithic rocks are associated with the metavolcanics, and the most felsic with metasedimentary rocks; this change is at or close to the boundary of the Perris and San Jacinto blocks.

2. *Wallrock metamorphism.*—Metamorphic grade increases eastward, with an abrupt increase in grade to higher amphibolite facies across a line in the central to eastern Perris block (Schwarcz, 1969).

3. *Plutonic rock types.*—Gabbroic rocks are restricted to the Santa Ana block and the western part of the Perris block (Baird and others, 1979) and similar relations are noted farther south (Gastil and others, 1975; Todd and Shaw, 1979). Granodiorite dominates in the San Jacinto block and quartz diorite in the Perris block (Baird and others, 1979, fig. 4). This change may mark the "quartz diorite boundary" of Moore (1959) in this region and is coincident with the discontinuities apparent in figure 10 and in the maps in figure 12 that represent the magmas and, presumably, their source materials.

4. *Plutonic rock mineralogy.*—Rocks east of a generally north-south line through the Perris block tend to be distinctly richer in potassic feldspar, commonly present as large phenocrysts, and richer in sphene (D. M. Morton, oral commun., 1981; Gastil and others, 1975).

5. *Plutonic rock structure and form.*—Plutons of the western Peninsular Ranges tend to be small, contain internal structures that suggest flow and (or) deformation, and have contact relations that suggest syntectonic emplacement (D. M. Morton, oral commun., 1980; Todd and Shaw, 1979). The eastern Peninsular Ranges and eastern Transverse Ranges are dominated by larger plutons that have irregular outlines and massive interiors; they are characteristically post-tectonic (Todd and Shaw, 1979).

6. *Radiometric ages.*—The extensive uranium-lead zircon dating program conducted by Silver and col-

TABLE 12.—*Average compositions (in percent) of the magmas for the batholithic rocks within structural blocks of southern California*

Structural block	Number of samples	Oxide							
		SiO_2	Al_2O_3	FeO	MgO	CaO	Na_2O	K_2O	TiO_2
San Gabrial block	47	60.26	18.51	5.61	2.72	6.26	3.86	1.80	0.99
San Bernardino block	124	62.06	18.55	4.60	2.09	5.44	4.08	2.26	0.92
Little San Bernardino block	25	61.02	18.53	5.18	2.45	5.91	3.95	1.99	0.96
San Jacinto block	90	61.00	18.53	5.18	2.46	5.92	3.95	1.99	0.96
Perris block	115	58.58	18.47	6.54	3.30	7.01	3.67	1.37	1.06
Santa Ana block	79	57.67	18.45	7.05	3.62	7.42	3.56	1.13	1.10
All batholithic rocks	480	60.08	18.51	5.71	2.78	6.34	3.84	1.75	1.00

TABLE 13.—*Average compositions (in percent) of differentiates separated from the magmas to form the batholithic rocks within structural blocks of southern California*

Structural block	Number of samples	Oxide							
		SiO_2	Al_2O_3	FeO	MgO	CaO	Na_2O	K_2O	TiO_2
San Gabrial block	47	50.18	21.63	8.54	4.44	9.55	3.88	0.29	1.50
San Bernardino block	124	51.32	22.28	7.61	3.69	8.87	4.53	0.26	1.43
Little San Bernardino block	25	50.62	21.88	8.18	4.15	9.29	4.13	0.28	1.47
San Jacinto block	90	51.22	22.22	7.70	3.76	8.94	4.47	0.26	1.44
Perris block	115	49.54	21.26	9.06	4.85	9.93	3.51	0.30	1.54
Santa Ana block	79	49.10	21.02	9.41	5.13	10.19	3.26	0.31	1.56
All batholithic rocks	480	50.36	21.73	8.39	4.32	9.44	3.98	0.28	1.49

leagues (summarized in Silver and others, 1979) has demonstrated an age "step" at 105 m.y. (million years) along a boundary coincident with the change from syntectonic to post-tectonic plutons noted in paragraph 5—older plutonic dates to the west, younger to the east. (Potassium-argon dates are also available, but these present further problems of varying cooling histories and argon retentions not relevant to this paper.)

7. *Isotopic and trace-element patterns.*—Strongly correlated with the age "step" (paragraph 6) is an abrupt increase in $\delta^{18}O$ (Taylor and Silver, 1978; further discussed in Silver and others, 1979) over normal igneous values of +6 to +8 in the west to +9 to +11 in the eastern part of the Peninsular Ranges. Contours of $\delta^{18}O$ values trend more northerly than do the strikes of major fault zones and do not appear significantly offset by the faults. The step crosses the Perris block coincident with the other changes just noted. Other isotopic and trace-element data (strontium, rare-earth elements) show close correlations to the patterns of oxygen data (Gromet and Silver, 1979; Silver and others, 1979).

The choice of end members *M*–1 and *M*–2 was not totally objective, but the derived map patterns are not highly sensitive to these choices. *M*–1 and *M*–2 can be changed significantly without eradicating the marked discontinuity near the San Jacinto fault zone. On the other hand, the map patterns can be eradicated almost completely by radical changes in the choice of end-member compositions. The most common difficulty with the alternative models that result, however, is that they call for far greater degrees of differentiation than the model proposed here.

In summary, the model calls for a regional discontinuity in the compositions of the magmas and in the compositions of the differentiates separated from them. The discontinuity in the magmas is presumed to represent a discontinuity in the compositions of the magma source materials. The discontinuity occurs mainly in the vicinity of the San Jacinto fault zone near the center of the Perris block, and corresponds generally to the location of other geochemical, mineralogical, petrological, radiometrical and structural discontinuities. In addition, most of the 17 samples found to be anomalous with respect to the other 480 are from a part of the region identified as anomalous in previous studies of strontium and oxygen isotopes.

DISCUSSION

Investigations cited and summarized in this paper are leading toward some firm conclusions about the origins of at least the Peninsular Ranges part of the southern

California batholithic rocks. The batholithic rocks are divided longitudinally into a western belt made up of older syntectonic plutons of quartz diorite and abundant gabbro that were derived from upper mantle rocks of a primitive nature, and an eastern belt of chiefly younger post-tectonic plutons of mainly granodiorite and quartz monzonite of a nonprimitive nature (Taylor and Silver, 1978). The oxygen-isotope data indicate that the eastern source materials once occurred in a near-surface environment. Baird, Baird, and Welday (1974) and Todd and Shaw (1979) concluded, on separate grounds, that the gabbroic magmas were distinct from those that supplied the quartz plutonites. Silver and colleagues proposed (see summary in Silver and others, 1979) that sources of the Peninsular Ranges rocks were fundamentally basaltic; rare-earth-element patterns show that variations in source rocks, not high-level crystal fractionation or differentiation, were responsible for zonation across the region. They believed that the simplest explanation for all observed trace-element and isotopic patterns is a two-end-member source for the batholithic rocks. Allegre and Othman (1980) showed, on the basis of neodymium-strontium isotopic relations, that one end member must have consisted of a large fraction of recycled older continental crust.

The model we have presented here seems compatible with these conclusions. *M*–1 is basaltic and could have been derived from upper mantle sources. More or less pure *M*–1, modified or unmodified by the redistribution of crystals, could have supplied the gabbroic magmas of the western Peninsular Ranges. *M*–2, a quartzofeldspathic type, represents the nonprimitive end member and may be composed, in some large part, of a partial melt from the continental crust. With but few exceptions, the magmas required for each of the 497 samples of the batholithic rocks range in composition between *M*–1 and *M*–2. The model calls for areal patterns with a discontinuity in the eastern part of the Peninsular Ranges, probably representing both the time and place where significant amounts of continental materials became involved.

Although we interpret *M*–1 and *M*–2 as representing magmas and *D*–1 and *D*–2 as representing differentiates, we recognize that *M*–1 and *M*–2 could also be interpreted as the extremes in a range of crustal rocks from which partial melts were derived. End-members *D*–1 and *D*–2 then could be interpreted as the extremes in a range of mineral assemblages separated from the crustal rocks, not by magmatic differentiation, but by residual concentration as refractory materials left behind on crustal melting. Also possible is that both differentiation and residual concentration occurred to varying degrees over the region, but the two processes are not distinguishable from our model or from the raw chemical data. However, the compositional discontinuity in the eastern part of the Peninsular Ranges is a necessary part of the model regardless of how the end members are interpreted.

SUMMARY AND CONCLUSIONS

The batholithic rocks of southern California were examined by a method of *Q*-mode factor analysis and were found to have a compositional structure similar to that of the Sierra Nevada batholith. The compositional structure indicates that a petrogenetic model with only four end members will account for 85–97 percent of the variation in each of the eight major oxide constituents. We assumed that two of the end members represent an assemblage of plagioclase and mafic minerals, largely hornblende, that ranges in composition between *D*–1 and *D*–2 of table 7. We further assumed that the other two end members represent a range of magmas from which plagioclase and the mafic minerals separated; the range was determined by computations based on the most likely source-magma compositions for the rocks of the southwesternmost Santa Ana block and the northeasternmost San Bernardino block. The limits of the range are given as end members *M*–1 and *M*–2 in table 7.

Each of 480 sample compositions can be closely approximated as a mixture of the four derived end-member compositions. The 17 sample compositions that cannot be approximated in this manner are regarded as anomalous. The mixing proportions indicate that the batholithic rocks as a group required differentiation of about 47 percent; that is, about 47 percent of the magma was removed in the form of plagioclase, hornblende, and other mafic minerals.

The model proposed here is comprised of the end-member compositions given in table 7 and of the mixing proportions in Appendix 2. The mathematical validity of the model can be verified by mathematically combining the magma compositions (*M*–1 and *M*–2 in table 7) and separating the differentiate compositions (*D*–1 and *D*–2 in table 7) according to the mixing proportions in Appendix 2. The results will give close approximations of the original data in Appendix 1. The goodness-of-fit of the model to the original data is given by the parameters in table 2. The loss in goodness-of-fit that would be obtained by using fewer than four end members, or the improvement by adding more end members, can be observed from the factor-variance diagram in figure 4.

The principal advantage of the model is that it allows examination of its separate components, specifically the magmas and the mineral assemblages (differentiates) that were separated from them. Comparison of the compositional variation in the batholithic rocks with the compositional variation in the magmas, has been of particular interest. The variation in the magmas, or the magma source materials, shows a discontinuity that is not evident in the original compositional data. The discontinuity is mainly near the San Jacinto fault zone close to the center of the Perris block. The general correspondence of the discontinuity to similar apparent discontinuities in mineralogic, petrologic, isotopic, and structural properties of the batholithic rocks suggest that the discontinuity is real and that the derived model is valid in at least a general way. The discontinuity is interpreted as the western limit of significant contribution of quartzo-feldspathic materials in the continental crust to the magmas that formed the batholithic rocks.

The compositional variations in the magmas, or their source materials, show no discontinuity at or near the San Andreas fault zone; this suggests that no large amount of displacement has occurred along this particular strand of the fault since the emplacement of the batholithic rocks.

REFERENCES CITED

Abbott, P. L., and Todd, V. R., eds., 1979, Mesozoic crystalline rocks: San Diego State University, Department of Geological Sciences, 286 p.

Allegre, C. J., and Othman, D. B., 1980, Nd-Sr isotopic relationship in granitoid rocks and continental crust development; a chemical approach to orogenesis: Nature, v. 286, p. 335–346.

Atwater, T., 1970, Implications of plate tectonics for the Cenozoic tectonic evolution of western North America: Geological Society of America Bulletin, v. 81, p. 3515–3536.

Baird, A. K., 1975, Plutonic zones in the Peninsular Ranges of southern California and Northern Baja California—Comment: Geology, v. 3, p. 676–677.

Baird, A. K., Baird, K. W., and Welday, E. E., 1974, Chemical trends across Cretaceous batholithic rocks of southern California: Geology, v. 2, p. 493–496.

———1979, Batholithic rocks of the northern Peninsular and Transverse Ranges, southern California, *in* Abbott, P. L., and Todd, V. R., eds., Mesozoic crystalline rocks: San Diego State University, Department of Geological Sciences, p. 111–132.

Baird, A. K., McIntyre, D. B., and Welday, E. E., 1967, Geochemical and structural studies in batholithic rocks of southern California; Part II, sampling of the Rattlesnake Mountain pluton for chemical composition and variation: Geological Society of America Bulletin, v. 78, p. 191–122.

Baird, A. K., Morton, D. M., Woodford, A. O., and Baird, K. W., 1974, The Transverse Ranges Province; a unique structural-petrochemical belt across the San Andreas fault system: Geological Society of America Bulletin, v. 85, p. 163–174.

Bateman, P. C., Clark, L. D., Huber, N. K., Moore, J. G., and Rinehart, C. D., 1963, The Sierra Nevada batholith—A synthesis of recent work across the central part: U.S. Geological Survey Professional Paper 414–D, p. D1–D46.

Bateman, P. C., and Dodge, F. C. W., 1970, Variation of major chemical constituents across the central Sierra Nevada batholith: Geological Society of America Bulletin, v. 81, p. 409–420.

Crowell, J. C., 1979, The San Andreas fault system through time: Quarterly of the Journal Geological Society of London, v. 136, p. 293–302.

DePaolo, D. J., 1980, Sources of continental crust; neodymium isotope evidence from the Sierra Nevada and Peninsular Ranges: Science, v. 209, no. 4457, p. 684–687.

Gastil, G., Morgan, G. J., and Krummenacher, D., 1978, Mesozoic history of Peninsular California and related areas east of the Gulf of California, *in* Howell, D. G., and McDougall, K. A., eds., Mesozoic paleogeography of the western United States, Pacific Coast paleogeography symposium 2: Pacific Section, Society of Economic Paleontologists and Mineralogists, p. 107–115.

Gastil, R. G., Phillips, R. P., and Allison, E. C., 1975, Reconnaissance geology of the State of Baja California: Geological Society of America Memoir 140, 170 p.

Gromet, P. L., and Silver, L. T., 1979, Profile of rare earth element characteristics across the Peninsular Ranges batholith near the international border, southern California, U.S.A., and Baja California, Mexico, *in* Abbott, P. L., and Todd, V. R., eds., Mesozoic crystalline rocks: San Diego State University, Department of Geological Sciences, p. 133–142.

Hadley, D., and Kanamori, H., 1977, Seismic structure of the Transverse Ranges, California: Geological Society of America Bulletin, v. 88, p. 1469–1478.

Hill, M. L., and Dibblee, T. W., 1953, San Andreas, Garlock, and Big Pine faults, California—A study of the character, history, and tectonic significance of their displacements: Geological Society of America Bulletin, v. 64, p. 443–458.

Imbrie, J., and Purdy, E. G., 1962, Classification of modern Bahamian carbonate sediments, *in* Ham, W. E., ed., Classification of carbonate rocks: American Association of Petroleum Geologists Memoir 1, p. 253–272.

Krummenacher, D., Gastil, R. G., Bushee, J., and Doupont, J., 1975, K-Ar apparent ages, Peninsular Ranges batholith, southern California and Baja California: Geological Society of America Bulletin, v. 86, p. 760–768.

Larsen, E. S., Jr., 1948, Batholith and associated rocks of Corona, Elsinore, and San Luis Rey quadrangles, southern California: Geological Society of America Memoir 29, 182 p.

Larsen, E. S., Jr., and Draisin, W. M., 1950, Composition of the minerals in the rocks of the southern California batholith: International Geological Congress, Report of 18th Session, Great Britain, 1948, pt. II, p. 66–79.

Luyendyk, B. P., Kamerling, M. J., and Terres, R., 1979, Geometric model for Neogene crustal rotations in southern California [abs.]: Geological Society of America Abstracts with Programs, v. 11, p. 470.

Miesch, A. T., 1976a, *Q*-mode factor analysis of compositional data: Computers & Geosciences, v. 1, p. 147–159.

———1976b, *Q*-mode factor analysis of geochemical and petrologic data matrices with constant row-sums: U.S. Geological Survey Professional Paper 574–G, 47 p.

———1976c, Interactive computer programs for petrologic modeling with extended *Q*-mode factor analysis: Computers & Geosciences, v. 2, p. 439–492.

———1979, Vector analysis of chemical variation in the lavas of Paricutin volcano, Mexico: Mathematical Geology, v. 11, p. 345–371.

———1980, Scaling variables and interpretation of eigenvalues in principal component analysis of geologic data: Mathematical Geology, v. 12, p.523–538.

Miesch, A. T., and Morton, D. M., 1977, Chemical variability in the Lakeview Mountains pluton, southern California batholith—A comparison of the methods of correspondence analysis and extended *Q*-mode factor analysis; U.S. Geological Survey Journal of Research, v. 5, p. 103–116.

Miesch, A. T., and Reed, B. L., 1979, Compositional structures in two batholiths of circum-Pacific North America: U.S. Geological Survey Professional Paper 574–H, 31 p.

Miller, C. F., 1977, Early alkalic plutonism in the calc-alkaline batholithic belt of California: Geology, v. 5, p. 685–688.

Moore, J. G., 1959, The quartz diorite boundary line in the western United States: Journal of Geology, v. 67, p. 198–210.

Morton, D. M., and Baird, A. K., 1976, The Paloma Valley ring dike complex: U.S. Geological Survey Journal of Research, v. 4, p. 83–89.

Morton, D. M., Baird, A. K., and Baird, K. W., 1969, The Lakeview Mountains pluton, southern California batholith, Part II; Chemical composition and variation: Geological Society of America Bulletin, v. 80, p. 1553–1564.

Nishimori, R. K., 1976, The petrology and geochemistry of the gabbros from the Peninsular Ranges batholith, California, and a model for their origin: Scripps Institute of Oceanography, Ph.D. thesis, 234 p.

Nockolds, S. R., and Allen, R., 1953, Geochemistry of some igneous rock series, I: Geochimica et Cosmochimica Acta, v. 4, p. 105–142.

Reed, B. L., and Lanphere, M. A., 1973, Alaska-Aleutian Range batholith; geochronology, chemistry, and relation to circum-Pacific plutonism: Geological Society of America Bulletin, v. 84, p. 2583–2610.

Richmond, J. F., 1965, Chemical variation in quartz monzonite from Cactus Flat, San Bernardino Mountains, California: American Journal of Science, v. 263, p. 53–63.

Schwarcz, H. P., 1969, Pre-Cretaceous sedimentation and metamorphism in the Winchester area, northern Peninsular Ranges, California: Geological Society of America Special Report 100, 63 p.

Silver, L. T., 1971, Problems of crystalline rocks of the Transverse Ranges [abs.]: Geological Society of America Abstracts with Programs, v. 3, p. 193–194.

Silver, L. T., Early, T. O., and Anderson, T. H., 1975, Petrological, geochemical and geochronological asymmetries of the Peninsular Ranges batholith [abs.]: Geological Society of America Abstracts with Programs, v. 7, p. 375–376.

Silver, L. T., Taylor, H. P., Jr., and Chappell, B., 1979, Some petrological, geochemical and geochronological observations of the Peninsular Ranges batholith near the international border of the U.S.A. and Mexico, *in* Abbott, P. L., and Todd, V. R., eds., Mesozoic crystalline rocks: San Diego State University, Department of Geological Sciences, p. 83–110.

Streckeisen, A. L., 1973, Plutonic rocks, classification and nomenclature recommended by the I.U.G.S. Subcommision on the systematics of igneous rocks: Geotimes, v. 18, p. 26–30.

Stuckless, J. S., and Miesch, A. T., 1981, Petrogenetic modeling of a potential uranium source rock, Granite Mountains, Wyoming: U.S. Geological Survey Professional Paper 1225, 34 p.

Stuckless, J. S., Miesch, A. T., Goldich, S. S., and Weiblen, P. W., 1981, A *Q*-mode factor model for the petrogenesis of the volcanic rocks from Ross Island and vicinity, Antarctica: American Geophysical Union, Dry Valley Drilling Project, Antarctica Research Series, v. 33, p. 257–280.

Taylor, H. P., Jr., and Silver, L. T., 1978, Oxygen isotope relationships in plutonic igneous rocks of the Peninsular Ranges batholith, southern and Baja California: U.S. Geological Survey Open-File Report 78–701, p. 423–426.

Todd, V. R., and Shaw, S. E., 1979, Structural, metamorphic and intrusive framework of the Peninsular Ranges batholith in southern San Diego County, California, *in* Abbott, P. L., and Todd, V. R., eds., Mesozoic crystalline rocks: San Diego State University, Department of Geological Sciences, p. 177–231.

Van Trump, G., Jr., and Miesch, A. T., 1977, The U.S. Geological Survey RASS-STATPAC system for management and statistical reduction of geochemical data: Computers & Geosciences, v. 3, p. 475–488.

Walawender, M. J., 1979, Basic plutons of the Peninsular Ranges batholith, southern California, *in* Abbott, P. L., and Todd, V. R., eds., Mesozoic crystalline rocks: San Diego State University, Department of Geological Sciences, p. 151–162.

Woodford, A. O., 1960, Bedrock patterns and strike-slip faulting in southwestern California: American Journal of Science, v. 258A, p. 400–417.

Yeats, R. S., 1981, Quaternary flake tectonics of the California Transverse Ranges: Geology, v. 9, p. 16–20.

FIGURE 12

Maps of the variability of SiO_2, Al_2O_3, FeO, MgO, CaO, Na_2O, K_2O, and TiO_2 in the batholithic rocks of southern California and in the magmas and differentiates as interpreted from the model. Class intervals are defined by the 20th, 40th, 60th, and 80th percentiles of the mapped variables.

SiO_2

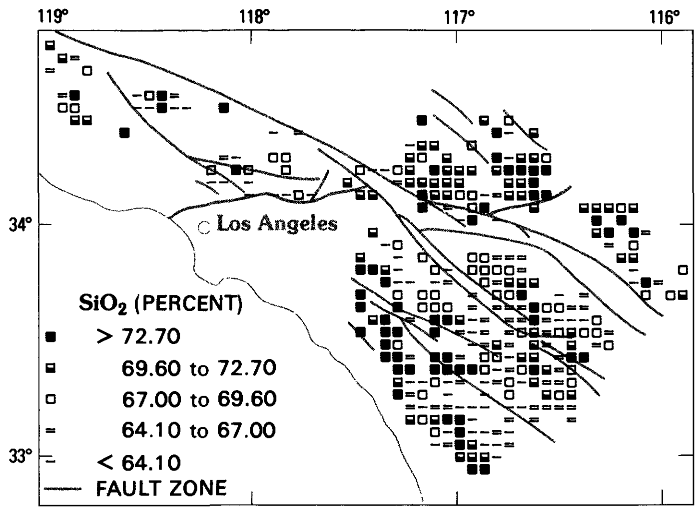

SiO_2 IN BATHOLITHIC ROCKS

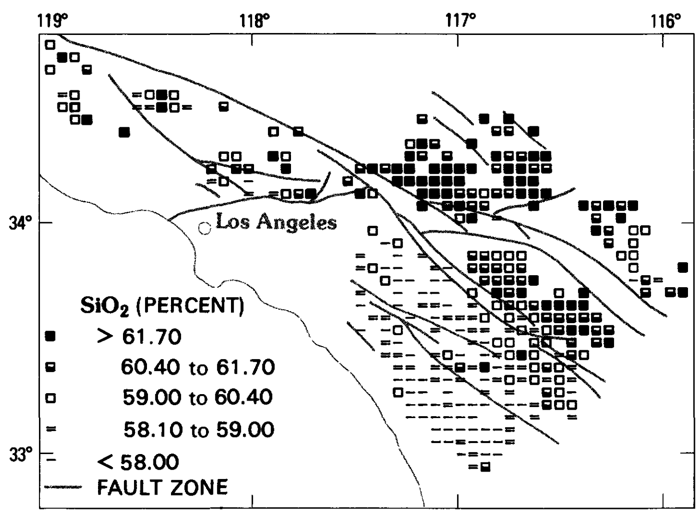

SiO_2 IN THE MAGMAS

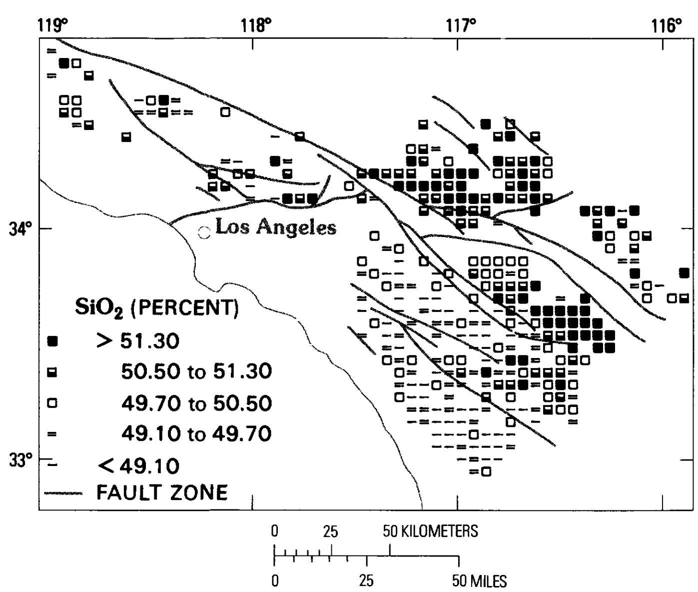

SiO_2 IN THE DIFFERENTIATES

Al_2O_3

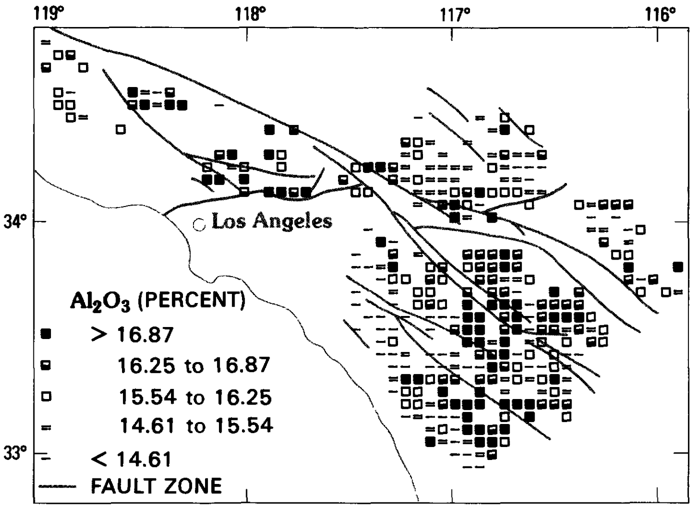

Al_2O_3 IN BATHOLITHIC ROCKS

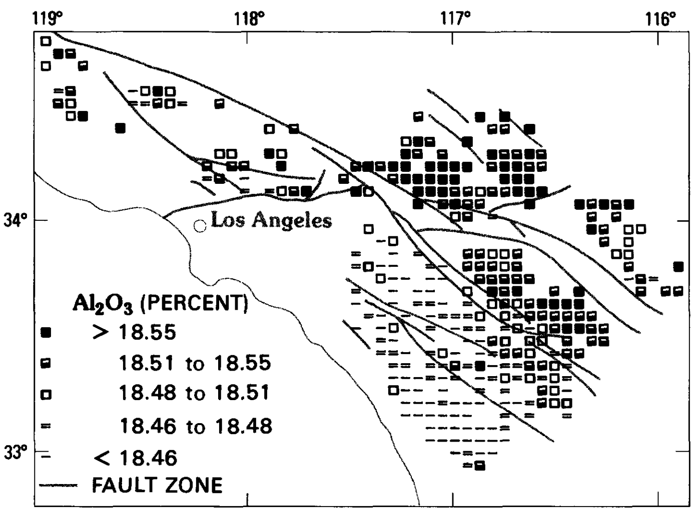

Al_2O_3 IN THE MAGMAS

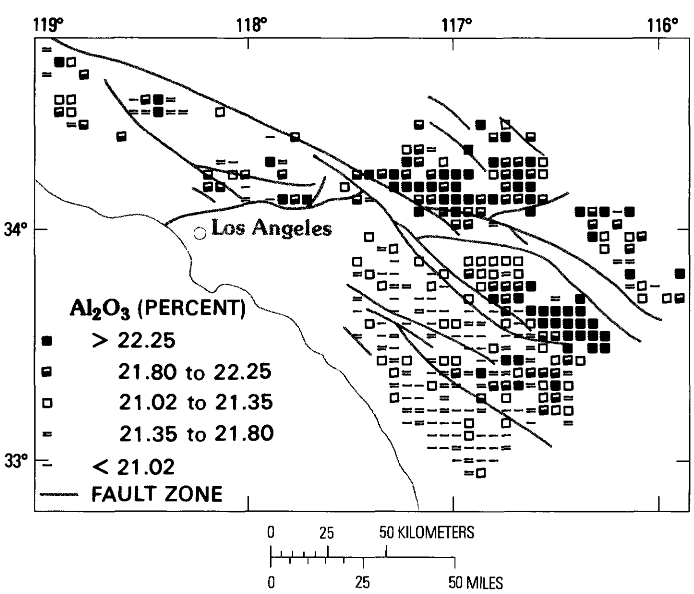

Al_2O_3 IN THE DIFFERENTIATES

FeO

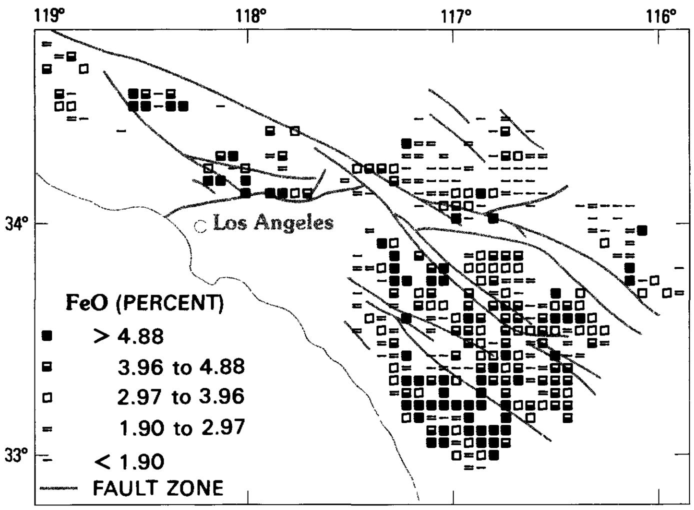

FeO IN BATHOLITHIC ROCKS

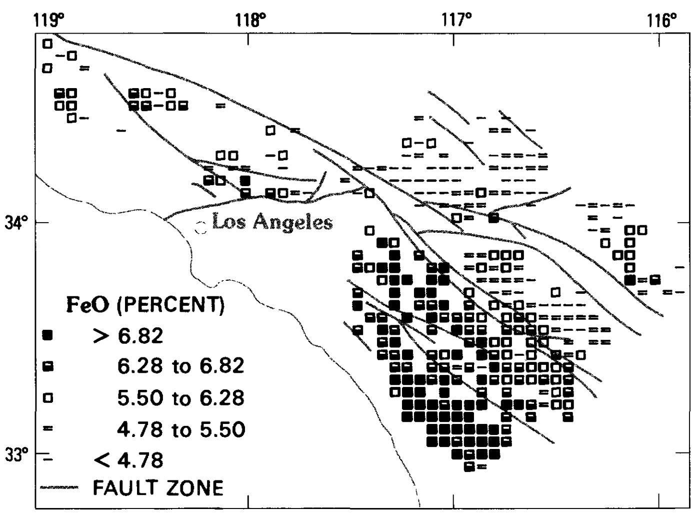

FeO IN THE MAGMAS

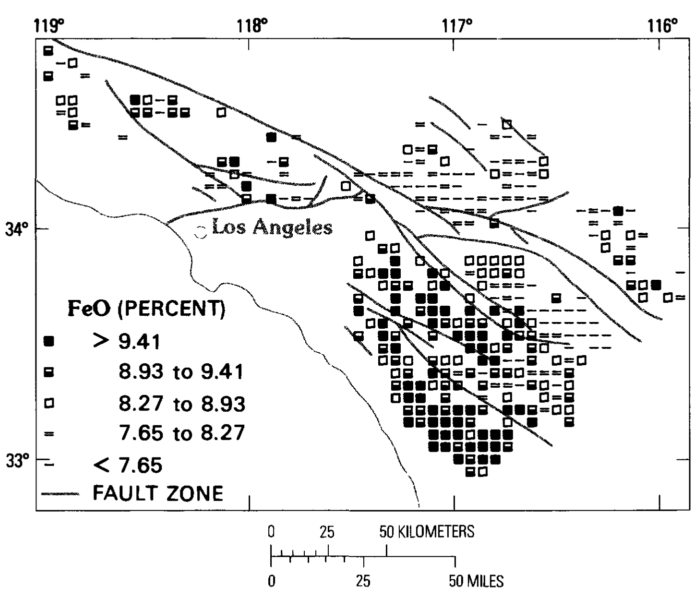

FeO IN THE DIFFERENTIATES

MgO

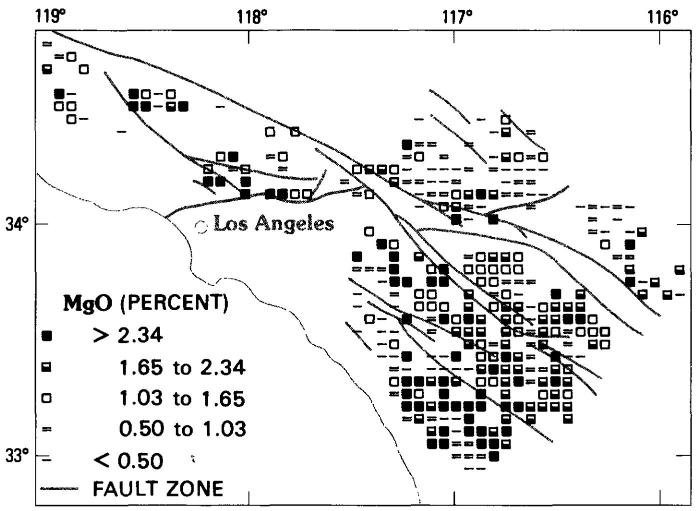

MgO IN BATHOLITHIC ROCKS

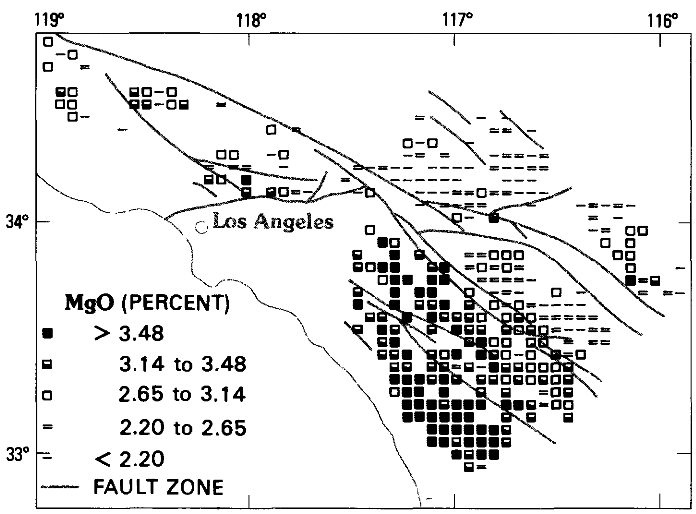

MgO IN THE MAGMAS

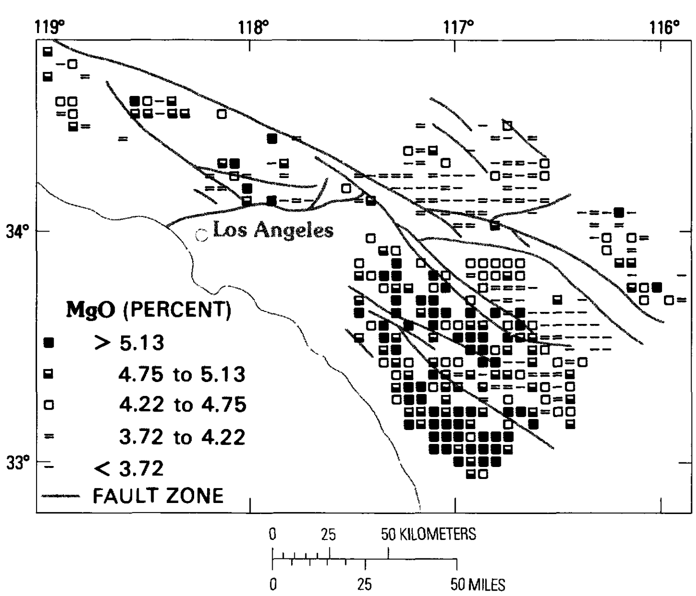

MgO IN THE DIFFERENTIATES

CaO

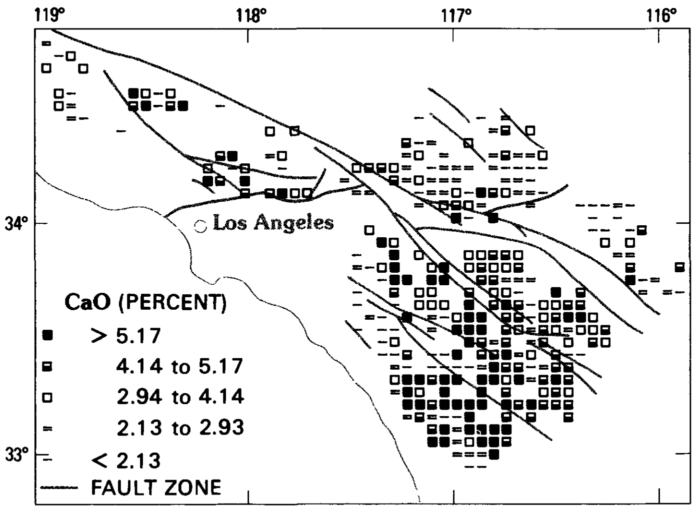

CaO IN BATHOLITHIC ROCKS

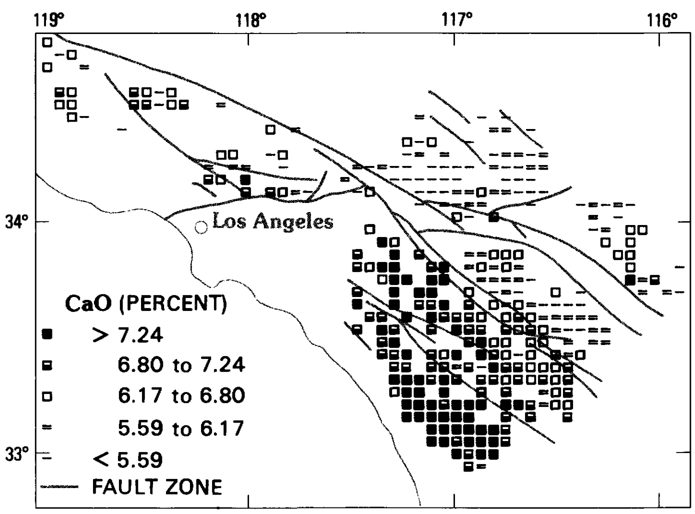

CaO IN THE MAGMAS

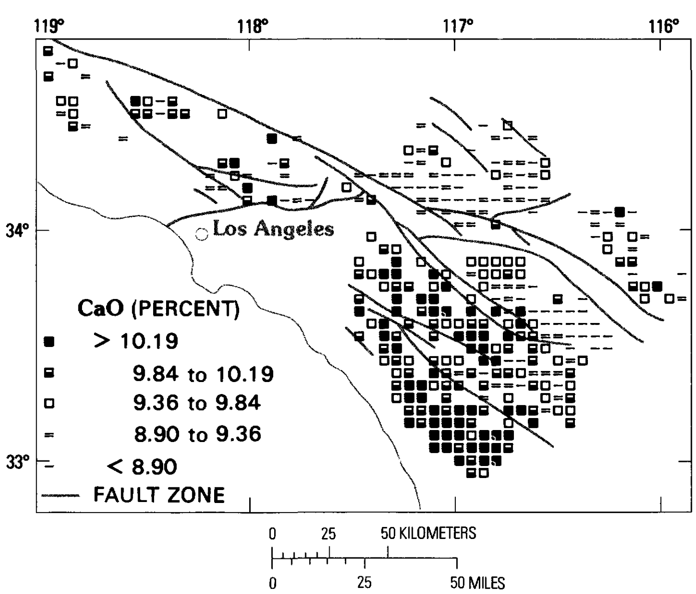

CaO IN THE DIFFERENTIATES

Na_2O

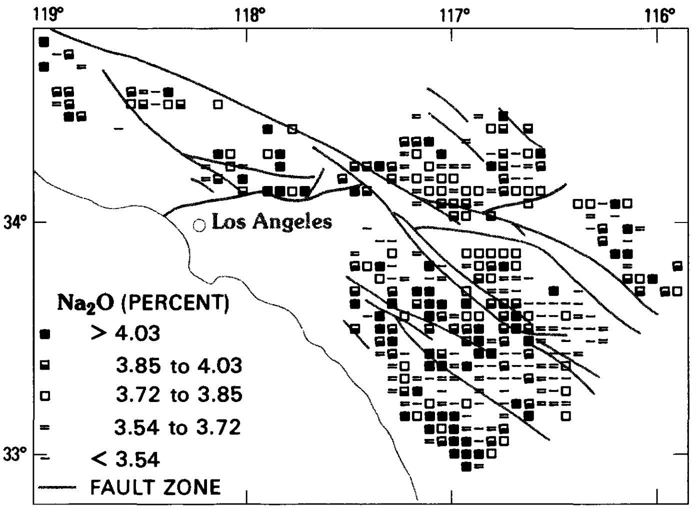

Na_2O IN BATHOLITHIC ROCKS

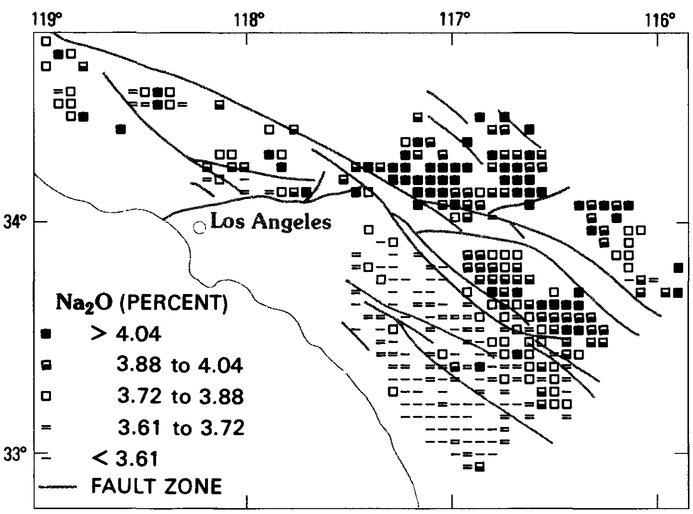

Na_2O IN THE MAGMAS

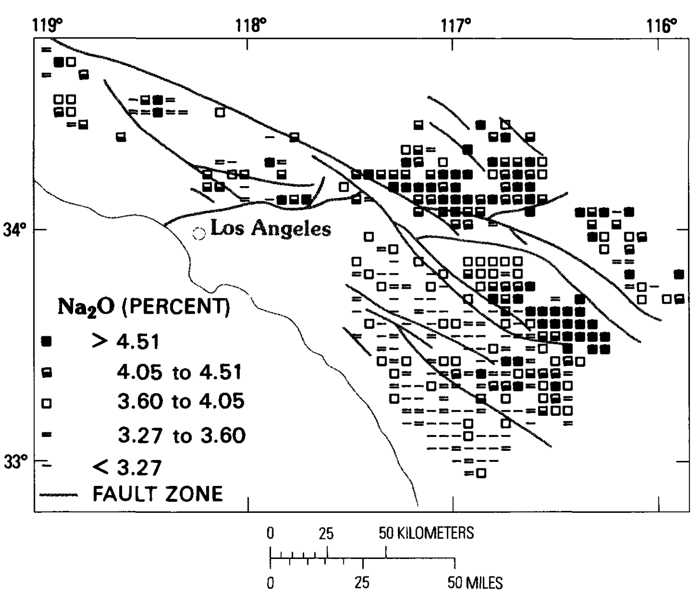

Na_2O IN THE DIFFERENTIATES

K_2O

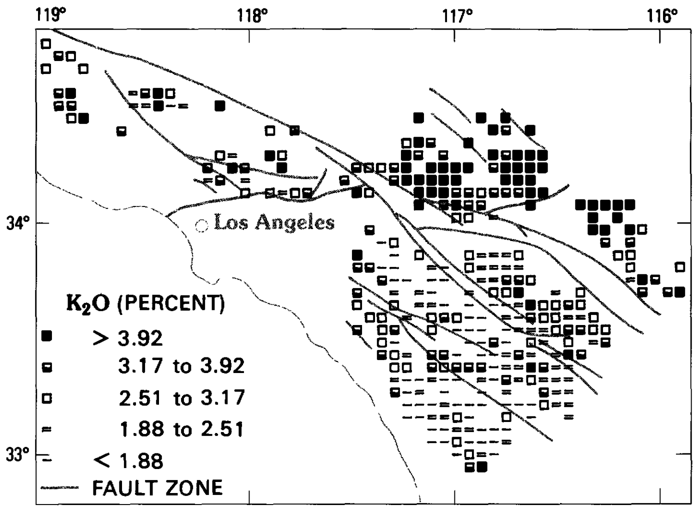

K_2O IN BATHOLITHIC ROCKS

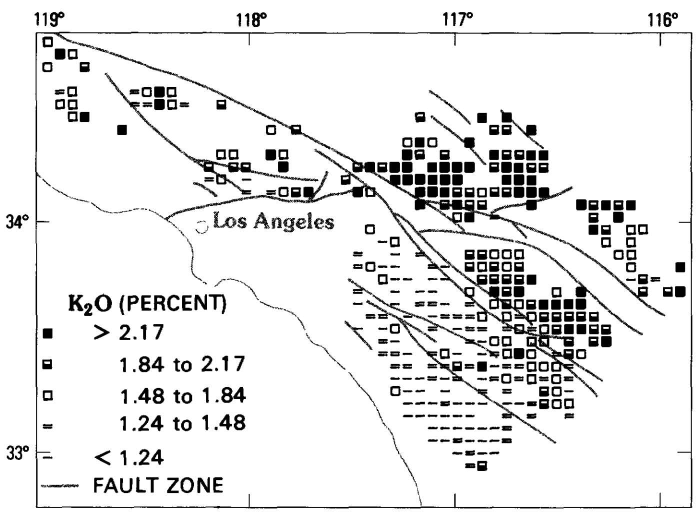

K_2O IN THE MAGMAS

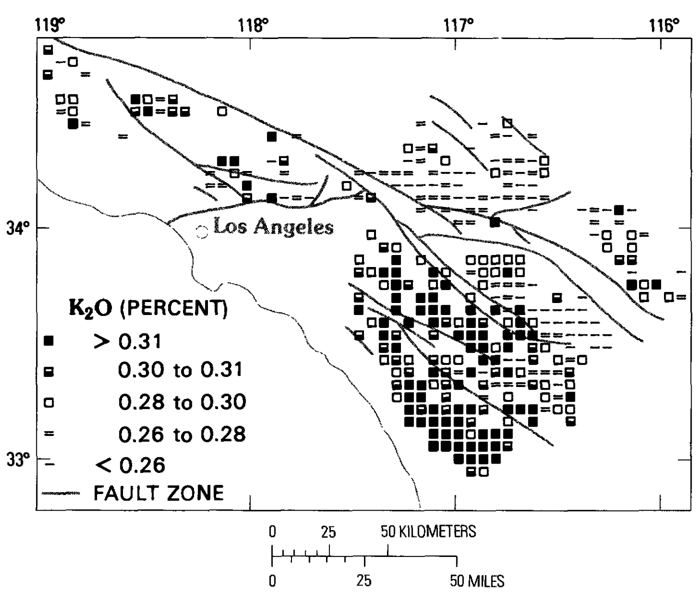

K_2O IN THE DIFFERENTIATES

TiO_2

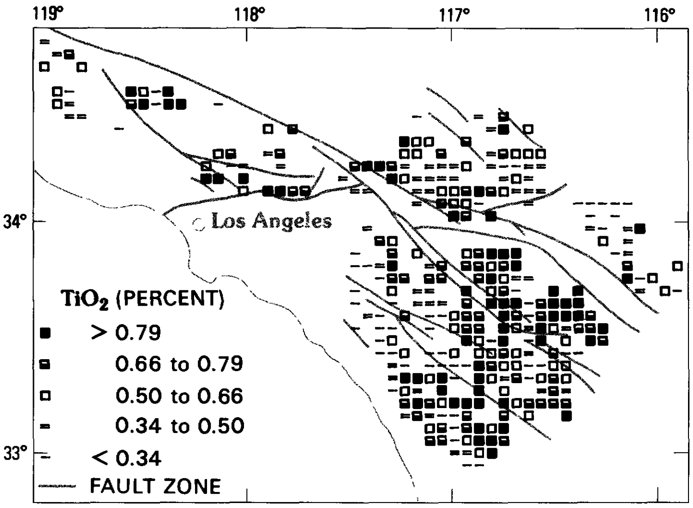

TiO_2 IN BATHOLITHIC ROCKS

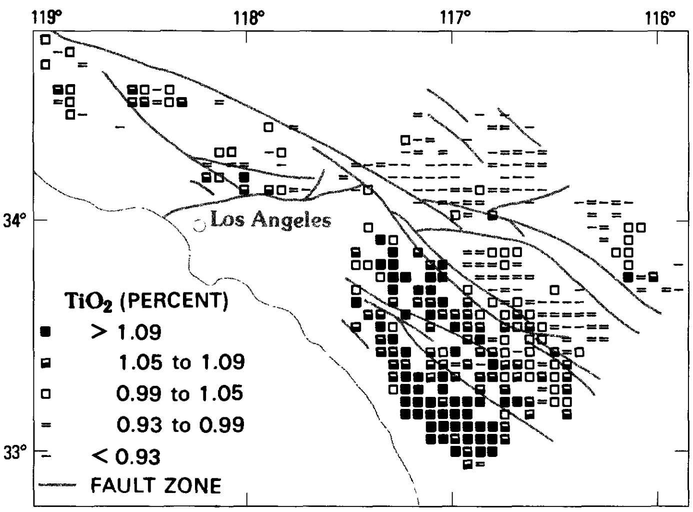

TiO_2 IN THE MAGMAS

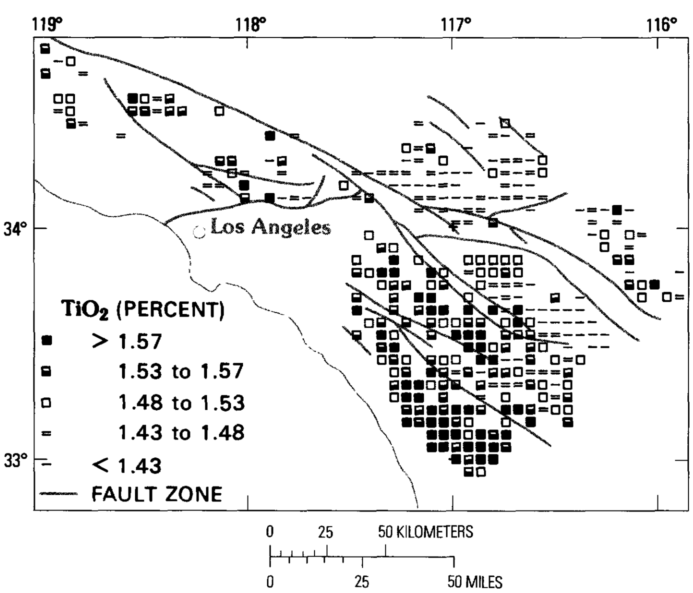

TiO_2 IN THE DIFFERENTIATES

APPENDIXES 1 AND 2

Chemical data on batholithic rocks of southern California (Appendix 1) and mixing proportions for end-members *M*–1, *M*–2, *D*–1, and *D*–2 (Appendix 2)

APPENDIX 1

Chemical data on batholithic rocks of southern California, in percent

Sample Number	SiO_2	Al_2O_3	FeO	MgO	CaO	Na_2O	K_2O	TiO_2
	San Gabriel block							
B 1	71.21	15.41	2.50	0.87	2.28	4.14	3.16	0.44
B 2	69.06	16.59	2.71	0.95	2.71	4.38	3.12	0.49
B 3	63.09	16.98	5.45	2.48	4.66	3.92	2.65	0.77
B 4	65.87	15.57	4.23	2.81	3.87	3.88	3.19	0.58
B 5	67.56	15.68	3.91	1.60	3.65	3.62	3.42	0.56
B 6	75.05	14.39	1.19	0.25	0.83	4.01	4.11	0.17
B 7	69.56	15.78	3.07	1.21	2.63	4.03	3.32	0.40
B 8	67.77	16.49	3.71	1.57	3.21	4.22	2.55	0.49
B 9	72.99	15.30	1.64	0.50	1.67	4.17	3.44	0.30
B 10	71.97	15.33	1.71	0.50	1.73	3.94	4.46	0.37
B 11	70.81	16.05	2.94	0.97	2.12	3.36	3.27	0.49
B 12	66.75	16.44	4.14	1.52	3.57	3.91	2.99	0.68
B 13	67.53	16.17	3.95	1.31	3.52	3.70	3.16	0.64
B 14	59.91	17.51	6.65	3.32	5.45	3.96	2.27	0.92
B 15	63.66	16.48	5.43	2.61	4.82	3.81	2.42	0.78
B 16	62.14	17.27	5.43	2.63	5.49	3.93	2.32	0.79
B 17	68.15	15.33	4.13	1.49	3.25	3.68	3.38	0.59
B 18	73.72	14.76	1.61	0.60	1.93	3.61	3.55	0.22
B 19	75.01	14.25	1.15	0.22	0.80	3.52	4.83	0.22
B 20	75.46	14.57	0.91	0.23	0.76	3.16	4.76	0.15
B 21	66.36	16.46	4.11	1.54	4.10	4.09	2.56	0.79
B 22	62.10	18.33	5.78	2.81	5.21	3.55	1.46	0.75
B 23	64.83	17.30	4.47	1.67	4.64	4.13	2.07	0.89
B 24	62.14	16.93	5.64	2.88	5.43	3.85	2.21	0.92
B 25	74.14	14.51	1.46	0.47	1.32	3.79	4.16	0.17
B 26	73.29	15.56	1.55	0.40	1.55	3.53	3.88	0.24
B 27	63.59	18.44	4.66	1.52	4.01	4.53	2.64	0.62
B 28	68.64	16.90	2.59	0.95	2.47	3.85	4.18	0.42
B 29	66.93	16.47	3.63	1.55	3.79	3.75	3.18	0.70
B 30	67.26	16.05	4.25	1.50	3.14	4.10	2.99	0.70
B 31	69.51	16.12	2.37	0.67	2.07	4.21	4.63	0.42
B 32	65.29	16.85	4.51	1.57	4.26	4.09	2.90	0.54
B 33	60.46	18.66	6.29	2.49	5.44	3.83	2.16	0.67
B 34	68.13	15.92	3.63	1.53	3.20	3.64	3.42	0.54
B 35	73.05	14.80	1.68	0.57	1.83	3.76	4.10	0.22
B 36	67.43	16.02	3.77	1.58	3.42	3.72	3.57	0.49
B 37	62.59	17.03	5.70	2.43	4.36	3.89	3.17	0.83
B 38	58.08	18.48	6.82	3.48	6.73	3.61	1.98	0.82
B 39	58.46	18.09	7.05	3.31	5.86	4.16	2.23	0.85
B 40	63.68	16.58	5.29	2.49	4.49	3.96	2.85	0.66
B 41	56.51	19.22	7.05	3.33	6.79	4.12	1.92	1.06
B 42	60.61	17.37	5.96	3.08	5.16	4.16	2.86	0.79
B 43	67.08	16.51	3.88	1.38	3.95	3.79	2.64	0.77
B 44	63.60	17.92	4.74	1.51	4.03	4.10	3.37	0.74
B 46	71.05	16.28	1.94	0.57	2.22	4.00	3.57	0.37
B 47	70.16	16.16	2.17	0.53	2.17	4.08	4.35	0.37
B 48	71.25	16.15	1.81	1.03	2.70	3.96	2.73	0.37
	San Bernardino block							
B 54	72.80	15.45	0.74	0.27	2.43	3.97	3.96	0.37
B 55	70.24	15.38	2.45	0.88	3.32	3.60	3.53	0.60
B 56	64.65	17.02	4.01	1.56	4.39	4.27	3.16	0.93
B 57	63.99	17.55	4.05	2.17	4.35	4.01	2.98	0.89
B 58	64.85	16.92	4.11	1.62	4.23	4.10	3.27	0.90
B 59	64.96	17.07	3.89	1.57	4.32	4.15	3.15	0.88
B 60	67.37	16.26	3.29	1.11	3.64	3.91	3.72	0.71
B 61	62.06	17.13	5.48	2.50	5.31	3.91	2.64	0.96
B 62	64.31	17.15	4.19	1.61	4.48	4.21	3.08	0.97
B 63	70.13	15.49	2.14	0.80	3.02	3.71	4.17	0.55
B 64	73.67	14.58	0.81	0.17	1.92	3.71	4.81	0.34
B 65	73.66	14.34	1.41	0.25	1.94	3.64	4.38	0.37
B 66	66.84	16.15	3.48	1.46	3.80	3.71	3.83	0.74
B 67	66.97	17.34	2.93	1.63	3.44	3.84	3.20	0.66
B 68	73.30	14.65	1.19	0.27	2.13	3.46	4.63	0.37
B 69	69.82	15.54	2.41	0.85	3.28	3.94	3.54	0.62
B 70	64.11	16.67	4.46	1.99	4.61	3.88	3.35	0.93
B 71	68.14	15.86	3.25	1.10	3.58	3.94	3.45	0.68
B 72	74.06	14.40	0.89	0.20	1.82	3.42	4.85	0.37
B 74	63.26	16.49	5.08	2.64	4.87	3.94	2.76	0.96
B 75	73.89	14.53	0.78	0.30	2.24	3.79	4.11	0.37
B 78	70.40	15.96	2.51	0.83	1.60	3.98	4.16	0.55
B 79	70.35	15.31	2.27	0.78	2.43	4.41	3.86	0.58
B 80	66.63	16.46	3.51	2.08	3.86	3.87	2.74	0.85
B 81	70.77	15.22	2.40	0.98	2.15	4.04	3.78	0.66
B 85	68.75	15.53	2.90	0.96	2.94	3.71	4.52	0.68
B 86	76.76	12.83	0.16	0.02	1.28	3.65	5.04	0.27
B 94	71.45	15.20	1.49	0.40	2.23	3.67	5.04	0.52
B 95	72.71	14.72	1.02	0.30	2.03	3.64	5.10	0.47
B 96	73.80	14.62	0.89	0.35	2.23	3.81	3.94	0.37
B 97	62.97	16.93	4.60	2.32	4.82	3.97	3.55	0.83
B 98	67.21	15.86	2.92	1.17	2.82	4.54	4.74	0.73
B 99	65.37	15.99	3.44	1.58	4.12	3.64	5.05	0.82
B100	73.31	15.55	0.13	0.10	2.45	4.03	4.16	0.27
B101	68.82	15.55	2.58	1.11	3.21	3.95	4.15	0.63
B102	67.58	16.13	2.77	1.22	3.45	4.05	4.12	0.68
B103	70.07	15.51	2.14	0.84	2.75	3.74	4.37	0.57
B104	68.46	16.26	2.50	1.03	3.06	4.19	3.95	0.55
B105	75.51	13.35	0.76	0.20	1.50	3.93	4.38	0.37
B106	71.97	14.80	1.64	0.60	2.43	3.81	4.25	0.50
B107	71.15	15.22	1.73	0.71	2.57	3.83	4.26	0.53
B108	63.94	16.15	5.20	2.48	4.62	4.01	2.91	0.68
B109	75.28	13.32	1.95	0.32	1.04	2.74	5.02	0.34
B110	75.96	12.85	1.05	0.20	1.47	2.98	5.14	0.35
B111	76.19	13.02	0.14	0.08	1.34	2.78	6.13	0.32
B112	75.73	12.36	1.39	0.35	1.70	3.27	4.81	0.39
B113	75.85	12.70	1.13	0.22	1.44	3.02	5.26	0.39
B114	77.40	12.11	0.69	0.08	1.28	2.87	5.22	0.33
B115	73.67	15.37	0.40	0.20	1.81	4.01	4.23	0.32
B116	63.70	16.70	4.76	2.18	4.75	3.85	3.31	0.75
B117	70.91	16.05	1.54	0.56	2.84	4.17	3.50	0.43
B118	73.59	14.63	1.10	0.31	2.23	3.47	4.28	0.38
B120	71.82	14.39	2.16	0.56	2.01	3.45	5.10	0.51
B121	68.79	15.48	3.02	1.25	2.61	3.82	4.24	0.77
B124	72.66	14.36	1.67	0.55	2.39	3.60	4.32	0.45
B125	73.18	14.67	1.12	0.37	2.08	3.80	4.31	0.47
B127	72.57	15.13	1.38	0.37	1.97	3.62	4.49	0.47
B128	63.78	16.91	4.50	2.07	4.89	3.81	3.28	0.77
B129	73.39	14.42	1.22	0.33	1.88	3.36	5.01	0.40
B130	72.84	15.25	1.30	0.49	1.78	3.48	4.43	0.44
B131	73.61	14.59	1.04	0.25	2.13	3.58	4.44	0.37
B132	73.20	14.95	1.25	0.30	2.24	3.62	4.03	0.40
B133	74.33	14.48	0.79	0.08	1.63	3.60	4.76	0.33
B134	73.95	14.64	0.90	0.18	1.85	3.79	4.35	0.34
B135	72.37	15.73	0.68	0.20	2.21	4.04	4.44	0.33
B136	71.72	15.20	1.51	0.55	2.52	3.81	4.18	0.52
B137	71.62	15.23	1.76	0.59	2.44	3.71	4.14	0.52
B138	72.45	14.96	1.42	0.40	2.27	3.70	4.34	0.46
B139	72.86	14.88	1.29	0.38	2.18	3.68	4.28	0.45
B140	72.44	14.99	1.42	0.38	2.24	3.58	4.50	0.45
B141	70.93	15.40	1.77	0.57	2.58	3.88	4.35	0.52
B142	71.81	15.15	1.54	0.51	2.34	3.62	4.54	0.48
B143	71.96	15.07	1.41	0.45	2.44	3.72	4.50	0.45
B144	72.13	14.72	1.69	0.51	2.35	3.62	4.49	0.48

APPENDIX 1.--Continued

Sample Number	Oxide SiO_2	Al_2O_3	FeO	MgO	CaO	Na_2O	K_2O	TiO_2
San Bernardino block--Continued								
B145	72.12	14.98	1.41	0.50	2.36	3.69	4.45	0.50
B146	73.32	14.66	1.22	0.33	2.07	3.71	4.27	0.42
B147	71.64	15.20	1.46	0.50	2.49	3.77	4.43	0.50
B148	71.87	15.27	1.40	0.50	2.50	3.81	4.16	0.49
B149	72.84	14.88	1.07	0.35	2.22	3.78	4.42	0.44
B150	72.08	15.18	1.36	0.42	2.37	3.78	4.34	0.47
B151	70.67	15.56	1.84	0.62	2.78	3.84	4.17	0.54
B152	65.95	16.37	3.90	1.67	4.31	3.79	3.33	0.70
B153	67.49	16.54	3.16	0.98	3.30	4.09	3.91	0.53
B155	61.93	16.89	5.10	2.42	5.18	3.74	3.90	0.84
B156	63.74	16.88	4.36	1.59	4.63	3.96	4.53	0.31
B157	71.88	15.31	1.33	0.33	2.15	3.98	4.61	0.42
B158	60.80	17.84	5.88	2.40	5.28	4.04	2.82	0.93
B159	64.43	16.55	4.58	2.25	4.76	3.54	3.16	0.74
B160	65.27	16.48	4.22	1.96	4.61	3.79	2.97	0.70
B161	68.35	16.39	3.86	1.66	1.84	3.74	3.48	0.68
B162	69.21	15.78	3.03	0.81	2.96	3.89	3.79	0.52
B163	74.59	15.17	0.86	0.22	1.83	3.81	2.79	0.73
B164	59.57	17.93	6.45	3.15	5.19	3.95	2.82	0.94
B165	74.49	14.43	0.86	0.20	2.18	3.66	3.86	0.32
B166	59.03	17.69	6.37	3.34	6.37	3.95	2.26	1.00
B168	59.70	17.36	6.36	3.14	6.11	3.76	2.60	0.97
B169	59.12	17.29	6.65	3.26	6.46	3.80	2.38	1.03
B170	70.61	16.45	1.53	0.49	3.19	4.33	2.94	0.46
B171	69.21	16.26	2.41	0.95	3.29	4.02	3.30	0.55
B172	61.21	16.90	6.02	2.80	5.72	4.12	2.30	0.94
B173	73.61	14.79	0.44	0.20	1.90	3.57	5.14	0.35
B174	72.10	14.97	1.56	0.57	2.51	3.44	4.39	0.45
B175	71.54	15.18	1.60	0.62	2.64	3.58	4.40	0.45
B176	71.18	16.15	1.40	0.53	3.17	4.03	3.09	0.45
B177	72.87	14.97	0.79	0.22	1.95	3.83	5.02	0.35
B178	74.89	14.44	0.21	0.08	1.59	3.42	5.08	0.29
B179	63.87	17.64	4.77	1.78	4.74	4.26	2.17	0.76
B180	72.32	15.27	0.92	0.52	2.33	4.11	4.11	0.42
B181	74.03	14.86	0.62	0.22	2.00	3.73	4.24	0.32
B182	72.67	14.49	1.45	0.53	2.37	3.31	4.73	0.45
B183	71.52	14.95	2.27	0.93	2.47	3.35	3.88	0.62
B184	75.38	13.80	0.91	0.18	1.06	2.54	5.73	0.40
B185	68.99	15.80	2.46	0.99	3.10	3.81	4.20	0.65
B186	71.38	15.73	1.73	0.85	2.22	3.84	3.73	0.50
B187	71.46	15.60	1.31	0.56	2.59	3.78	4.25	0.43
B188	71.10	15.23	1.93	0.72	2.57	3.52	4.45	0.49
B189	74.77	14.73	0.21	0.07	1.58	3.74	4.63	0.28
B190	73.35	15.24	0.49	0.20	2.26	3.81	4.26	0.39
B191	73.04	15.18	0.59	0.12	2.19	3.69	4.87	0.32
B192	72.48	15.53	1.01	0.41	2.28	3.76	4.18	0.36
B193	73.60	15.16	0.64	0.20	1.96	3.83	4.26	0.35
B194	69.38	16.08	2.29	0.95	3.08	3.99	3.70	0.54
B195	74.59	14.61	0.26	0.15	1.98	3.64	4.46	0.32
B196	68.12	16.35	2.63	1.07	3.23	3.96	4.03	0.61
B197	73.91	14.92	0.41	0.21	2.04	3.55	4.62	0.33
Little San Bernardino block								
B198	72.14	15.80	1.13	0.50	1.83	3.77	4.49	0.34
B199	72.49	15.06	1.79	0.45	1.80	3.80	4.37	0.24
B200	69.47	16.50	1.76	0.50	2.46	4.82	4.30	0.19
B201	70.43	15.90	2.34	0.76	2.33	3.88	3.94	0.41
B202	72.69	16.29	1.23	0.42	1.57	3.35	4.27	0.18
B203	72.40	16.64	1.17	0.29	1.28	3.75	4.33	0.15
B204	73.58	14.47	1.49	0.55	1.87	3.69	4.13	0.22
B205	71.21	14.97	2.15	0.69	2.02	3.33	5.19	0.43
B206	74.73	13.64	1.59	0.22	0.84	3.52	5.24	0.23
B207	73.43	15.04	1.25	0.43	1.58	3.91	4.17	0.20

Sample Number	Oxide SiO_2	Al_2O_3	FeO	MgO	CaO	Na_2O	K_2O	TiO_2
B208	73.92	13.84	2.02	0.48	1.21	4.06	4.11	0.35
B209	68.91	14.62	2.80	3.02	3.16	3.47	3.65	0.38
B210	66.99	16.49	3.71	1.49	3.70	3.89	3.23	0.50
B211	71.33	16.04	1.96	0.61	2.51	4.15	3.09	0.31
B212	70.36	16.07	2.33	0.78	2.93	4.14	3.02	0.37
B213	62.87	17.35	5.70	2.25	4.84	3.62	2.59	0.77
B214	61.34	16.75	5.98	3.10	5.84	3.90	2.19	0.89
B215	75.13	14.17	0.99	0.25	1.10	3.82	4.46	0.08
B216	67.02	16.90	1.47	2.33	4.67	3.88	3.09	0.64
B217	72.26	14.74	2.19	0.30	1.58	3.76	4.89	0.27
B218	65.78	16.52	3.61	2.16	2.94	4.89	3.50	0.61
B219	68.12	16.09	3.19	1.81	2.48	4.01	3.80	0.51
B220	71.61	15.45	1.90	0.64	1.96	3.88	4.32	0.25
B221	64.72	16.34	4.80	2.67	3.41	3.93	3.48	0.64
B222	64.45	15.64	5.40	2.20	4.75	3.61	3.15	0.80
San Jacinto block								
B223	66.88	17.22	3.39	1.29	4.59	4.20	1.72	0.71
B224	71.27	15.72	2.14	0.72	2.73	3.39	3.50	0.53
B225	67.79	17.35	2.89	1.05	4.17	4.13	1.98	0.64
B226	66.49	16.78	4.21	1.64	4.40	3.22	2.28	0.99
B227	64.61	16.49	4.14	2.32	4.97	3.36	3.19	0.92
B228	68.69	16.05	3.20	1.12	3.78	3.68	2.79	0.69
B229	63.94	18.34	3.80	1.56	5.42	4.11	1.82	1.00
B230	67.61	16.21	3.67	1.35	4.01	3.62	2.77	0.76
B231	69.36	16.47	2.79	1.05	3.28	3.79	2.66	0.59
B232	64.29	17.64	4.36	1.75	4.96	4.06	1.93	1.01
B233	64.86	15.92	5.14	2.43	4.74	3.40	2.70	0.81
B234	67.55	16.88	3.46	1.32	4.11	3.91	2.01	0.76
B235	68.60	16.90	3.00	1.10	3.90	4.01	1.87	0.62
B236	68.00	15.78	3.68	1.54	3.82	3.37	3.19	0.64
B237	65.74	17.30	3.84	1.36	4.76	4.03	2.12	0.84
B238	68.19	16.24	3.21	1.14	4.00	3.84	2.66	0.72
B239	66.00	17.11	3.86	1.39	4.65	3.98	2.17	0.84
B240	67.46	17.22	3.09	1.13	4.09	4.02	2.31	0.68
B241	67.83	17.04	3.17	1.18	3.74	4.03	2.34	0.66
B242	67.17	16.90	3.65	1.36	3.97	3.89	2.28	0.78
B243	66.09	17.31	3.69	1.44	4.68	3.94	2.05	0.81
B244	64.96	16.50	4.36	2.52	5.14	3.59	2.12	0.81
B245	66.34	16.29	4.64	1.29	4.09	3.81	2.74	0.80
B246	69.67	16.33	2.73	0.93	3.07	3.87	2.87	0.53
B247	67.70	16.92	3.37	1.24	3.83	4.11	2.16	0.68
B248	70.43	15.89	2.78	0.92	3.04	3.82	2.59	0.54
B249	68.30	16.44	2.94	1.16	3.94	3.73	2.80	0.69
B250	69.17	16.34	2.64	1.00	3.62	3.54	3.06	0.62
B251	63.83	16.86	5.10	2.10	5.40	3.74	2.00	0.96
B252	67.92	17.00	3.18	1.17	3.63	4.06	2.36	0.68
B253	66.45	16.62	4.03	1.59	4.30	3.82	2.30	0.89
B254	67.45	17.03	3.45	1.33	3.87	3.97	2.21	0.71
B255	75.57	13.68	1.13	0.31	1.65	2.88	4.51	0.27
B256	66.56	16.45	4.04	1.51	4.31	3.60	2.68	0.85
B257	65.81	17.22	3.93	1.43	4.62	3.87	2.25	0.86
B258	66.73	16.72	3.98	1.45	4.10	3.91	2.27	0.84
B259	73.00	14.61	2.26	0.45	1.90	3.38	4.09	0.32
B260	65.86	16.74	4.58	1.50	3.89	4.23	2.42	0.78
B261	67.01	16.94	3.70	1.34	4.01	3.83	2.39	0.78
B262	71.26	15.94	2.07	0.99	2.78	3.46	3.02	0.49
B263	70.58	15.10	3.53	0.78	2.59	3.73	3.13	0.57
B264	72.61	14.98	2.27	0.55	2.21	3.45	3.59	0.34
B265	64.74	16.80	4.85	2.07	4.48	3.83	2.35	0.90
B266	75.41	14.29	0.46	0.15	1.18	2.75	5.62	0.15
B267	75.19	13.61	1.65	0.18	1.12	2.62	5.48	0.16
B268	69.90	15.43	3.58	1.09	3.00	3.52	2.98	0.50
B269	63.96	17.57	4.74	1.94	5.03	4.06	1.69	1.01
B270	75.26	13.73	1.64	0.32	1.31	3.84	3.70	0.22
B271	75.13	14.17	1.36	0.27	1.24	3.77	3.87	0.20
B272	72.69	14.56	3.30	0.58	2.20	3.95	2.36	0.37

APPENDIX 1.--Continued

Sample Number	Oxide SiO_2	Al_2O_3	FeO	MgO	CaO	Na_2O	K_2O	TiO_2
San Jacinto block--Continued								
B273	65.62	16.97	4.63	1.79	4.51	3.98	1.57	0.94
B274	66.32	16.88	3.67	1.82	4.24	3.61	2.59	0.87
B275	70.18	16.01	2.20	0.98	3.16	3.44	3.39	0.64
B276	66.77	16.46	3.97	1.79	3.83	3.54	2.85	0.79
B277	64.05	16.69	5.01	2.70	4.29	3.46	2.87	0.92
B278	65.89	17.12	4.29	1.81	3.95	3.60	2.54	0.80
B279	70.28	15.77	3.24	0.65	2.45	3.80	3.36	0.44
B280	68.94	16.25	3.76	0.68	2.60	4.08	3.22	0.47
B281	70.36	15.70	2.94	0.89	3.16	3.43	2.90	0.63
B282	73.79	14.41	1.75	0.47	1.75	2.86	4.55	0.41
B283	66.23	16.08	4.53	2.10	3.25	2.99	3.96	0.86
B284	68.84	16.20	2.76	1.13	3.25	3.35	3.77	0.71
B285	66.83	16.39	3.41	1.72	4.25	3.39	3.21	0.80
B286	63.47	17.29	4.54	2.55	5.24	3.50	2.43	0.98
B287	69.17	15.63	2.96	1.22	3.71	3.36	3.22	0.73
B288	65.22	16.62	4.29	2.24	4.99	3.46	2.21	0.98
B289	68.85	15.99	2.65	1.34	3.59	3.67	3.24	0.67
B290	64.38	16.87	4.53	1.97	5.05	3.79	2.43	0.97
B291	69.21	15.43	3.00	1.14	3.54	3.35	3.67	0.67
B292	69.67	15.22	3.09	1.23	3.72	3.37	2.98	0.71
B293	68.89	15.53	3.22	1.37	3.52	3.49	3.24	0.74
B294	69.56	15.61	2.98	1.23	3.42	3.49	3.01	0.71
B295	62.78	17.27	4.90	2.65	5.47	3.55	2.34	1.03
B296	68.72	16.09	3.04	1.40	3.41	3.32	3.23	0.78
B297	65.50	16.85	3.86	2.16	4.40	3.39	2.97	0.87
B298	64.97	16.71	4.19	2.29	4.74	3.35	2.81	0.93
B299	65.85	17.13	3.49	1.69	4.46	3.68	2.78	0.92
B300	61.79	17.89	4.89	2.76	5.71	3.74	2.25	0.98
B301	65.68	16.69	3.90	2.11	4.56	3.29	2.88	0.89
B302	64.92	17.00	4.22	2.11	4.43	3.32	3.12	0.87
B303	67.89	16.87	2.87	1.28	3.93	3.29	3.14	0.73
B304	62.41	18.06	4.68	2.52	5.52	3.63	2.23	0.96
B305	62.25	17.73	4.97	2.56	5.22	4.03	2.22	1.02
B306	65.08	17.24	3.91	2.08	4.50	3.23	3.08	0.88
B307	65.56	16.66	3.82	2.16	4.64	3.30	3.02	0.86
B308	63.18	17.76	4.53	2.44	5.14	3.60	2.35	1.00
B309	68.70	16.08	3.04	1.40	3.42	3.32	3.23	0.80
B310	63.96	16.46	5.33	2.51	4.38	3.35	3.07	0.93
B311	64.18	17.31	4.83	2.11	4.60	3.64	2.47	0.84
B312	77.23	12.84	0.90	0.15	0.67	3.50	4.50	0.21
B313	75.87	13.66	1.29	0.19	1.34	3.39	3.97	0.29
B314	73.09	14.63	2.51	0.39	1.72	3.87	3.43	0.36
B315	64.60	17.43	4.80	1.86	4.77	3.78	1.92	0.84
B317	65.13	17.56	4.25	1.52	5.02	3.97	1.74	0.82
B318	63.96	17.52	4.57	1.80	5.34	3.85	1.97	1.00
B319	65.26	17.46	4.16	1.52	4.97	3.96	1.80	0.86
B320	63.77	17.74	4.58	1.83	5.43	3.78	1.83	1.03
B321	63.53	18.31	4.59	1.69	5.28	3.77	1.86	0.98
B322	65.58	16.81	4.33	1.76	4.69	3.90	1.96	0.98
B323	63.62	18.08	4.56	1.93	5.07	4.12	1.65	0.98
B324	66.09	17.16	4.53	1.50	4.41	4.08	1.46	0.77
Perris block								
B325	66.27	16.03	4.57	1.94	4.48	3.63	2.29	0.80
B326	64.42	15.81	5.16	2.88	5.14	3.48	2.38	0.73
B327	66.35	15.55	4.83	1.85	4.62	3.90	2.24	0.66
B328	68.65	15.28	4.06	1.35	3.84	3.79	2.48	0.55
B330	72.16	12.94	1.75	3.50	1.45	3.66	4.30	0.23
B331	72.79	14.29	2.51	0.75	2.21	3.91	3.24	0.30
B332	74.07	14.00	1.92	0.60	1.85	3.75	3.56	0.27
B333	73.74	14.19	1.97	0.61	2.17	3.86	3.18	0.27
B334	75.29	13.58	1.60	0.45	1.41	3.72	3.73	0.22
B336	60.86	16.99	6.44	3.38	6.71	3.42	1.42	0.78

Sample Number	Oxide SiO_2	Al_2O_3	FeO	MgO	CaO	Na_2O	K_2O	TiO_2
B337	69.53	14.58	3.66	1.64	3.84	3.35	2.87	0.53
B338	63.95	19.74	3.97	0.89	4.35	5.36	1.38	0.37
B339	63.45	16.86	5.04	2.65	6.29	3.81	1.20	0.70
B340	63.34	16.31	5.56	2.81	5.92	3.81	1.54	0.71
B341	54.16	19.25	7.65	4.80	9.01	3.06	1.08	0.98
B342	60.27	16.86	6.45	3.51	7.04	3.63	1.44	0.80
B343	64.76	15.94	5.18	2.60	5.49	3.54	1.81	0.67
B344	63.46	16.10	5.73	2.94	5.57	3.64	1.81	0.76
B345	65.94	15.13	5.35	2.48	5.31	3.44	1.70	0.64
B346	74.21	13.37	2.41	0.50	2.01	4.21	3.03	0.25
B347	62.31	16.75	7.11	1.31	6.90	3.54	1.25	0.82
B348	74.94	13.45	2.03	0.42	1.68	4.28	2.97	0.24
B350	68.91	15.74	3.99	1.24	3.45	3.92	2.27	0.49
B351	68.83	15.77	3.82	1.37	3.63	4.11	2.02	0.45
B352	63.36	16.31	5.66	2.74	6.04	3.34	1.89	0.67
B353	63.03	17.21	5.36	2.63	6.45	3.49	1.20	0.64
B354	67.46	15.64	4.45	1.76	4.31	3.50	2.27	0.61
B355	68.21	15.09	4.01	1.67	3.95	3.63	2.88	0.56
B356	68.71	15.91	4.03	1.14	3.31	4.06	2.35	0.49
B357	61.38	16.34	6.38	3.58	6.89	3.28	1.42	0.74
B358	64.19	16.06	5.44	2.74	5.72	3.65	1.52	0.67
B359	61.53	16.61	6.28	3.30	6.72	3.15	1.67	0.74
B360	68.74	15.54	4.08	1.29	3.72	4.39	1.76	0.48
B361	68.55	16.29	3.65	1.38	3.49	4.05	2.15	0.44
B363	64.47	14.07	6.32	3.11	5.43	3.79	2.09	0.72
B364	74.69	13.51	2.14	0.61	2.16	4.11	2.51	0.27
B366	69.53	15.68	3.63	1.20	3.51	4.33	1.69	0.42
B367	75.02	12.81	1.06	2.49	0.91	3.85	3.75	0.10
B368	74.22	14.10	2.06	0.56	2.14	3.92	2.72	0.27
B369	75.92	12.82	1.86	0.45	1.39	3.75	3.58	0.22
B370	65.54	15.12	5.12	2.59	4.85	3.45	2.51	0.82
B371	65.44	17.12	4.11	1.81	5.43	4.03	1.29	0.77
B372	65.43	16.48	4.34	1.80	5.07	3.82	2.17	0.90
B373	64.18	18.02	4.03	1.90	5.35	4.26	1.49	0.78
B374	64.46	16.73	5.04	1.88	5.71	3.34	2.15	0.69
B375	62.31	18.36	4.26	3.14	5.58	4.20	1.39	0.77
B376	62.99	17.20	5.60	2.63	5.43	3.33	2.06	0.77
B377	65.19	17.19	4.54	1.95	5.75	3.97	0.81	0.60
B378	67.17	16.40	4.20	1.60	4.97	3.89	1.25	0.52
B380	65.15	17.77	4.20	1.86	5.44	3.80	1.19	0.59
B381	62.76	18.45	4.41	2.14	6.08	4.20	1.12	0.84
B382	64.47	17.64	4.25	1.82	5.51	4.13	1.38	0.81
B383	64.38	17.84	4.00	1.90	5.85	4.01	1.20	0.82
B384	65.79	17.82	3.64	1.43	4.91	4.19	1.58	0.64
B385	64.08	17.32	4.54	2.15	5.69	4.00	1.36	0.87
B386	64.13	15.30	4.44	4.08	6.51	3.27	1.77	0.50
B387	73.77	14.91	1.79	0.45	1.48	3.64	3.72	0.24
B388	75.54	13.20	1.59	0.51	1.30	4.19	3.47	0.19
B389	74.26	13.97	1.92	0.49	1.40	4.36	3.39	0.22
B390	69.09	16.81	2.61	0.94	4.12	4.51	1.50	0.42
B391	70.98	16.02	2.09	0.81	3.53	4.33	1.87	0.36
B392	61.90	19.52	3.93	1.69	5.09	4.63	2.48	0.75
B394	66.46	16.65	3.94	1.72	4.71	3.91	1.89	0.72
B395	65.11	16.82	4.02	2.03	5.45	3.95	1.75	0.87
B396	72.41	15.00	1.87	0.71	2.84	3.57	3.28	0.32
B397	67.15	17.17	3.25	1.30	4.06	4.08	2.40	0.58
B398	64.77	17.41	4.19	1.99	5.06	3.91	1.84	0.83
B399	67.67	16.58	3.45	1.40	4.22	3.85	2.19	0.63
B400	68.40	16.57	3.01	1.17	4.25	4.65	1.47	0.49
B401	61.08	16.88	6.39	3.19	6.55	3.50	1.62	0.79
B402	69.23	14.42	4.16	1.98	2.84	2.86	3.58	0.93
B403	61.11	16.54	6.93	2.86	6.34	3.78	1.55	0.90
B404	66.67	16.13	5.20	0.38	5.08	3.61	2.23	0.69
B405	63.25	17.39	4.94	2.75	5.41	3.35	2.14	0.77
B406	71.33	13.91	3.20	2.05	2.66	2.46	3.76	0.63

APPENDIX 1.--Continued

Sample Number	Oxide							
	SiO_2	Al_2O_3	FeO	MgO	CaO	Na_2O	K_2O	TiO_2
Perris block--Continued								
B407	71.97	15.41	2.02	0.62	2.61	4.09	2.93	0.34
B408	64.37	16.61	4.85	2.44	5.60	3.68	1.69	0.75
B409	66.48	16.31	3.92	1.81	5.04	3.87	1.92	0.65
B410	66.65	16.19	3.84	2.13	4.67	3.73	2.25	0.54
B411	65.14	16.76	4.93	0.20	9.30	2.59	0.61	0.47
B412	57.13	20.18	6.42	3.58	7.17	3.66	1.06	0.80
B413	67.00	15.46	4.51	2.15	4.40	3.48	2.36	0.62
B415	67.93	15.11	4.08	2.05	3.85	3.29	3.22	0.49
B416	74.79	14.39	1.22	0.37	1.75	3.62	3.73	0.13
B417	62.39	15.83	5.85	3.78	6.13	3.11	2.09	0.81
B418	74.14	13.87	1.64	0.41	1.71	3.52	4.45	0.26
B420	61.13	17.45	6.66	2.73	6.29	3.06	1.73	0.95
B421	76.29	12.85	1.64	0.85	1.15	3.01	3.94	0.27
B422	72.74	14.53	2.29	0.64	2.19	3.42	3.90	0.29
B423	63.51	15.79	5.91	3.06	5.44	3.08	2.47	0.73
B424	74.15	15.09	1.17	0.42	2.04	4.21	2.73	0.17
B425	72.13	14.60	2.12	0.86	2.62	3.59	3.79	0.30
B426	68.22	15.38	4.27	1.58	4.19	4.00	1.79	0.57
B427	62.88	16.01	6.01	3.13	6.51	3.47	1.13	0.85
B428	77.04	12.35	0.99	0.20	0.89	3.47	4.95	0.10
B429	59.97	18.83	5.67	1.99	5.70	7.18	0.10	0.57
B430	65.65	16.57	4.38	2.10	4.79	3.11	2.82	0.59
B431	67.18	15.35	4.73	1.99	4.16	3.50	2.47	0.63
B432	64.33	17.09	4.81	2.35	5.40	3.30	1.97	0.75
B433	65.94	16.24	4.31	2.27	4.93	3.63	2.06	0.62
B434	70.65	15.59	2.64	1.08	3.46	4.04	2.19	0.34
B435	64.42	17.04	4.52	2.18	5.58	3.97	1.51	0.77
B436	62.94	17.50	3.05	5.69	4.18	4.19	1.86	0.57
B437	65.61	17.31	3.76	1.78	4.97	4.19	1.72	0.66
B438	64.17	17.32	4.50	2.10	5.25	3.79	2.09	0.78
B439	65.64	16.80	3.85	1.91	5.10	3.98	2.04	0.67
B440	69.98	15.40	3.59	1.00	3.58	4.19	1.82	0.44
B441	66.77	16.47	4.01	1.78	4.61	3.71	1.90	0.74
B442	66.11	15.96	4.54	1.98	4.85	3.77	1.98	0.81
B447	70.07	16.05	2.69	0.90	3.38	3.95	2.50	0.47
B448	62.42	17.82	4.49	2.21	6.18	4.90	1.09	0.89
B449	66.36	16.12	4.55	2.15	4.54	3.64	2.00	0.63
B450	74.09	14.15	1.48	0.47	1.59	3.19	4.81	0.22
B451	69.88	15.54	3.37	1.29	3.77	3.79	1.92	0.44
B452	67.00	15.78	3.96	1.82	4.73	3.48	2.45	0.79
B453	66.51	16.59	4.09	1.76	4.39	3.64	2.29	0.75
B454	66.04	16.62	3.88	1.87	4.57	3.63	2.63	0.75
B455	67.83	15.76	4.00	1.80	3.91	3.50	2.50	0.69
B456	66.25	15.98	4.49	1.93	4.90	3.77	1.88	0.81
Santa Ana block								
B458	74.36	13.84	2.27	0.35	1.78	4.25	2.88	0.27
B459	76.20	13.31	1.46	0.17	1.11	4.02	3.57	0.17
B460	74.83	13.70	1.97	0.40	1.97	4.27	2.61	0.25
B461	75.88	12.09	2.54	0.38	1.48	3.91	3.50	0.22
B462	70.01	14.12	4.19	1.36	3.27	3.49	2.97	0.59
B464	72.75	13.77	3.02	0.89	2.50	3.58	3.09	0.41
B465	74.85	13.50	2.12	0.28	1.41	3.96	3.66	0.22
B466	73.21	13.99	3.02	0.31	1.79	4.42	2.97	0.29
B469	74.91	13.46	2.06	0.48	2.03	3.88	2.92	0.25
B470	75.04	13.41	2.33	0.35	1.76	3.85	2.97	0.28
B471	79.10	10.92	1.30	0.05	0.73	3.52	4.23	0.15
B472	72.51	14.55	2.71	0.54	2.35	4.29	2.70	0.34
B473	67.36	15.86	4.86	1.44	4.07	4.09	1.68	0.65
B474	65.86	15.06	5.09	2.74	5.17	3.30	2.13	0.65
B475	75.82	12.99	1.98	0.38	1.69	3.56	3.35	0.23

Sample Number	Oxide							
	SiO_2	Al_2O_3	FeO	MgO	CaO	Na_2O	K_2O	TiO_2
B476	70.82	13.92	3.71	1.45	3.33	3.66	2.67	0.44
B478	69.63	14.86	3.76	1.64	3.72	3.68	2.26	0.47
B479	74.84	13.70	2.37	0.35	1.81	3.54	3.14	0.25
B480	75.24	13.34	2.04	0.45	1.93	3.79	2.97	0.25
B482	77.21	12.75	1.32	0.05	0.77	4.12	3.68	0.10
B484	59.55	18.10	6.58	3.25	6.76	3.80	1.12	0.85
B485	73.26	14.53	2.26	0.55	2.17	3.70	3.24	0.29
B486	65.71	15.93	4.70	2.43	5.19	3.89	1.53	0.62
B487	58.14	18.37	6.79	3.65	7.72	3.62	0.86	0.85
B489	74.18	14.45	1.54	0.13	1.18	4.64	3.73	0.13
B490	75.99	13.35	1.49	0.23	1.26	3.87	3.64	0.18
B491	75.16	13.65	2.01	0.22	1.62	4.03	3.09	0.22
B492	67.26	15.67	4.42	1.88	4.42	3.47	2.27	0.61
B493	71.19	15.44	2.47	0.39	2.48	5.51	2.24	0.29
B494	64.42	16.05	5.21	2.75	5.39	3.59	1.92	0.67
B495	64.55	15.80	5.10	2.95	5.52	3.67	1.73	0.68
B496	72.59	14.03	3.62	0.74	2.75	4.22	1.57	0.48
B497	67.14	14.72	4.88	2.23	4.70	3.78	1.79	0.76
B498	61.14	16.05	6.64	3.69	6.50	3.49	1.59	0.90
B499	66.62	15.12	6.10	1.74	4.39	3.79	1.50	0.75
B500	61.79	16.72	6.06	3.22	6.13	3.55	1.70	0.83
B502	65.93	16.87	3.35	1.67	6.34	3.70	1.82	0.34
B503	60.08	17.45	6.19	3.43	7.25	3.47	1.33	0.79
B504	74.79	13.91	1.79	0.37	1.91	3.77	3.23	0.23
B506	71.54	14.66	3.21	0.74	2.73	4.46	2.28	0.39
B507	66.05	15.78	4.78	2.00	4.96	4.39	1.44	0.59
B508	72.63	14.55	2.70	0.54	2.45	4.47	2.33	0.32
B510	74.43	13.80	2.14	0.44	2.17	4.15	2.60	0.27
B513	53.86	18.93	8.14	4.64	9.16	3.61	0.71	0.95
B514	56.68	18.26	7.03	4.29	8.27	3.48	1.13	0.86
B515	77.17	12.41	1.74	0.02	0.93	4.19	3.41	0.13
B516	76.96	12.82	1.79	0.15	1.71	4.35	2.04	0.18
B517	69.05	14.43	4.54	1.68	4.11	3.67	1.96	0.55
B518	60.46	17.06	6.14	3.82	6.88	3.57	1.29	0.78
B519	63.48	15.92	5.67	3.12	5.59	3.78	1.71	0.74
B520	73.16	13.92	3.08	0.40	2.07	4.69	2.38	0.30
B521	73.95	14.32	2.22	0.37	2.00	4.40	2.49	0.23
B522	60.40	17.46	6.20	3.24	6.65	3.84	1.42	0.81
B523	58.70	17.73	6.83	3.71	7.37	3.62	1.19	0.86
B524	64.04	15.29	6.01	2.71	5.65	4.05	1.43	0.81
B525	65.91	14.92	5.22	2.32	5.17	3.96	1.75	0.76
B528	73.17	14.08	2.97	0.37	2.25	4.78	2.08	0.30
B529	61.20	17.19	6.03	3.14	6.20	3.57	1.93	0.74
B530	59.81	17.49	6.14	3.82	7.12	3.42	1.47	0.73
B531	61.53	16.46	6.36	3.24	6.10	3.34	2.11	0.86
B533	54.76	18.75	7.82	4.96	8.48	3.40	0.85	0.96
B536	55.28	17.66	8.06	4.93	8.75	3.39	1.00	0.93
B537	59.88	16.86	6.88	3.67	6.79	3.43	1.67	0.83
B538	73.04	14.10	2.67	0.62	2.33	4.15	2.75	0.34
B539	72.52	14.36	3.06	0.65	2.75	4.52	1.75	0.39
B540	72.49	14.31	2.71	0.60	2.34	4.20	3.00	0.34
B541	72.78	13.91	3.07	0.65	2.35	4.11	2.77	0.37
B542	70.34	14.97	3.96	0.82	3.24	4.91	1.23	0.52
B543	56.32	17.46	7.56	4.94	8.43	3.40	1.07	0.81
B544	64.55	16.75	5.30	2.33	5.63	3.57	1.33	0.54
B546	65.75	15.90	5.04	1.81	4.56	3.66	2.60	0.67
B547	59.48	17.81	6.10	3.54	6.55	3.94	1.60	0.98
B548	64.05	16.90	4.74	2.43	5.67	3.91	1.51	0.79
B549	70.45	14.68	3.91	0.84	2.87	4.23	2.50	0.52
B550	76.45	12.97	1.35	0.02	0.51	3.89	4.72	0.10
B551	72.03	15.33	3.03	0.60	2.44	4.25	1.98	0.34
B553	77.36	12.96	0.45	0.02	0.70	3.69	4.74	0.08
B555	63.72	16.68	5.19	2.51	5.80	3.77	1.48	0.85
B556	65.54	15.91	4.68	2.34	4.80	3.83	2.14	0.76
B557	59.80	18.24	5.95	3.15	6.48	3.85	1.57	0.96

APPENDIX 2

Mixing proportions

Sample Number	End member *M*-1	*M*-2	*D*-1	*D*-2
San Gabriel block				
B 1	1.2174	0.9289	-0.6709	-0.4755
B 2	0.9619	0.8786	-0.5231	-0.3174
B 3	0.9302	0.6186	-0.3118	-0.2369
B 4	1.2767	0.7197	-0.5559	-0.4404
B 5	0.9208	0.9135	-0.3952	-0.4391
B 6	1.2507	1.2092	-0.7926	-0.6673
B 7	1.1276	0.9123	-0.5895	-0.4504
B 8	1.2485	0.7044	-0.6100	-0.3429
B 9	1.1917	1.0451	-0.7145	-0.5224
B 10	0.7177	1.2399	-0.4496	-0.5080
B 11	0.6233	1.1228	-0.2827	-0.4634
B 12	0.8445	0.8223	-0.3519	-0.3150
B 13	0.7706	0.9073	-0.3155	-0.3624
B 14	0.9792	0.4384	-0.2641	-0.1535
B 15	1.1089	0.5788	-0.3939	-0.2937
B 16	0.9389	0.5381	-0.2886	-0.1884
B 17	1.0423	0.8977	-0.4700	-0.4700
B 18	1.1551	1.1495	-0.6630	-0.6416
B 19	0.8019	1.4285	-0.5291	-0.7014
B 20	0.5837	1.5388	-0.3978	-0.7248
B 21	0.9391	0.7171	-0.3907	-0.2654
B 22	0.7831	0.4762	-0.1414	-0.1178
B 23	0.8008	0.6209	-0.2773	-0.1444
B 24	0.9681	0.5208	-0.2828	-0.2061
B 25	1.1512	1.2196	-0.7038	-0.6670
B 26	0.7134	1.2828	-0.4335	-0.5626
B 27	0.7229	0.6464	-0.2956	-0.0737
B 28	0.3545	1.1692	-0.1861	-0.3376
B 29	0.6434	0.9085	-0.2393	-0.3126
B 30	1.0392	0.7829	-0.4777	-0.3444
B 31	0.5875	1.1692	-0.3648	-0.3919
B 32	0.9966	0.7151	-0.4309	-0.2808
B 33	0.6869	0.5134	-0.1251	-0.0752
B 34	0.8412	0.9545	-0.3684	-0.4272
B 35	1.0494	1.1927	-0.6240	-0.6180
B 36	0.8666	0.9352	-0.3847	-0.4171
B 37	0.7273	0.7084	-0.2085	-0.2272
B 38	0.7242	0.4060	-0.0590	-0.0712
B 39	0.9959	0.3676	-0.2722	-0.0913
B 40	1.1020	0.6300	-0.4273	-0.3047
B 41	0.5382	0.3488	0.0236	0.0894
B 42	0.9570	0.5350	-0.3101	-0.1818
B 43	0.7424	0.8197	-0.2780	-0.2841
B 44	0.3696	0.8393	-0.0817	-0.1272
B 46	0.7325	1.1015	-0.4289	-0.4051
B 47	0.6038	1.1752	-0.3727	-0.4064
B 48	1.0573	0.9368	-0.5685	-0.4256
San Bernardino block				
B 54	0.7080	1.2247	-0.4546	-0.4781
B 55	0.7045	1.0839	-0.3346	-0.4538
B 56	0.5472	0.7952	-0.1855	-0.1568
B 57	0.4363	0.7923	-0.0867	-0.1418
B 58	0.5181	0.8350	-0.1629	-0.1903
B 59	0.5160	0.8225	-0.1667	-0.1718
B 60	0.5270	1.0037	-0.2191	-0.3116
B 61	0.7139	0.6223	-0.1693	-0.1669
B 62	0.4926	0.7891	-0.1410	-0.1407
B 63	0.5426	1.1837	-0.2808	-0.4455
B 64	0.6369	1.3884	-0.4281	-0.5972
B 65	0.8435	1.2957	-0.5139	-0.6253
B 66	0.4837	1.0171	-0.1670	-0.3337
B 67	0.3876	0.9667	-0.1231	-0.2312
B 68	0.5702	1.3892	-0.3572	-0.6022
B 69	0.7879	1.0210	-0.4022	-0.4067
B 70	0.5139	0.8303	-0.1225	-0.2218
B 71	0.7682	0.9463	-0.3541	-0.3604
B 72	0.5272	1.4569	-0.3500	-0.6341
B 74	0.8694	0.6447	-0.2744	-0.2397
B 75	0.8799	1.2560	-0.5439	-0.5920
B 78	0.5754	1.1626	-0.3299	-0.4082
B 79	0.9923	0.9954	-0.5698	-0.4178
B 80	0.7478	0.8041	-0.2722	-0.2797
B 81	0.8413	1.0596	-0.4558	-0.4451
B 85	0.4104	1.1881	-0.1866	-0.4119
B 86	1.0616	1.4356	-0.6989	-0.7983
B 94	0.2961	1.3932	-0.2011	-0.4882
B 95	0.3964	1.4304	-0.2761	-0.5507
B 96	0.9281	1.2204	-0.5649	-0.5835
B 97	0.5656	0.7990	-0.1500	-0.2146
B 98	0.6223	1.0403	-0.3450	-0.3177
B 99	0.1145	1.1810	0.0293	-0.3249
B100	0.6653	1.2826	-0.4638	-0.4840
B101	0.6535	1.0780	-0.3283	-0.4032
B102	0.5175	1.0506	-0.2423	-0.3257
B103	0.4882	1.2123	-0.2585	-0.4420
B104	0.6614	1.0296	-0.3529	-0.3381
B105	1.2093	1.2510	-0.7557	-0.7046
B106	0.7563	1.2086	-0.4381	-0.5268
B107	0.6321	1.2025	-0.3601	-0.4746
B108	1.2012	0.6206	-0.4870	-0.3349
B109	0.6404	1.5559	-0.3669	-0.8295
B110	0.7476	1.5435	-0.4569	-0.8342
B111	0.2485	1.7961	-0.2146	-0.8300
B112	1.1397	1.3705	-0.6659	-0.8443
B113	0.7591	1.5381	-0.4642	-0.8331
B114	0.8734	1.5886	-0.5394	-0.9226
B115	0.6849	1.2952	-0.4731	-0.5070
B116	0.7195	0.7742	-0.2294	-0.2643
B117	0.8083	1.0521	-0.4734	-0.3870
B118	0.6657	1.3399	-0.4026	-0.6030
B120	0.5096	1.3764	-0.2935	-0.5925
B121	0.5248	1.1163	-0.2401	-0.4011
B124	0.8158	1.2503	-0.4657	-0.6004
B125	0.7314	1.2730	-0.4523	-0.5521
B127	0.4719	1.3466	-0.2979	-0.5205
B128	0.5882	0.8055	-0.1571	-0.2365
B129	0.4652	1.4625	-0.2998	-0.6279
B130	0.4224	1.3774	-0.2644	-0.5354
B131	0.6876	1.3436	-0.4301	-0.6011
B132	0.7061	1.2742	-0.4245	-0.5557
B133	0.6287	1.4218	-0.4263	-0.6241
B134	0.8028	1.3048	-0.5161	-0.5915
B135	0.5352	1.2980	-0.3801	-0.4530
B136	0.6184	1.2242	-0.3616	-0.4811
B137	0.6047	1.2280	-0.3425	-0.4901
B138	0.6140	1.2863	-0.3714	-0.5289
B139	0.6512	1.2892	-0.3958	-0.5446
B140	0.5245	1.3352	-0.3205	-0.5392
B141	0.5696	1.2175	-0.3343	-0.4528
B142	0.4753	1.3185	-0.2846	-0.5091
B143	0.5632	1.2942	-0.3429	-0.5145
B144	0.6402	1.2850	-0.3720	-0.5532
B145	0.5508	1.2966	-0.3306	-0.5168
B146	0.7554	1.2815	-0.4623	-0.5746
B147	0.5304	1.2744	-0.3194	-0.4854
B148	0.6137	1.2324	-0.3650	-0.4811
B149	0.6469	1.2973	-0.4073	-0.5369
B150	0.5771	1.2738	-0.3536	-0.4973
B151	0.5503	1.1946	-0.3100	-0.4349
B152	0.6898	0.8747	-0.2527	-0.3118
B153	0.6108	1.0084	-0.3028	-0.3163
B155	0.4314	0.8466	-0.0503	-0.2276
B156	0.6582	0.9458	-0.2783	-0.3258
B157	0.5937	1.2770	-0.3885	-0.4822
B158	0.5699	0.6217	-0.0971	-0.0945
B159	0.6619	0.8163	-0.1758	-0.3024
B160	0.8222	0.7752	-0.2971	-0.3003
B161	0.6458	0.9970	-0.2746	-0.3683
B162	0.7669	1.0411	-0.3915	-0.4165
B163	0.7325	1.1465	-0.4256	-0.4535
B164	0.6338	0.5702	-0.0955	-0.1084
B165	0.9658	1.2500	-0.5862	-0.6295
B166	0.8182	0.4391	-0.1585	-0.0987
B168	0.7335	0.5355	-0.1201	-0.1489
B169	0.8207	0.4652	-0.1485	-0.1373
B170	0.8835	0.9454	-0.5081	-0.3209
B171	0.7430	0.9793	-0.3765	-0.3458
B172	1.0757	0.4596	-0.3519	-0.1834
B173	0.3673	1.4962	-0.2835	-0.5801
B174	0.5195	1.3222	-0.2926	-0.5492
B175	0.5281	1.2866	-0.3003	-0.5144
B176	0.7910	1.0308	-0.4448	-0.3771
B177	0.5045	1.3977	-0.3611	-0.5411
B178	0.4426	1.5445	-0.3357	-0.6514
B179	0.8881	0.5737	-0.3306	-0.1312
B180	0.7911	1.1830	-0.4966	-0.4775
B181	0.7332	1.3216	-0.4761	-0.5787
B182	0.5015	1.3937	-0.2884	-0.6068
B183	0.5930	1.2168	-0.2818	-0.5280
B184	0.0000	1.8051	-0.0365	-0.7686
B185	0.4551	1.1473	-0.2176	-0.3848
B186	0.6726	1.1476	-0.3764	-0.4438
B187	0.5206	1.2551	-0.3147	-0.4610
B188	0.4868	1.2859	-0.2640	-0.5087
B189	0.6386	1.4182	-0.4551	-0.6017
B190	0.5585	1.3280	-0.3777	-0.5087
B191	0.4142	1.4301	-0.3084	-0.5359
B192	0.5742	1.2855	-0.3648	-0.4950
B193	0.6465	1.3172	-0.4323	-0.5313
B194	0.6755	1.0501	-0.3523	-0.3733
B195	0.6606	1.3934	-0.4458	-0.6082
B196	0.4675	1.0851	-0.2234	-0.3292
B197	0.4803	1.4336	-0.3356	-0.5783
Little San Bernardino block				
B198	0.4478	1.3347	-0.3044	-0.4782
B199	0.8866	1.2342	-0.5413	-0.5795
B200	0.9771	1.0126	-0.6330	-0.3567
B201	0.7056	1.1290	-0.3941	-0.4406
B202	0.2879	1.4270	-0.2046	-0.5103
B203	0.3669	1.3695	-0.2850	-0.4514
B204	1.0912	1.2119	-0.6478	-0.6554
B205	0.3380	1.4218	-0.1933	-0.5665
B206	0.9024	1.4280	-0.5792	-0.7512
B207	0.9836	1.2223	-0.6171	-0.5889

APPENDIX 2.--Continued

Sample Number	End member M-1	M-2	D-1	D-2
Little San Bernardino block--Continued				
B208	1.3615	1.1131	-0.8115	-0.6631
B209	1.3327	0.9114	-0.6194	-0.6246
B210	0.8695	0.8661	-0.3869	-0.3487
B211	1.0856	0.9661	-0.6212	-0.4305
B212	1.0926	0.9137	-0.5971	-0.4092
B213	0.6930	0.6728	-0.1555	-0.2103
B214	1.1242	0.4543	-0.3542	-0.2242
B215	1.1917	1.2863	-0.7610	-0.7171
B216	0.5367	0.9199	-0.1936	-0.2630
B217	0.8028	1.2984	-0.4994	-0.6017
B218	1.2019	0.7027	-0.6238	-0.2808
B219	0.8707	0.9628	-0.4292	-0.4043
B220	0.8327	1.1981	-0.5017	-0.5290
B221	0.9761	0.7734	-0.3945	-0.3550
B222	0.9861	0.7372	-0.3458	-0.3775
San Jacinto block				
B223	0.9859	0.6163	-0.4217	-0.1804
B224	0.5269	1.1874	-0.2494	-0.4648
B225	0.8099	0.7333	-0.3553	-0.1879
B226	0.3335	0.8727	0.0324	-0.2386
B227	0.3873	0.8940	-0.0063	-0.2749
B228	0.7662	0.9098	-0.3189	-0.3571
B229	0.3394	0.6504	-0.0075	0.0177
B230	0.7027	0.8791	-0.2533	-0.3286
B231	0.7688	0.9180	-0.3496	-0.3372
B232	0.5791	0.6307	-0.1327	-0.0771
B233	0.9301	0.7230	-0.2860	-0.3670
B234	0.8227	0.7338	-0.3230	-0.2334
B235	0.9812	0.7210	-0.4435	-0.2587
B236	0.7323	0.9621	-0.2682	-0.4262
B237	0.6757	0.6984	-0.2248	-0.1493
B238	0.7945	0.8537	-0.3348	-0.3134
B239	0.7069	0.7113	-0.2417	-0.1766
B240	0.7020	0.7919	-0.2888	-0.2051
B241	0.7869	0.7907	-0.3413	-0.2363
B242	0.7418	0.7718	-0.2798	-0.2338
B243	0.6834	0.7075	-0.2253	-0.1656
B244	0.9483	0.6390	-0.2984	-0.2888
B245	0.8296	0.7806	-0.3135	-0.2967
B246	0.8339	0.9386	-0.4089	-0.3636
B247	0.9322	0.7245	-0.4146	-0.2421
B248	1.0296	0.8927	-0.5081	-0.4142
B249	0.6344	0.9222	-0.2490	-0.3075
B250	0.5227	1.0323	-0.2031	-0.3520
B251	0.8156	0.5936	-0.2161	-0.1931
B252	0.7942	0.7917	-0.3493	-0.2366
B253	0.7450	0.7447	-0.2511	-0.2386
B254	0.8024	0.7573	-0.3275	-0.2322
B255	0.7274	1.4937	-0.4254	-0.7958
B256	0.6158	0.8424	-0.1786	-0.2796
B257	0.5904	0.7457	-0.1681	-0.1680
B258	0.7911	0.7382	-0.2928	-0.2364
B259	0.8759	1.2565	-0.4897	-0.6427
B260	1.0092	0.6565	-0.4307	-0.2350
B261	0.6684	0.7997	-0.2364	-0.2317
B262	0.6928	1.0889	-0.3289	-0.4529
B263	1.0899	0.9518	-0.5424	-0.4993
B264	0.9418	1.1636	-0.5102	-0.5951
B265	0.8129	0.6700	-0.2551	-0.2279
B266	0.1626	1.7666	-0.1621	-0.7672
B267	0.4676	1.6743	-0.2933	-0.8486

Sample Number	End member M-1	M-2	D-1	D-2
B268	1.0436	0.9379	-0.4854	-0.4961
B269	0.7386	0.5526	-0.2010	-0.0901
B270	1.5060	1.1208	-0.8940	-0.7327
B271	1.2724	1.1995	-0.7740	-0.6979
B272	1.7592	0.7880	-0.9433	-0.6039
B273	0.9636	0.5577	-0.3389	-0.1824
B274	0.4859	0.8500	-0.1016	-0.2343
B275	0.4204	1.1421	-0.1659	-0.3966
B276	0.6237	0.8767	-0.1874	-0.3130
B277	0.5948	0.7799	-0.1031	-0.2716
B278	0.5477	0.8156	-0.1293	-0.2340
B279	0.9333	1.0080	-0.4850	-0.4563
B280	0.9770	0.9052	-0.5050	-0.3773
B281	0.7293	1.0214	-0.3135	-0.4372
B282	0.4173	1.4874	-0.2221	-0.6825
B283	0.1947	1.1170	0.0732	-0.3850
B284	0.2175	1.1809	-0.0330	-0.3655
B285	0.3901	0.9863	-0.0627	-0.3137
B286	0.4279	0.7348	0.0064	-0.1691
B287	0.5701	1.0460	-0.2011	-0.4150
B288	0.6260	0.7331	-0.1171	-0.2420
B289	0.6420	0.9983	-0.2687	-0.3716
B290	0.6324	0.7067	-0.1502	-0.1890
B291	0.5500	1.1095	-0.2079	-0.4516
B292	0.8084	0.9822	-0.3271	-0.4634
B293	0.6962	0.9963	-0.2730	-0.4195
B294	0.7272	0.9919	-0.2983	-0.4208
B295	0.4824	0.6804	-0.0083	-0.1546
B296	0.3890	1.0707	-0.0928	-0.3669
B297	0.3528	0.9094	-0.0053	-0.2569
B298	0.4075	0.8574	-0.0096	-0.2552
B299	0.3154	0.8865	-0.0172	-0.1847
B300	0.4704	0.6234	-0.0057	-0.0882
B301	0.3563	0.9111	0.0039	-0.2713
B302	0.2546	0.9323	0.0568	-0.2437
B303	0.1444	1.0893	0.0494	-0.2832
B304	0.3335	0.6797	0.0641	-0.0773
B305	0.6179	0.5864	-0.1186	-0.0857
B306	0.0977	0.9747	0.1468	-0.2192
B307	0.3589	0.9237	-0.0018	-0.2808
B308	0.3225	0.7292	0.0577	-0.1094
B309	0.3749	1.0721	-0.0838	-0.3632
B310	0.5617	0.8145	-0.0804	-0.2958
B311	0.5814	0.7289	-0.1146	-0.1957
B312	1.2970	1.3622	-0.8076	-0.8516
B313	1.1211	1.3030	-0.6676	-0.7565
B314	1.2809	1.0455	-0.7273	-0.5991
B315	0.7331	0.6313	-0.1986	-0.1658
B317	0.7599	0.6091	-0.2398	-0.1292
B318	0.5452	0.6453	-0.0892	-0.1013
B319	0.7249	0.6300	-0.2229	-0.1320
B320	0.4567	0.6404	-0.0264	-0.0707
B321	0.2819	0.6737	0.0641	-0.0197
B322	0.7896	0.6504	-0.2489	-0.1910
B323	0.6313	0.5529	-0.1475	-0.0368
B324	1.1072	0.5289	-0.4441	-0.1920
Perris block				
B325	1.0270	0.6908	-0.3763	-0.3415
B326	1.2220	0.6021	-0.4297	-0.3943
B327	1.4513	0.5810	-0.6315	-0.4008
B328	1.3916	0.7255	-0.6483	-0.4688
B330	1.7953	0.9791	-0.9467	-0.8277

Sample Number	End member M-1	M-2	D-1	D-2
B331	1.5502	0.9483	-0.8582	-0.6404
B332	1.4352	1.0775	-0.8182	-0.6945
B333	1.5518	0.9864	-0.8744	-0.6637
B334	1.4987	1.1368	-0.8786	-0.7569
B336	1.2551	0.3337	-0.3420	-0.2469
B337	1.3087	0.8591	-0.5859	-0.5819
B338	1.1805	0.3435	-0.6150	0.0910
B339	1.4054	0.3488	-0.5089	-0.2453
B340	1.5226	0.3666	-0.5774	-0.3118
B341	0.5722	0.1931	0.1996	0.0352
B342	1.3682	0.2810	-0.4121	-0.2372
B343	1.4111	0.4971	-0.5270	-0.3812
B344	1.4100	0.4402	-0.5073	-0.3428
B345	1.6812	0.4779	-0.6754	-0.4837
B346	2.0244	0.8481	-1.1517	-0.7208
B347	1.2062	0.3612	-0.3572	-0.2102
B348	2.0263	0.8663	-1.1735	-0.7192
B350	1.4198	0.6986	-0.6824	-0.4360
B351	1.6113	0.6087	-0.7936	-0.4264
B352	1.2370	0.5046	-0.3927	-0.3489
B353	1.2389	0.3859	-0.3839	-0.2410
B354	1.2425	0.7050	-0.5080	-0.4395
B355	1.2820	0.7921	-0.5759	-0.4982
B356	1.4016	0.6942	-0.6872	-0.4086
B357	1.4453	0.3245	-0.4348	-0.3350
B358	1.5523	0.4009	-0.5916	-0.3615
B359	1.1839	0.4262	-0.2977	-0.3125
B360	1.8643	0.4958	-0.9396	-0.4205
B361	1.3819	0.6714	-0.6709	-0.3825
B363	2.0647	0.3651	-0.8853	-0.5446
B364	2.0905	0.8017	-1.1718	-0.7204
B366	1.8375	0.5314	-0.9395	-0.4295
B367	2.0478	0.9741	-1.1496	-0.8722
B368	1.7444	0.9050	-0.9761	-0.6733
B369	1.8090	1.0659	-1.0442	-0.8307
B370	1.2524	0.6511	-0.4604	-0.4430
B371	1.1371	0.4786	-0.4329	-0.1828
B372	0.8761	0.6609	-0.2943	-0.2427
B373	0.8987	0.4922	-0.3191	-0.0718
B374	0.8425	0.6663	-0.2210	-0.2878
B375	0.9793	0.3972	-0.3103	-0.0662
B376	0.8043	0.6020	-0.1637	-0.2427
B377	1.4700	0.3375	-0.5895	-0.2180
B378	1.5581	0.4664	-0.6848	-0.3397
B380	1.0473	0.4904	-0.3671	-0.1706
B381	0.8412	0.4006	-0.2394	-0.0024
B382	0.9697	0.4813	-0.3410	-0.1100
B383	0.8729	0.4801	-0.2686	-0.0844
B384	0.9437	0.5656	-0.3808	-0.1286
B385	1.0219	0.4591	-0.3388	-0.1422
B386	1.7529	0.4200	-0.6622	-0.5106
B387	1.0528	1.1913	-0.6190	-0.6251
B388	1.9236	0.9767	-1.1362	-0.7641
B389	1.7926	0.9340	-1.0611	-0.6655
B390	1.4990	0.5528	-0.7762	-0.2757
B391	1.5496	0.6817	-0.8332	-0.3981
B392	0.3044	0.6424	-0.0475	0.1007
B394	1.0670	0.6235	-0.4249	-0.2656
B395	0.9725	0.5664	-0.3392	-0.1997
B396	1.0863	1.0770	-0.5842	-0.5791
B397	0.8499	0.7583	-0.3735	-0.2347
B398	0.7902	0.6071	-0.2416	-0.1558
B399	0.9724	0.7382	-0.4102	-0.3005
B400	1.6440	0.4768	-0.8424	-0.2784
B401	1.2272	0.3712	-0.3480	-0.2504

APPENDIX 2.--Continued

Sample Number	End member M-1	M-2	D-1	D-2
	Perris block--Continued			
B402	0.6372	1.0920	-0.1744	-0.5547
B403	1.3768	0.3126	-0.4490	-0.2403
B404	0.9711	0.7182	-0.3703	-0.3189
B405	0.6742	0.6510	-0.1048	-0.2204
B406	0.7566	1.2203	-0.2567	-0.7202
B407	1.2854	0.9295	-0.7204	-0.4945
B408	1.1790	0.5061	-0.4077	-0.2774
B409	1.2244	0.5982	-0.5067	-0.3159
B410	1.2343	0.6591	-0.5153	-0.3781
B411	0.9239	0.5092	-0.1467	-0.2864
B412	0.4703	0.2809	0.1185	0.1304
B413	1.3006	0.6849	-0.5267	-0.4588
B415	1.1394	0.8811	-0.4749	-0.5456
B416	1.2384	1.2007	-0.7388	-0.7003
B417	1.2209	0.5101	-0.3363	-0.3948
B418	1.0601	1.2860	-0.6292	-0.7169
B420	0.6256	0.5349	0.0153	-0.1758
B421	1.3384	1.2911	-0.7400	-0.8895
B422	1.0345	1.1845	-0.5660	-0.6530
B423	1.1152	0.6262	-0.3193	-0.4221
B424	1.5740	0.9303	-0.9321	-0.5723
B425	1.1126	1.1130	-0.6041	-0.6215
B426	1.6943	0.5408	-0.7948	-0.4404
B427	1.5244	0.3121	-0.5077	-0.3287
B428	1.4103	1.3798	-0.8749	-0.9152
B429	2.6100	-0.3401	-1.3843	0.1144
B430	0.6489	0.8630	-0.1454	-0.3665
B431	1.3082	0.7015	-0.5398	-0.4698
B432	0.7463	0.6594	-0.1526	-0.2531
B433	1.2086	0.6159	-0.4664	-0.3581
B434	1.5552	0.7281	-0.8070	-0.4764
B435	1.1509	0.4707	-0.4200	-0.2016
B436	1.4615	0.3951	-0.5794	-0.2773
B437	1.0942	0.5450	-0.4529	-0.1863
B438	0.7841	0.6277	-0.2259	-0.1859
B439	1.0627	0.6097	-0.4216	-0.2508
B440	1.7744	0.5888	-0.9042	-0.4591
B441	1.0250	0.6584	-0.3863	-0.2970
B442	1.1911	0.6003	-0.4619	-0.3296
B447	1.1217	0.8412	-0.5649	-0.3980
B448	1.3424	0.2424	-0.5602	-0.0246
B449	1.2736	0.6097	-0.5074	-0.3760
B450	0.7420	1.4328	-0.4471	-0.7277

Sample Number	End member M-1	M-2	D-1	D-2
B451	1.5397	0.6778	-0.7416	-0.4759
B452	0.9229	0.7731	-0.3253	-0.3706
B453	0.8337	0.7454	-0.2872	-0.2919
B454	0.7106	0.7977	-0.2244	-0.2839
B455	1.0197	0.7925	-0.4010	-0.4112
B456	1.2100	0.5883	-0.4708	-0.3274
	Santa Ana block			
B458	1.9135	0.8606	-1.1011	-0.6730
B459	1.7670	1.0704	-1.0623	-0.7751
B460	2.0496	0.8175	-1.1759	-0.6912
B461	2.1629	0.9533	-1.2337	-0.8826
B462	1.4343	0.8453	-0.6722	-0.6074
B464	1.5710	0.9421	-0.8209	-0.6921
B465	1.6721	1.0488	-0.9802	-0.7407
B466	1.9508	0.8012	-1.1159	-0.6360
B469	1.8732	0.9285	-1.0555	-0.7461
B470	1.8369	0.9476	-1.0367	-0.7479
B471	2.0347	1.2250	-1.2098	-1.0498
B472	1.7620	0.7959	-0.9843	-0.5736
B473	1.5866	0.5076	-0.7271	-0.3671
B474	1.5042	0.5765	-0.5789	-0.5018
B475	1.7422	1.0713	-0.9861	-0.8274
B476	1.7772	0.7606	-0.8813	-0.6565
B478	1.6282	0.6953	-0.7726	-0.5509
B479	1.5948	1.0462	-0.8869	-0.7542
B480	1.8548	0.9585	-1.0452	-0.7680
B482	1.9808	1.0664	-1.2051	-0.8421
B484	1.1093	0.2486	-0.2721	-0.0859
B485	1.3515	1.0358	-0.7494	-0.6378
B486	1.6495	0.4253	-0.6999	-0.3748
B487	1.0815	0.1737	-0.2007	-0.0545
B489	1.6731	0.9822	-1.0446	-0.6107
B490	1.6631	1.1061	-0.9912	-0.7781
B491	1.8256	0.9594	-1.0607	-0.7244
B492	1.2329	0.7007	-0.4954	-0.4382
B493	2.1502	0.5189	-1.2684	-0.4007
B494	1.3882	0.5007	-0.5172	-0.3717
B495	1.5606	0.4386	-0.6090	-0.3902
B496	2.2246	0.5550	-1.1734	-0.6061
B497	1.7294	0.4977	-0.7516	-0.4754
B498	1.4506	0.3243	-0.4534	-0.3215
B499	1.7833	0.4276	-0.7683	-0.4426

Sample Number	End member M-1	M-2	D-1	D-2
B500	1.2032	0.4107	-0.3525	-0.2615
B502	1.2378	0.5842	-0.5065	-0.3155
B503	1.1302	0.3147	-0.2648	-0.1800
B504	1.5663	1.0441	-0.8981	-0.7124
B506	1.9503	0.6488	-1.0632	-0.5359
B507	1.9119	0.3398	-0.8939	-0.3578
B508	1.9738	0.6965	-1.1051	-0.5652
B510	1.9703	0.8275	-1.1149	-0.6828
B513	1.0880	0.0000	-0.1165	0.0285
B514	1.0534	0.1775	-0.1530	-0.0779
B515	2.1895	0.9767	-1.3064	-0.8598
B516	2.5641	0.7164	-1.4776	-0.8029
B517	1.8413	0.5840	-0.8553	-0.5699
B518	1.3600	0.2735	-0.3995	-0.2339
B519	1.5813	0.3836	-0.6068	-0.3582
B520	2.2689	0.6373	-1.2865	-0.6197
B521	1.9913	0.7746	-1.1445	-0.6214
B522	1.2333	0.2972	-0.3680	-0.1625
B523	1.1810	0.2259	-0.2744	-0.1325
B524	1.8796	0.2871	-0.7876	-0.3791
B525	1.7953	0.4217	-0.7808	-0.4362
B528	2.3401	0.5816	-1.3256	-0.5961
B529	1.0731	0.4469	-0.2912	-0.2288
B530	1.1585	0.3245	-0.2768	-0.2062
B531	1.0718	0.4949	-0.2703	-0.2964
B533	1.0072	0.0829	-0.0706	-0.0195
B536	1.3371	0.0609	-0.2591	-0.1390
B537	1.2498	0.3334	-0.3295	-0.2537
B538	1.8314	0.8159	-1.0151	-0.6322
B539	2.2172	0.5596	-1.2106	-0.5662
B540	1.7085	0.8473	-0.9539	-0.6018
B541	1.8661	0.8006	-1.0206	-0.6461
B542	2.3167	0.3555	-1.2362	-0.4360
B543	1.4461	0.0870	-0.3423	-0.1908
B544	1.4404	0.4186	-0.5373	-0.3217
B546	1.1315	0.6895	-0.4431	-0.3779
B547	0.9797	0.3356	-0.2268	-0.0885
B548	1.1964	0.4501	-0.4272	-0.2193
B549	1.7151	0.6954	-0.8955	-0.5150
B550	1.4935	1.2775	-0.9442	-0.8267
B551	1.7885	0.6883	-0.9721	-0.5048
B553	1.3364	1.3784	-0.8653	-0.8495
B555	1.2041	0.4383	-0.4052	-0.2371
B556	1.2864	0.5755	-0.5126	-0.3493
B557	0.7757	0.3869	-0.1188	-0.0438

☆U.S. GOVERNMENT PRINTING OFFICE 1984—776-041/4035